ACTA FACULTATIS TECHNICAE

TECHNICAL UNIVERSITY IN ZVOLEN

2

ISSUE: XXIV
ZVOLEN 2019

Medzinárodný zbor recenzentov / International Reviewers Board

Witold Biały (PL)
Silesian University of Technology, Faculty of Organization and Management
Igor Ďukič (HR)
University of Zagreb, Faculty of Forestry
Jiří Dvořák (CZ)
Czech University of Life Sciences Prague, Faculty of Forestry and Wood Sciences
Ladislav Dzurenda (SK)
Technical University in Zvolen, Faculty of Wood Sciences and Technology
Roman Gálik (SK)
Slovak University of Agriculture in Nitra, Faculty of Engineering
Zhivko Gochev (BG)
University of Forestry, Faculty of Forest Industry
Radek Knoflíček (CZ)
Brno University of Technology, Faculty of Mechanical Engineering)
Zdeněk Kopecký (CZ)
Mendel University in Brno, Faculty of Forestry and Wood Technology
Ján Kosiba (SK)
Slovak University of Agriculture in Nitra, Faculty of Engineering
Dražan Kozak (HR)
Josip Juraj Strossmayer University of Osijek, Mechanical Engineering Faculty
Antonín Kříž (CZ)
University of West Bohemia, Faculty of Mechanical Engineering
Stanislaw Legutko (PL)
Poznan University of Technology
Oleg Machuga (UA)
National Forestry University of Ukraine, Lviv
Milan Malcho (SK)
University of Zilina, The Faculty of Mechanical Engineering
Stanislav Marchevský (SK)
Technical University of Košice, Faculty of Electrical Engineering and Informatics
Ján Mihalík (SK)
Technical University of Košice, Faculty of Electrical Engineering and Informatics
Miroslav Müller (CZ)
Czech University of Life Sciences Prague, Faculty of Engineering
Nataša Náprstková (CZ)
UJEP in Ustí nad Labem, Faculty of Production Technology and Management
Jindřich Neruda (CZ)
Mendel University in Brno, Faculty of Forestry and Wood Technology

Alena Očkajová (SK)
Matej Bel University, Faculty of Natural Sciences
Marián Peciar (SK)
Slovak University of Technology in Bratislava, Faculty of Mechanical Engineering
Krzysztof Zbigniew Rokosz (PL)
Koszalin University of Technology, Faculty of Mechanical Engineering
Juraj Ružbarský (SK)
Technical University of Košice, Faculty of Manufacturing Technologies
Ruslan Safin (RU)
Kazan National Research Technological University
Sergey Spiridonov (RU)
State Institution of Higher Professional Education, Saint Petersburg State
Dana Stančeková (SK)
University of Žilina,Faculty of Mechanical Engineering
Vladimír Štollmann (SK)
Technical University in Zvolen, Faculty of Forestry
Marian Šušniar (HR)
University of Zagreb, Faculty of Forestry
Paweł Tylek (PL)
University of Agriculture in Krakow, Faculty of Forestry
Valery Zhylinski (BY)
Belarusian State Technological University

TABLE OF CONTENTS

SCIENTIFIC PAPERS

SCIENTIFIC PAPERS

QUALITATIVE CLASSIFICATION OF VERTICAL LOG SPLITTERS IN FORESTRY BASED ON THE EVALUATION OF THE MOST IMPORTANT PARAMETERS

KVALITATÍVNA KLASIFIKÁCIA VERTIKÁLNYCH ŠTIEPAČIEK GUĽATINY V LESNÍCTVE NA ZÁKLADE VYHODNOTENIA NAJDÔLEŽITEJŠÍCH PARAMETROV

Pavol Harvánek [a], Ján Kováč [b]

Department of Environmental and Forestry Machinery, Faculty of Technology, Technical University in Zvolen, T.G.Masaryka 24, 960 01 Zvolen
email: [a] xharvanek@is.tuzvo.sk, [b] jan.kovac@ituzvo.sk

ABSTRACT: Due to the large number of manufacturers that focus on producing one type of machine on the market, it is necessary to make their products more transparent. This article focuses on the separating and evaluation of vertical log splitters in forestry according to basic technical parameters. The task of the article is to select different types of vertical log splitters from known manufacturers and to make them more transparent to the end user. For each vertical log splitter, the basic data sets are, the basic parameters such as splitting force, maximum stroke of the linear hydraulic motor due to the maximum chip size and splitting rate. From these data, histograms are subsequently created to enable the user to make clearer splitters based on the manufacturer's basic information. The output from the article will be able to separate the splitters into power groups according to the maximum splitting force and to groups according to their cylinder stroke and cutting speeds. From the parameters it was found that the manufacturers are focused on the production of splitters of two power categories, namely low power with splitting power max. 12t and high power with a splitting force max 25t .

Key words: Vertical log splitter, log splitting, regression analysis, splitting force.

ABSTRAKT: Z dôvodu veľkého množstva výrobcov, ktorý sa zameriavajú na výrobu jedného typu stroja na trhu je potrebne ich produkty sprehľadniť. Tento článok je zameraný na rozdelenie a vyhodnotenie vertikálnych štiepačiek v lesníctve podľa základných technických parametrov. Úlohou článku je vybrať rôzne typy vertikálnych štiepačiek od známych výrobcov a sprehľadniť ich pre koncového užívateľa. Pre každú vertikálnu štiepačku sú v databázovom súbore uvedené základné parametre ako štiepacia sila, maximálny zdvih priamočiareho hydromotora kvôli údaju o maximálnej výške štiepaného kmeňa a rýchlosť štiepania. Z uvedených údajov sú následne vytvorené histogramy, ktoré dokážu užívateľovi sprehľadniť vyrábane štiepačky na základe základných informácií od výrobcu. Výstupom z článku bude možnosť rozdeliť štiepačky do výkonových skupín podľa maximálnej štiepacej sily a do skupín podľa ich zdvihu valca a rýchlosti štiepania. Z parametrov bolo zistene že, výrobcovia sú zameraný na výrobu štiepačiek dvoch výkonových kategórii a to nízko výkonové so štiepacou silou max. 12t a vysoko výkonové so štiepacou silou max 25t.

Kľúčové slová: Vertikálna štiepačka, štiepanie, regresná analýza, štiepacia sila.

INTRODUCTION

Heating with solid fuels and mainly wood belongs to the traditional and most demanded types of heating in cottages and of course households. Increasing energy prices force people to think about other ways of heating even in family houses. Transverse cutting of wood in homes can be solved by either a motorized chainsaw or an electric chainsaw, or a circular saw. Wood splitting requires more physical effort using conventional hand tools such as axes, wedges, etc. Of course, there are machines for such work and those are wood splitters. They can provide large splitting forces and split any wood with difficult shape. On the market there are wood splitters of different power categories, that is, suitable for any household at an affordable price.

Wood splitting is done by penetrating the symmetrical wedge into the wood in the plane of the wood of the cut-out. (Minárik *et al*. 2015). At the beginning of the penetration (Figure 1), the wedge is pressed into wood by its blade and cuts (separates) the fiber walls, while the force F on the wedge increases proportionally to the depth of penetration. This stage is characterized by the fact that the normal tension σ is rapidly increasing. On further movement, the contact surface increases with the wood and the wood is pressed around the wedge to interrupt. In the bent portions of the cut, potential energy is accumulated (Mikleš *et al*. 2004, Koreň 1983). Splited wood can also be used as input material for wood chip disintegrator, for made biomass fuel (Stochlová *et al*. 2019).

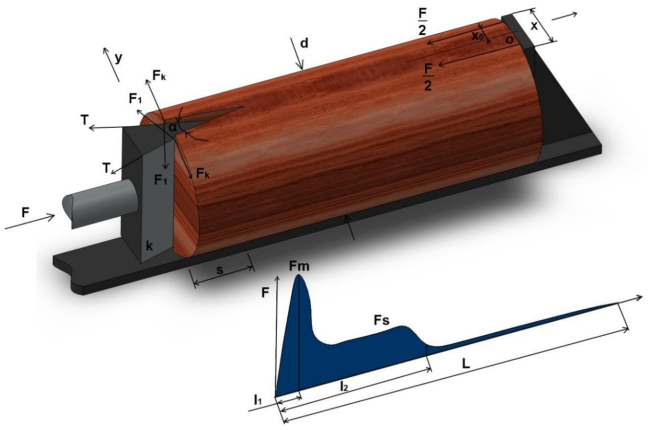

Fig. 1 Scheme of forces in the splitting process (Remper, Krilek, 2012)
k – splitting wedge, o – support, d – diameter of splitting log, L – splitting length, F – wedge pressure, α – wedge angle, Fm – maximum pressure, F1 – wedge pressure, Fk – splitting force , s – wedge path, x – support width, xo – support reaction points, l1 – wedge penetration length with maximum pressure, l2 – wedge penetration length with average pressure, Fs – average pressure

Obr. 1 Schéma pôsobenia síl v procese štiepenia
k – štiepací klin, o – opora, d – priemer štiepaného výrezu, L – dĺžka štiepaného výrezu, F – tlak na klin, α – uhol lícny klina, F_m – maximálny tlak, F1 – tlak lícny klina, F_k – sila spôsobujúca rozštiepnutie výrezu, s – dráha klina, x – šírka opory, x_o – ramená pôsobiska opornej reakcie, l_1 – dĺžka vniknutia klina s maximálnym tlakom, l_2 – dĺžka vniknutia klina s priemerným tlakom, F_s – priemerný tlak

When the wedge exceeds the distance l_1 at the expense of this energy, the wood begins to chop it by way of separating the fibers in the transverse direction near the blade edge. If there is sufficient potential energy in the bent portions, the cut begins to cut to the end. If this energy is inadequate, it is necessary to move the wedge further into the cut. The process of the cleavage process depends on the relationship of the thickness of the cut to its length (Štollmann *et al*. 2001, Kováč *et al*. 2017).

According to the splitting curve (Figure 1) it is obvious that the splitting force initially increases until the sides of the wood have reached sufficient potential energy, when the cleavage force begins to fall and the wood is cleaved by its own energy.

From the above it can be seen that the greatest forces of stress and deformation in the cleavage process arise at the onset of the cracks before the wedge. Hence, the blade itself plays an effective role only in the discovery of cracks and does not actually participate in other splitting processes. The depth of penetration of the wedge depends not only on the thickness to the length of the cut but also on the structure and physical state of the wood, the wedge angle, the support struts and other factors (Kováč *et al*. 2014, Marko *et al*. 2000, Jamaaoui *et al*. 2017).

The size of the cleavage force can be determined by the formula:

$$Fs = p \,.\, L \,.\, a_d \,.\, a_w \,.\, a_p \qquad [\mathrm{N}] \tag{1}$$

Where p is resistance of the splitting [N.cm^{-2}],
L is trunk length [cm],
d is trunk diameter [cm],
a_d, a_w, a_p is coefficients for influence of wood, moisture and support dimensions [-].

MATERIAL AND METHODS

Division of vertical log splitter:

By direction of movement of the splitting wedge:
- Horizontal,
- Vertical.

By drive:
- Powered by its own electric motor,
- Powered by hydraulic system of another machine.

By construction:
- Self-propelled (own self-propelled construction),
- Traffic (behind the tractor).

Scheme of vertical log splitter

Fig. 2 Vertical log splitter. (www.remab.sk)
1.transportation handle, 2. main beam, 3. control handle, 4. electro-hydraulic motor, 5. oil tank, 6. wheels, 7. splitting wedge, 8. clamping arms, 9. bottom table, 10. bottom beam, 11. base plate.

Obr. 2 Vertikálna štiepačka
1.transportná rukoväť 2. hlavný nosník, 3. ovládacia páka, 4. elektro-hydraulický motor, 5. olejová nádrž, 6. kolesá, 7. štiepací klin, 8. upínacie ramená, 9. spodný stôl, 10. spodný nosník, 11. základová doska.

The following parameters were chosen to examine the suitability of the use of the log splitters according to the technical parameters: splitting force, stroke of the cylinder due to the possibility of determining the height of the wood and the rate of splitting. The regression analysis will be used for evaluation. Regression analysis examines linear dependence between two quantitative variables and is a specific case of multiple regression. Simple regression estimates the regression coefficients β0 and β1 in the equation (Schmidtová and Vacek 2013):

$$y_i = \beta_0 + \beta_{1xi} + \varepsilon_i \tag{2}$$

Where y_i is the value of the dependent variable Y (criteria) in the i-th observation [-],
x_i is the value of the independent variable X (predictor) in this observation [-],
β_0 is the regression constant (the x-axis and regression line intersection) [-],
β_1 is regression coefficient (regression line directive) [-],
ε_i is a random error of observation [-].

The regression coefficient is interpreted depending on the type of research. In the case of the experiment (in which variable X is manipulated), it expresses how much the expected value of the variable Y increases when the value of the variable X is increased by 1 unit. In the case of an observation study, the coefficient is interpreted as the expected dif-

ference in the values of the Y variable of the two observations whose value of the variable X varies by one unit (Schmidtová and Vacek, 2013).

For research, a database file was created where 60 different types of log splitters are currently used in the world. They are listed ascending by manufacturer in Table 1. Due to the regression analysis it was possible to create a histogram of the results described in the article conclusion.

Table 1. Database file of log splitters
Tabuľka 1. Databázový súbor štiepačiek

Nr.	Manufacturer / title of log splitter	Splitting force (t)	Cylinder stroke (cm)	Speed of splitting (cm/s)	Nr.	Manufacturer / title of log splitter	Splitting force (t)	Cylinder stroke (cm)	Speed of splitting (cm/s)
1	Binderberger H12 eco Z	12	115	19	31	POSCH SpaltAXT 10	8	54	8
2	Binderberger H12 ss Z	12	115	25	32	POSCH SpaltAXT 10 Sp.	9,3	54	8
3	Binderberger H12 ss E	12	115	15	33	RABAUD F7 LOISIR	7	55	20
4	Binderberger H12 SE EZ	12	115	15	34	RABAUD F10 LOISIR	10	55	18
5	Binderberger H20 eco Z	20	115	15	35	RABAUD F13 LOISIR	13	55	18
6	Binderberger H20 ss Z	20	115	22	36	RABAUD F15 LOISIR	15	55	16
7	Binderberger H20 ss E	20	115	11	37	RABAUD F13 LOISIR	14	105	18
8	Binderberger H20 SE EZ	20	115	11	38	RABAUD F15 LOISIR	18	105	16
9	Binderberger H27 ss Z	27	115	16	39	RABAUD F12 MINI	12	55	22
10	Binderberger H27 SE E	27	115	11	40	RABAUD F 13 ECO	13	115	18
11	Binderberger H27 SE EZ	27	115	11	41	RABAUD F 14 ECO	14	115	16
12	Binderberger H33 ss Z	33	115	16	42	RABAUD F25	25	130	14
13	Binderberger H33 ss E	33	115	11	43	RABAUD F32	32	130	11
14	Binderberger H33 SE EZ	33	115	11	44	RABAUD F 15 FARMER	15	65	16
15	Lancman STX 13	13	117	15	45	RIKO UK THPLS7TP	7	104	16
16	Lancman STX 17	17	117	12	46	RIKO UK COLLA. 100 PI	10	150	32
17	Lancman STX 21	21	117	10	47	RIKO UK COLPRO. 12 PI	12	150	29
18	Lancman STX 22	22	117	11	48	RIKO IK UF Titanium 14	14	115	18
19	Lancman STX 26	26	117	13	49	RIKO IK UF Titanium 18	18	115	16
20	Pezzolato KING 20	20	112	22	50	RIKO IK UF Titanium 20	20	115	16
21	POSCH Hydro Combi 10	10	100	32	51	RIKO IK UF Titanium 25	25	115	13
22	POSCH Hydro Combi 13	13	100	23	52	RIKO UK UF BMF 14	13	115	17
23	POSCH Hydro Combi 16	16	100	19	53	Rosselli Apollo M	5	50	8
24	POSCH Hydro Combi 18	18	100	19	54	Rosselli Apollo T	5	50	16
25	POSCH Hydro Combi 20	20	100	22	55	Rosselli ECO 96 M	5	50	8
26	POSCH Hydro Combi 22	22	100	23	56	Rosselli ECO 96 T	5	50	16
27	POSCH Hydro Combi 24	24	100	18	57	Rosselli REX M	7	50	8
28	POSCH Hydro Combi 26	26	100	23	58	Rosselli REX T	7	50	16
29	POSCH SpaltAXT 6	6	54	5	59	Rosselli ECO 99 M	9	50	8
30	POSCH SpaltAXT 8	7,2	54	8	60	Rosselli ECO 99 T	9	50	16

Assuming the data is a random sample from the population, the regression coefficients and the correlation coefficient are calculated by the best point estimates of unknown parameters. In addition, hypotheses can be tested (the zero hypothesis that a coefficient equal to zero, expresses, that there is no relationship between the variables in the base file) and to construct their interval estimates. Hypothesis tests and interval estimates of regression coefficients assume that errors ei are independent of each other (which means that even yi are independent), normal division with an average of 0 and the same spread for all X values. Based on sample n observation of variables X and Y, the method of smallest squares estimates the unknown parameters β0 and β1 so that the sum of the second potency of the residues is minimal. The residue ei is the difference between the actual value of the dependent variable yi and the value calculated from the regression function by fitting the value xi (Schmidtová and Vacek 2013):

$$e_i = y_i - x_i \tag{3}$$

RESULTS AND DISCUSSION

By implementing the proposed methodology, histograms of dependence on splitting force and splitting speeds, histogram of the splitting force and stroke of the hydromotor, and histogram of hydromotor stroke and speed of splitting were created. Methods of 3D histograms depend on the author (Melicherčík and Krilek 2018).

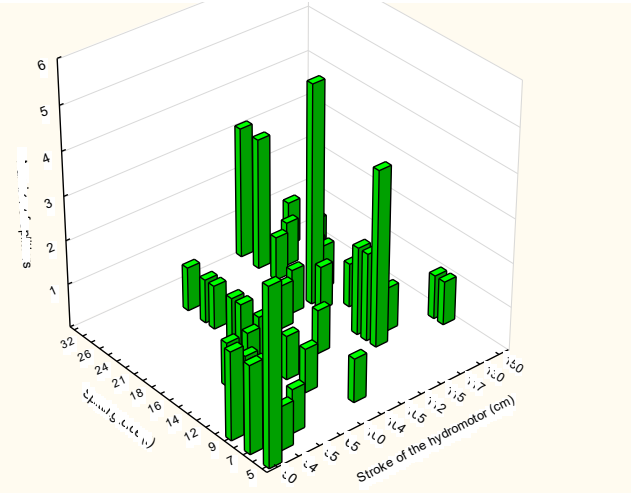

Fig. 3. Splitting force and cylinder stroke histogram

Obr. 3. Histogram početnosti štiepacej sily a zdvihu valca

From Fig. 3, it seems that manufacturers concentrate mainly on two production groups, with a splitting force of 5 to 12 tonnes with a cylinder stroke of 50 to 55 cm. The second area of the more powerful splitting machines with a splitting force of 14 to 25 tons with a cylinder stroke of 112 to 130 cm. We can also divide areas as low-power and high-performance splitting machines.

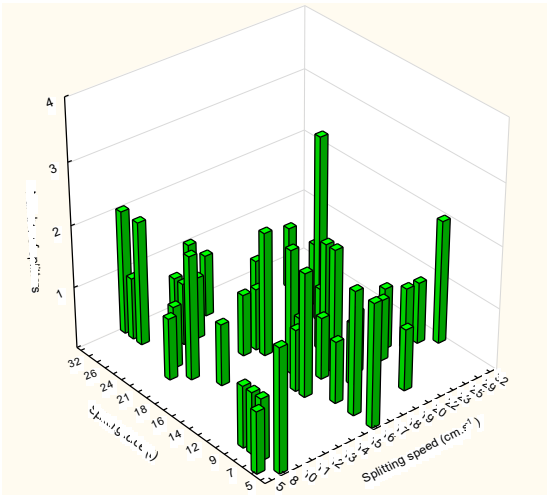

Fig. 4. Splitting force and splitting speed histogram
Obr. 4. Histogram početnosti štiepacej sily rýchlosti štiepania

It can not be clearly stated from Fig. 4 which combination of splitting power and splitting speeds prevails with manufacturers. However, it is clear that for low-power splitters with a splitting force of max. 12 t, the normal cutting rate is from 5 to 10 cm.s^{-1}. On other side high-performance, where the splitting speed can be 20 to 32 cm.s^{-1}.

In Fig. 5, occurrence rates are seen in the combination of cylinder stroke and splitting speed. It can be said that in low-power splitting machines where the cylinder stroke is up to 55 cm, the rate of splitting speed is in the range 5 to 10 cm.s^{-1}, but some reach a speed of up to 16 cm.s^{-1}. For high-performance splitting machines, the area is higher, the most widely used stroke is in the range 112 to 130 cm where the splitting speed is from 10 to 20 cm.s^{-1}.

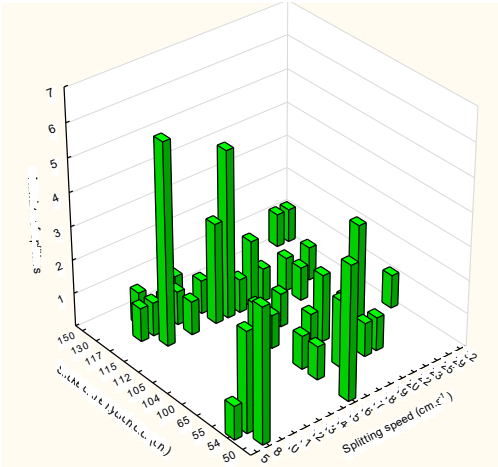

Fig. 5. Cylinder stroke and splitting speed histogram
Obr. 5. Histogram početnosti zdvihu valca a rýchlosti štiepania

The results were obtained by regression analysis in the STATISTICA 12 software, which also enabled the 3D histogram shown above.

CONCLUSION

In the current modern times, when it is a tendency to make work easier and to try to replace human work by mechanical automatization, a large number of manufacturers are emerging on the market producing machines designed for the same business.

The purpose of the article is to make the offered splitting machines available to end--users from various world manufacturers. In the article, 60 pieces of different log splitters from different manufacturers were selected. A database file has been created for all the log splitters, which contains the parameters for each base pump.

The output of the article is that the splitter makers focus mainly on two groups of splitters, which we can also designate as high and low power log splitters. Low power splitters work most often with a splitting force of 5 to 12 t when lifting the cylinder from 50 to 55 cm and cutting speed from 5 to 10 $cm.s^{-1}$. High-performance splitters work most often with a splitting force of 14 to 25 t when lifting the cylinder from 112 to 130 cm and cutting speeds from 20 to 32 $cm.s^{-1}$.

REFERENCES

JAMAAOUI, A., POP, O., DUBOIS, F. 2017. Wedge splitting test on douglas genotypes using an integrated mixed-mode approach. In *Theoretical and applied fracture mechanics*, pp 44-51. ISSN: 0167-8442. 2017.

KOREN. J. 1983. *Beztrieskové rezanie dreva. Vedecké* a *pedagogické aktuality.* 1. vyd. Zvolen: Technická Univerzita vo Zvolene, 1983. 105 p. č.6/1983.

KOVAC, J., KRILEK, J., JOBBAGY, J., DVORAK, J. 2017. *Technika* a *mechanizácia* v *lesníctve*. 1. vyd. Zvolen: Technická Univerzita vo Zvolene, 2017. 354 p. ISBN 978-80-228-3021-8.

KOVAC, J., KRILEK, J., KUCERA, M., BARCIK, S. 2015. The impact of design parameters of a horizontal wood splitter on splitting force. In *Drvna industrija*, vol. 65, no. 4 pp 263-271. ISSN: 0012-6772. 2015. DOI: 10.5552/drind.2014.1335

KRILEK J., REMPER M. 2012. Vplyv tvaru štiepacieho klina na proces štiepania, In Chip and chipless woodworking processes. *The 8th international science conference*, September 6-8, 2012, Technical University in Zvolen, 2012, pp. 205-210.

MARKO. J., HOLIK. J. 2000. Teória delenia dreva, Vedecké studie 1. vyd. Zvolen: Technická Univerzita vo Zvolene, 2000, 66 p. ISBN 80-228-0891-1.

MELICHERČÍK, J., KRILEK, J., 2018: Analýza technických parametrov harvesterových hlavíc v lesníctve = Analysis of technical parameters of harvester heads in forestry. In Kolokvium ku grantovej úlohe č. 1/0826/15. Technická univerzita vo Zvolene, 2018. - ISBN 978-80-228-3128-4.

MIKLES, M. HOLIK, J. MIKLES. J. 2004. *Lesné stroje.* 1. vyd. Zvolen: Technická Univerzita vo Zvolene, 2004, 331 p. ISBN 80-228-1403-2.

MINARIK, M., HRICOVA, J. 2015. Log splitter design and construction. In *Drvna industrija*, vol. 66, no. 1, pp 11-16. ISSN: 0012-6772. DOI: 10.5552/drind.2015.1349

SCHMIDTOVÁ, J., VACEK, V. 2013. *Applied statistics*. Technical University in Zvolen, 2013. 139 p. ISBN 978-80-228-2496-5

STOCHLOVÁ, P., NOVOTNA, K., COSTA, M., RODRIGUES, A. 2019. Biomass production of poplar short rotation coppice over five and six rotations and its aptitude as a fuel. In *BIOMASS & BIOENERGY*, pp 183-192. ISSN: 0961-9534. 2019.

STOLLMANN, V., MIKLES, M. 2001. *Lesnícke mechanizačné prostriedky.* 1. vyd. Zvolen: Technická Univerzita vo Zvolene, 2001, 285 p. ISBN 80-228-0998-5.

Contribution has been prepared within the solving of scientific grant project VEGA project no. 1/0642/18 "Analysis of the impact of structural parts of forestry mechanisms in the forest environment in terms of energy and ecology".

Corresponding author:
Ján Kováč, tel. +421 45 5206 517, E- mail: jan.kovac@tuzvo.sk

USING ECOLOGICAL MATERIALS FOR BINDING AMMONIA AND CERTAIN GREENHOUSE GASES IN PROCESS OF PIGS FATTENING

VYUŽITIE EKOLOGICKÝCH MATERIÁLOV NA VIAZANIE AMONIAKU A VYBRANÝCH SKLENÍKOVÝCH PLYNOV VO VÝKRME OŠÍPANÝCH

Štefan Boďo [a)], Roman Gálik [b)]

Department of Building Equipment and Technology Safety, Faculty of Engineering, Slovak University of Agriculture in Nitra, Tr. A. Hlinku 2, 949 76 Nitra, Slovakia
email: [a)] stefan.bodo@uniag.sk, [b)] roman.galik@uniag.sk

ABSTRACT: In this article we focus on the possibility of using environmentally friendly materials applied to the floor in the process of pigs fattening to reduce ammonia and selected greenhouse gases. We focused on the possibility of reducing the production of CO_2, N_2O and NH_3 by zeolite. It has been applied in recommended dose according to the seller's instruction on the floor in the hall after its cleaning process. From the results obtained it was indicated, that the temperature and the relative humidity affects production of CO_2 and N_2O. By zeolite application, we had observed a statistically significant difference in CO_2 and N_2O reduction in hall treated with zeolite and in the hall without treatment ($0.002 < 0.05$). In the case of NH_3 production, we did not notice any decrease in the production of harmful substances after the application of zeolite ($0.98 > 0.05$).

Keywords: zeolite, pig fattening, ammonia, greenhouse gases, reduction

ABSTRAKT: V tomto príspevku sa zaoberáme možnosťou využitia ekologických materiálov aplikovaných na podlahu vo výkrme ošípaných na redukciu amoniaku a vybraných skleníkových plynov. Zamerali sme sa na možnosť zníženia produkcie CO_2, N_2O, NH_3 pomocou zeolitu. Aplikovaný bol v odporúčanej dávke predajcom na podlahu kotercov v hale po ich vyčistení. Z dosiahnutých výsledkov vyplýva, že teplota a relatívna vlhkosť majú vplyv na produkciu CO_2 a N_2O. Použitím zeolitu sme zaznamenali štatisticky významný rozdiel zníženia produkcie CO_2 a N_2O v hale ošetrenej zeolitom a hale bez ošetrenia ($0,002 < 0,05$). V prípade produkcie NH_3 sme nezaznamenali zníženie produkcie škodlivých látok v hale s použitím zeolitu($0,98 > 0,05$).

Kľúčové slová: zeolit, výkrm ošípaných, amoniak, skleníkové plyny, redukcia

INTRODUCTION

Pig's production is quite a risky business for farmers. The risk of pig plague from neighbouring states, low ransom prices, outdated technology and lack of funds to build new buildings cause that many farms end with pigs breeding. GHG production in live-

stock farming results in emission charges. About 20 to 35 % of greenhouse gas emissions come from agriculture (IPCC 2001). According to the European Environment Agency (2010), pigs breeding in Europe represents almost 25 % of livestock emissions. GHG such as carbon dioxide (CO_2) and nitrous oxide (N_2O) are involved in global warming and climate change (IPCC 2007). Air pollution is the third biggest threat to our planet following the loss of biodiversity and climate change. Global concentrations of those two most important greenhouse gases have increased significantly over the last 150 years (IPCC, 2001) and affect environment - increased greenhouse gas emissions (Zavattaro et al. 2012). Those gases come also from livestock farms, where it is used straw as a litter (Brown et al. 2001; Freibauer & Kaltschmitt 2001). The nitrous oxide warming potential is 290 to 310 times higher than the carbon dioxide warming potential (IPCC 2007). Usually, it can be estimated that the carbon dioxide produced livestock are compensated by photosynthesis of plants used as feed (Philippe et al. 2011). Carbon dioxide emissions differ from the breeding, weaning and fattening systems of pigs (Dubeňová et al. 2011; Dubeňová et al. 2013; Philippe et al. 2007a; Philippe et al. 2007b; Cabaraux et al. 2009). The main producer of CO_2 is production and animals. Manure removal methods affect the production of harmful gases in pig fattening (Mihina et al. 2011). The process of releasing GHG into the atmosphere depends on methods of livestock farming, nutrition, manure processing, its storage and application into the soil (Palkovičová et al. 2009). Number and weight of animals, method and time of manure removal, temperature in the object, humidity, pH reaction of litter, C : N ratio, type and performance of the ventilation system significantly affect the gas concentration in the stable (Topisirovic et al. 2010; Topisirovic et al. 2010b). Many factors must be considered for successful emission assessment, including seasonal time, quantity and depth of litter, animal density, type of floor and its area, feeding and watering procedures, ventilation, temperature and relative humidity (Brouček 2018). Changing the management of pigs manure from liquid systems to solid-liquid separation systems, along with mitigation measures, could simultaneously reduce greenhouse gas emissions (Wang et al. 2017). Thus, the emissions of gas from farm buildings depend on breeding technology (Cabaraux et al. 2009). However, there is also the possibility to reduce the production of greenhouse gases by biological additives (Jelinek et al. 2004). As reported by Galajda et al., it is appropriate to use zeolite bio-filters for greenhouse gas elimination and ammonia. Likewise Zeocem company, recommends using zeolite for adsorption of ammonia. Biotechnology additives secure the bonding of ammonia emission in excrements which results into the prevention of ammonia nitrogen release in the environment (Švenková 2007).

MATERIAL AND METHODS

On the farm for pig fattening we tried natural mineral zeolite. It is used for cleaning of natural and other gases from CO_2, N_2O H_2S, SO_2 and NH_3. The seller recommends to apply the amount of 10 % from the amount of consumed feed. The measurements we made on a farm with fattening pigs hall, which one consist from two parts, whereby each part had ten stalls. Due the fact that measurement took place in winter time, the windows were closed, as well as all the doors. The air has been exchanged by natural ventilation through a chimney in the roof of the hall. During feed establishment and cleaning processes the

fans support the air ventilation from hall. After the treatment, the hall was closed and the fans turned off to keep the temperature in hall. We applied 150 kg of zeolite into one part of the hall for two weeks in average 1.2 kg of zeolite on stall per day. Preferably, the zeolite has been applied to the places from which the excrement has been removed. Subsequently, we measured the values of pollutant production. In the first part of the hall, where we did not apply zeolite, was placed 72 pigs with an average live weight of 85kg. In the second part of the hall, where we applied zeolite, was 89 pigs with average live weight of 40kg. During 24 hours we monitored the pollutant concentration as well as its quantity emitted. For the measurement of CO_2 emissions, N_2O and NH_3, we used INNOVA 1412 gas analyser and INNOVA 1309 multi-point sampler with Comet temperature recording device. Both devices have been monitored from inside and outside. The data have been processed using the MS Excel statistical program. Significance level $\alpha = 0.05$.

RESULTS AND DISCUSSION

When monitoring the CO_2 concentration in the hall without treatment, we recorded an average concentration of 4510.4 $mg.m^{-3}$. Measured and calculated values for CO_2 are in the Table 1. When monitoring the CO_2 concentration in the hall with a zeolite applicate we recorded an average concentration of 3890 $mg.m^{-3}$.

Table 1. Measured and calculated values CO_2
Tabuľka 1. Namerané a vypočítané hodnoty pre CO_2

Measuring	Air velocity[1)] ($m.s^{-1}$)	Applied Agent[2)]	Temperature (°C)[3)]	Relative air humidity[4)] (%)	Average concentration of CO_2[5)] ($mg.m^{-3}$)	Emission factor CO_2[6)] (kg CO_2/animal place/year)
No. 1 -	0.464	Untreated	14.9±1.9	61.8±5.5	4510.4 ±1529.9	719.1
No. 2 -	0.648	Zeolite	14.1±2.35	63.5±6.5	3890.0 ±1330.3	701.6

Rýchlosť prúdenia vzduchu, [2)] Aplykovaná látka, [3)] Teplota, [4)] Relatívna vlhkosť, [5)] Priemerná koncentrácia, [6)] Emisný factor

This is, for example to compare, between a part of the hall without treatment and part of the hall with treatment is a statistically significant difference in CO_2 concentration ($P < a$; $0.00 < 0.05$). Figure 1 shows the temperature course outside, in hall treated with zeolite and in hall without treatment. When comparing the effect of temperature on CO_2 concentration without treatment, as well as with usage of zeolite was recorded statistically is significant difference ($P < a$; $0.00 < 0.05$). When comparing the temperature in hall treated with zeolite treatment statistically is significant difference ($P < a$; $0.00 < 0.05$).

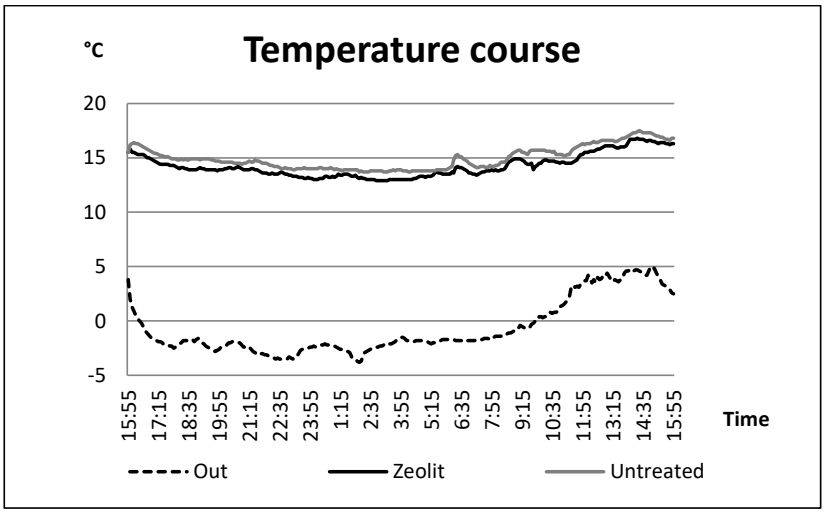

Fig. 1. Outdoor temperature, in the hall treated with and without zeolite
Obr. 1. Priebeh teploty vonku, v hale ošetrenej zeolitom a neošetrenej hale

When comparing the effect of relative humidity on the concentration of CO_2 without and with the application of zeolite we can see statistically significant difference ($P < a$; $0.00 < 0.05$). When comparing the relapsing course humidity hall is also an statistically significant difference ($P < a$; $0.00 < 0.05$). Figure 2 shows the relative humidity course during outdoor measurements.

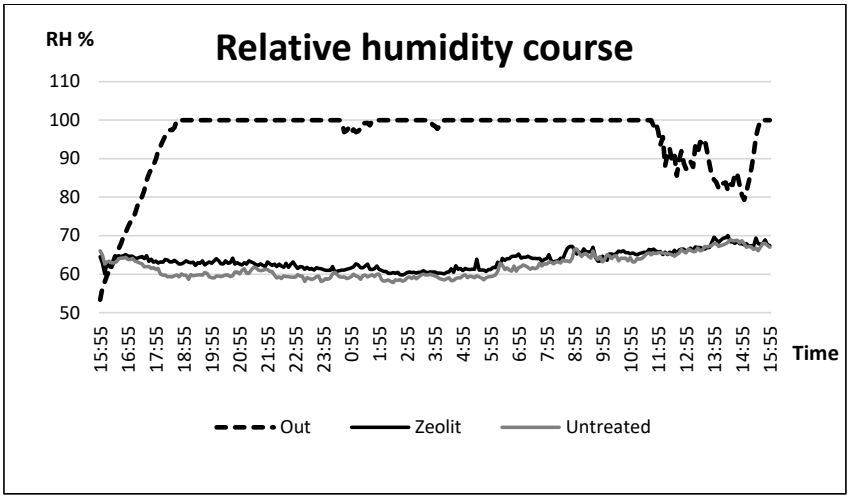

Fig. 2. Outdoor air humidity, treated in the hall with and without zeolite
Obr. 2. Priebeh relatívnej vlhkosti vzduchu vonku, v hale ošetrenej zeolitom a v neošetrenej hale

We observed N_2O production without zeolite in average of 3.0 mg.m^{-3} and with zeolite the value was 2.57 mg.m^{-3}. Measured and calculated values for N_2O are listed in Table 2. between the hall without and with the zeolite applied. There is a statistically significant difference in concentration of N_2O ($P < a$; $0.00 < 0.05$). When comparing the effect of temperature on the concentration of N_2O without zeolite is statistically significant difference ($P < a$; $0.00 < 0.05$) as well after the zeolite application is significant difference ($P < a$; $0.00 < 0.05$). When comparing the effect of relative humidity on concentration of N_2O without and with zeolite applied, was recorded statistically significant difference ($P < a$; $0.00 < 0.05$).

Table 2 Measured and calculated values of N_2O
Tabuľka 2 Namerané a vypočítané hodnoty pre N_2O

Measuring	Air velocity (m.s^{-1})	Applied agent	Temperature (°C)	Relative air humidity (%)	Average concentration of N_2O (mg.m^{-3})	Emission factor N_2O (kg N_2O/animal place/year)
No. 1 -	0.464	Untreated	14.9±1.9	61.8±5.5	3 ±1.28	0.48
No. 2 -	0.648	Zeolite	14.1±2.35	63.5±6.5	2.6 ±1.4	0.47

The measurement of NH_3 production in hall without zeolite, the average value was 4.2 mg.m^{-3}, with zeolite treatment the average value was 4.1 mg.m^{-3}. Measured a calculated values for NH_3 are given in Table 3. Between the hall without treatment and with zeolite treatment hall there is statistically no significant difference in production NH_3 ($P < a$; $0.98 > 0.05$). When comparing the effect of temperature on the production of NH_3 without treatment we have not seen statically significant difference ($P > a$; $0.87 > 0.05$), but with treatment, we recorded statistically significant difference ($P < a$; $0.002 < 0.05$). When comparing the effect of relative humidity on production NH_3 without treatment, as well as with treatment we have not seen statistically significant difference ($P > a$; $0.78 > 0.05$, $P > a$; $0.49 > 0.05$).

Table 3 Measured and calculated values of NH_3
Tabuľka 3 Namerané a vypočítané hodnoty pre NH_3

Measuring	Air velocity (m.s^{-1})	Applied agent	Temperature (°C)	Relative air humidity (%)	Average concentration of NH_3 (mg.m^{-3})	Emission factor NH_3 (kg N_2O/animal place/year)
No. 1 -	0.464	Untreated	14.9±1.9	61.8±5.5	4.2 ±3.6	0.67
No. 2 -	0.648	Zeolite	14.1±2.35	63.5±6.5	4.1 ±1.4	0.74

When testing the correlation between the qualitative attributes (CO_2 and temperature, CO_2 and relative humidity, N_2O and temperature, N_2O and relative humidity, NH_3 and

temperature, NH_3 and relative humidity), we observed a weak correlation coefficient in hall with and without zeolite treatment.

The results obtained indicate that the temperature and relative humidity affects production of CO_2 and N_2O. When using zeolite, we have noticed a statistically significant difference in CO_2 and N_2O reduction against the hall without treatment. In the case of NH_3 production, we did not notice a decrease in the production of harmful substances in hall with zeolite as reported by Galajda et al. (2000).

CONCLUSION

THE results show that the time effect of the zeolite on the hall floor plays an important role. We think it is important to measure the floor temperature in the hall, especially in winter months. The floor temperature is important for fermentation of NH_3. Our results have shown that by applying ecological materials on the floor, we can reduce the emitted amount of CO_2 or N_2O into the air. Zeolite is a natural rock with excellent physical properties mainly with high sorption capacity. In conclusion, this technology is characterized as a low investment and low operating costs compared to other reducing technologies.

REFERENCES

BROUČEK, J. 2018. Nitrous oxide release from poultry and pig housing. In *Polish Journal of Environmental Studies* Vol. 27, No. 2 (2018), p. 467-479.

CABARAUX, J.F. et al. 2009. Gaseous emissions from weaned pigs raised on different floor systems. In *Agriculture, Ecosystems and Environment* 130, p. 86–92.

DUBEŇOVÁ, M. et al. 2011. Vplyv hmotnosti ošípaných na koncentráciu amoniaku vo vybranom objekte počas zimného obdobia. *Technics in Agrisector Technologies 2011*: Proceedings of Scientific Works. FE SUA in Nitra, p. 20–24.

DUBEŇOVÁ, M.. et al. 2013. Ammonia concentration in farrowing pens with permanent limited range of motion for lactating sows. In. *Res. Agr. Eng*. 59,

Special Issue, p. 9–14.

GALAJDA, R. et al. 2000. Redukcia amoniaku z odvádzaného vzduchu z objektov ustajnenia zvierat [online]. [Cit. 2019-01-12]**.** Available on: <http://docplayer.net/39299133-Redukcia-amoniaku-z-odvadzaneho-vzduchu-z-objektov-ustajnenia-zvierat-reduction-of-ammonia-in-the-waste-air-from-animal-housings.html>.

HOUGHTON, J. T., et al. IPCC, 2001. (Eds.), Climate Change 2001: In: *The Scientific Background,* vol. 94. Cambridge University Press, Cambridge, UK.

IPCC, 2007. Climate Change 2007: The Physical Science Basic. In *Contribution of Working Group I to the Fourth Assessment Report of the Intergovernmental Panel on Climate Change.* Cambridge Univesity Press, Cambridge, United Kingdom/New York, NY, USA.

JELÍNEK, A. et al. 2004. Research of biological agents effects on reduction of ammonia concentration. In stables of intensive farm animals breeding. In *Res. Agr. Eng., 50*, 2004 (2): p. 43–53

MIHINA, Š. et al. 2011. Produkcia škodlivých plynov v objektoch pre výkrm ošípaných s rôznym spôsobom odstraňovania hnoja. In Rural buildings 2011: *Proceedings of Scientific Works. FE SUA* in Nitra. p. 84–92.

PALKOVIČOVÁ, Z. et al. 2009. Emissions of greenhouse gases and ammonia from intensive pig breeding. In *Folia Veterinaria* 53, s. 168–170.

PHILIPPE, F. X. et al. 2007a. Comparison of ammonia and greenhouse gas emissions during the fattening of pigs, kept either on fully slatted floor or on deep litter. In *Livestock Science* 111, p.144–152.

PHILIPPE, F.X. et al. 2007b. Gaseous emissions during the fattening of pigs kept either on fully slatted floors or on straw flow. In *Animal* 1, s. 1515–1523.

ŠVENKOVÁ,J., 2007. Znižovanie emisií škodlivín plynov úpravou technických a technologických systémov v chove hospodárskych zvierat. Autoreferát dizertačnej práce. Slovenská poľnohospodárska univerzita v Nitre. 20 p.

TOPISIROVIC, G., RADOJIČIC, D. & DRAŽIC, M. 2010a. Mogućnosti poboljšanja efektada rada ventilacionog sistema u odeljenjima prasilište i odgajalište na farmi svinja 'Farkaždin'. In *Poljoprivredna tehnika* 35, p. 5–16.

TOPISIROVIC, G., RADOJIČIC, D. & RADIVOJEVIC, D. 2010b. Predlog poboljšanja ambijentalnih uslov u objektima za tov svinja na farmi 'Vizelj'. In *Poljoprivredna tehnika* 35, p. 17–25.

ZAVATTARO, L. et al. 2012. Mitigation of environmental impacts of nitrogen use in agriculture. In *Agriculture, Ecosystems and Environment* 147, p. 1– 3.

WANG. Y. et al. 2017. Mitigating Greenhouse Gas and Ammonia Emissions from Swine Manure Management: A System Analysis. In *Environmental science & technology 2017 Apr* 18. 51(8), p. 4503-4511

www page of ZEOLIT Zeocem a.s., [online] [Cit.2019-03-12]. Mechanizmus účinku vlastností zeolitu [Cit. 2019-05-12]. Available on: <www.zeocem.com/sk/zeolit>.

Corresponding author:
Štefan Boďo, stefan.bodo@uniag.sk, tel: +421 37 641 5666

SIMULATION AND MANUFACTURING PREDICTION OF PRODUCTION LINE

SIMULÁCIA A PREDIKCIA VÝROBY VÝROBNEJ LINKY

Roman Bambura [a)], Miroslav Dado [b)], Erika Sujová [c)], Andrej Augustín

Department of Manufacturing Technology and Quality Management, Faculty of Technology, Technical University in Zvolen, Študentská 26, 960 01 Zvolen, Slovakia
email: [a)] bambura.r@gmail.com, [b)] dado@tuzvo.sk, [c)] erika.sujova@tuzvo.sk

ABSTRACT: The aim of this article is to simulate and analyse efficiency of production line with prediction of manufacturing for future production line. This research was performed as case study in production plant in Slovak company specialized in development and manufacturing of aluminium components for automotive. The simulation model of production line was created in Tecnomatix Plant Simulation software (TPS). The first simulation represents the current state of the production line. The second simulation represents production line prediction with reduced cycle times for RCX and RCY stations. From the results of the second simulation we can state that there was an increase in production from 4241 castings to 5267 castings, but the proportion of defective castings is up to 82.3% compared to 7.3 % in the first simulation. This situation was caused by the blocking of the RCY station and the late removal of the castings by the conveyor before cooling to the FC station. This situation was solved in the third simulation by adding a conveyor in front of the cooling tunnel to remove the castings with suitable temperature for direct supply to the FC station. This optimization reduced RCY blocking by 34.14 % and also increased production from 5267 castings to 6909 castings, with a percentage reduction of defective castings from 82.3 % to 27 %.

Key words: simulation model, production line, Industry 4.0

ABSTRAKT: Cieľom tohto príspevku je simulovať a analyzovať efektívnosť výrobnej linky s predikciou výroby pre budúcu výrobnú linku. Tento výskum bol realizovaný ako prípadová štúdia vo výrobnom závode v slovenskej spoločnosti špecializujúcej sa na vývoj a výrobu hliníkových komponentov pre automobilový priemysel. Simulačný model výrobnej linky bol vytvorený v softvéri Tecnomatix Plant Simulation (TPS). Na základe dát a faktov o výrobnom procese boli vytvorené 3 simulácie. Prvá simulácia reprezentuje súčasný stav výrobnej linky. Druhá simulácia reprezentuje predikciu výrobnej linky s redukovanými cyklovými časmi pre stanice RCX a RCY. Z výsledkov druhej simulácie môžeme pozorovať nárast výroby z 4241 odliatkov na 5267 odliatkov, avšak podiel chybných odliatkov je až 82,3 % oproti 7,3% v prvej simulácii. Táto situácia bola zapríčinená blokáciou pracoviska RCY a nevčasným odoberaní odliatkov dopravníkom pred ich vychladením pre stanicu FC. Táto situácia bola vyriešená v tretej simulácii pridaním dopravníka pred chladiaci tunel na odoberanie odliatkov s vhodnou teplotou pre priame zásobovanie FC stanice. Táto optimalizácia znížila blokovanie stanice RCY o 34,14 % a takisto sa zvýšila produkcia z 5267 odliatkov na 6909 odliatkov a s percentuálnym znížením počtu chybných odliatkov z 82,3 % na 27 %.

Kľúčové slová: simulačný model, výrobná linka, Priemysel 4.0

INTRODUCTION

With ever evolving digitalization of industries, optimization of the production processes in currently one of the most common optimization tasks in production (Alavi & Habek, 2016). The company must work in such a way that the input-output transformation proceeds with the optimal consumption of production inputs, the optimal choice of production processes, resources and optimal utilization of production capacity (Simanova & Gejdos, 2016). For such an optimization of production processes, companies often use simulation software to create simulation models of a production line. The simulation model can be characterized as a system that mimics the actual idea of the simulated system and its movement wth defined objects, configurations and sequences identical to physical world (Gregor et al., 1992). Therefore, simulation is an efficient tool for planning, operating and evaluating manufacturing systems. Estimation of simulation model complexity provides several advantages in the planning phase of a simulation project (Popovics & Monostroni, 2016). Tecnomatix Plant Simulation (TPS) is the simulation software that enables to create production system models to help user define system characteristics and optimize performance. Various scenarios of future production system and processes can be simulated without disturbing existing production with biggest advantage to be able to use them in the planning process long before the changes are introduced into the production process. The simulation provides the information needed for quick and reliable decisions in the initial stages of production planning. In addition, TPS allows to optimize material flow, resource utilization, and logistics for levels of production plant planning, through local plans to specific lines (TPS, 2019).

Development in the industry is aimed to improve the production processes from automation to digitization. The latest trend in businesses is implementation of the Industry 4.0 strategy, which predicts the future development of digital production. Many authors deal with the characteristics and the definition of the concept of Industry 4.0 (Sujová et al. 2019). The trend and the current challenge for businesses is the Industry 4.0 concept aimed at digitizing all business processes (Sujová et al., 2018).

Bauer et al. (2014) defined Industry 4.0 as intelligent real-time, horizontal and vertical integration of humans and machines with objects and information and communication technology systems to enable a flexible and dynamic management of complex systems. Industry 4.0 philosophy and the associated method of digital factory require a wide range of tasks and skills to be managed for their successful application and efficient operating. One of the key competencies for their reliable operation is mastering computer simulation of various processes that take place within the enterprise (Neradilova & Fedorko, 2017). Programmable logic controllers (PLC) and programmable platforms are often used for data collection which are necessary for simulation model to represent real production (Kosa et al., 2019).

MATERIAL AND METHODS

Simulation model of production line was created in TPS software which environment represents effective method to solve our research needs and allows to analyse production process efficiency. First step for simulation model creation is to obtain relevant data about

production line and production processes. Deductive approach was used for creation of the simulation model. Chosen method is based on multilevel modelling. Firstly, we created simulation model of real production line which represent present state of production line. Secondly, production line was optimized with addition of conveyor belt.

Production line can be divided into 3 parts. First part represents Casting line (CL), second part is Conveyor (CO) between CL and Fettling line with cooling system (FC) which represent third part of simulation model.

The casting line consists of two RC X and RC Y casting lines and two robots, conveyors and a robot to move pieces from conveyors from casting lines to a conveyor carrying castings to the elevator. RC X and Y have the same cycle times, availability and same production plan and maintenance time. After casting, the castings go to the removal site where the casting number and casting time are saved to the table. From the casting line robot picks and place casting to the conveyor where the castings are cleaned. Subsequently, the robot transfers them to a conveyor connected with the elevator.

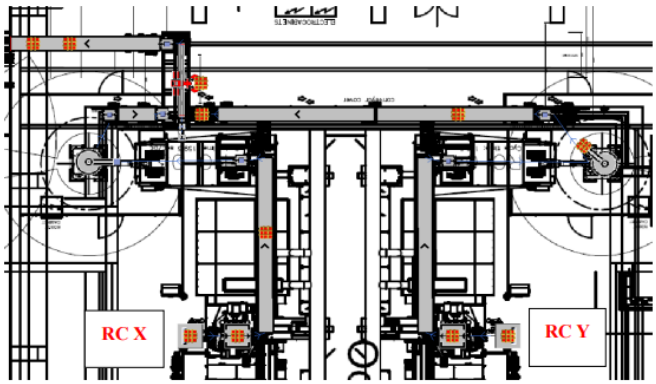

Fig. 1. Casting line simulation
Obr. 1. Simulácia odlievacej linky

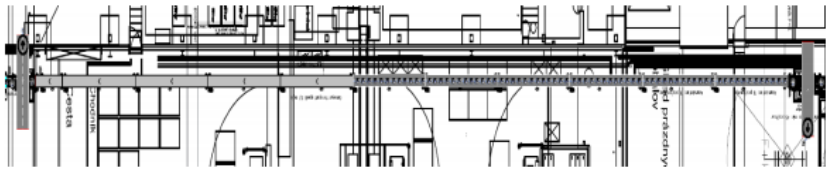

Fig. 2. Simulation of conveyor between CL and FC
Obr. 2. Simulácia dopravníka medzi CL a FC

We used the TransferStation to load and unload the elevator parts with fixed loading and unloading time and loading and unloading position.

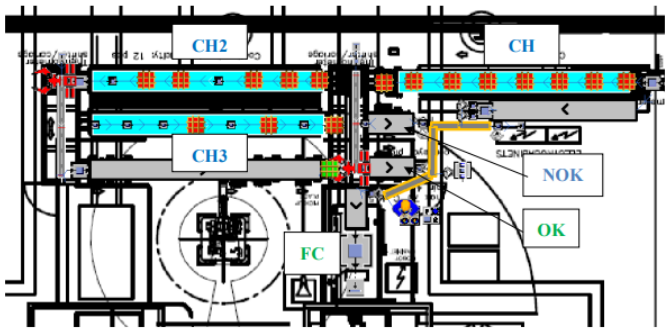

Fig. 3. Simulation of fettling line with cooling system
Obr. 3. Simulácia apretačnej linky s chladiacim systémom

Cooling system is set with the same cooling time. The robot is programmed to wait for the first cooling system. When the casting is lifted by robot, the location is determined, and casting will change colour based on its temperature. The red castings have a temperature above 80 °C and continue to the next tunnel. Castings with a temperature between 35-80 °C have a green colour and the robot carries them to the OK conveyor. Castings below 35 °C are blue, the robot stores them to NOK (not OK) conveyor.
Input data for simulation model:

- Casting line RCX and RCY
  - Cycle time – 166-184 s,
  - Availability – 85 %,
  - Maintenance time – 25 min,
  - Production plan (Figure 4).

	Shift	From	To	Mo	Tu	We	Th	Fr	Sa	So	Pauses
1	Shift-1	6:00	14:00	☑	☑	☑	☑	☑	☐	☐	
2	Shift-2	14:00	22:00	☑	☑	☑	☑	☑	☐	☐	
3	Shift-3	22:00	6:00	☑	☑	☑	☑	☑	☐	☐	

Fig. 4. Production plan for RCX CL and RCY CL
Obr. 4. Plán výroby pre RCX CL a RCY CL

- Fettling line with cooling system
  - Cycle time – 30 s,
  - Availability – 72 %,
  - Maintenance time – 20 min,
  - Production plan (Figure 5).

	Shift	From	To	Mo	Tu	We	Th	Fr	Sa	So	Pauses
1	Shift-1	6:00	14:00	☑	☑	☑	☑	☑	☑	☐	9:05-9:35
2	Shift-2	14:00	22:00	☑	☑	☑	☑	☑	☐	☐	17:05-17:35
3	Shift-3	22:00	6:00	☑	☑	☑	☑	☑	☐	☐	1:05-1:35

Fig. 5. Production plan for FC
Obr. 5. Plán výroby pre FC

- Transportation
  - Conveyor speed – 0,1 $m.s^{-1}$,
  - Step rate of conveyors and cooling tunels – 80 s,
  - Elevator speed – 0,2 $m.s^{-1}$,
  - Robot speed – 0,2 $m.s^{-1}$.

RESULTS

The aim of our research is to analyse production line efficiency with simulation method and subsequently with addition of other components predict future production data for production line. Simulation analysis provides information about machines and production processes behaviour and efficiency presented in tables or graphs.

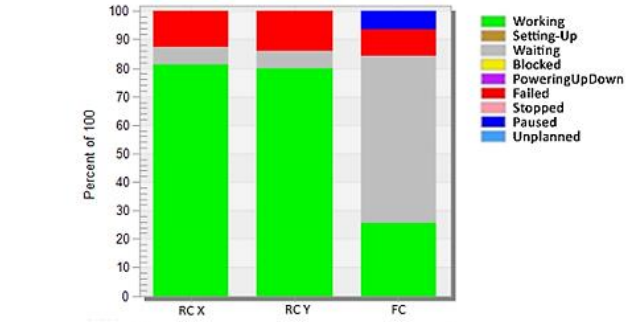

	RC X	RC Y	FC
Working	81,11%	79,92%	25,60%
Setting-up	0,00%	0,00%	0,00%
Waiting	6,24%	6,24%	58,83%
Blocked	0,00%	0,00%	0,00%
PoweringUpDown	0,00%	0,00%	0,00%
Failed	12,64%	13,84%	9,32%
Stopped	0,00%	0,00%	0,00%
Paused	0,00%	0,00%	6,25%
Unplanned	0,00%	0,00%	0,00%

Fig. 6. Efficiency analysis of real production line
Obr. 6. Analýza efektívnosti skutočnej výrobnej linky

Working, Setting-up, Waiting, Blocked. PoweringUpDown, Failed, Stopped, Paused and Unplanned times are shown in Figure 6 as percentages of overall process time. Results shown that most efficient workstation is RCX with 81,11 %. FC workstation has lowest

efficiency with 25,6 % of working time which is caused by waiting for castings at 58.83 % of overall process time. Total amount of produced castings was 4241 with 3932 OK castings and 309 NotOk castings.

First manufacturing prediction of production line was done with reduction of cycle times of RCX and RCY by half. This reduction essentially allows to simulate future production with four CL.

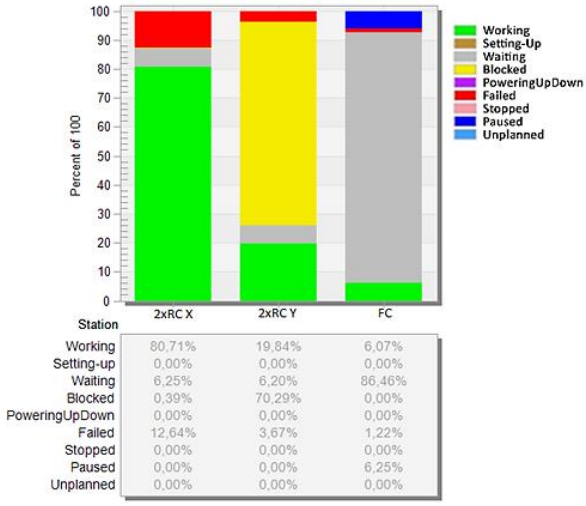

Fig. 7. Efficiency analysis with reduced cycle times
Obr. 7. Analýza efektívnosti pri znížení cyklových časov

The RCY casting line is blocked 70,29 % of overall process time. This is due to the shorter conveyor and the priority of removing castings from the conveyor for RCX casting line. The FC finishing line waiting time represents 86,46 % of overall process time which is more than in the first variant because the conveyor is unable to remove castings before they cool, so the FC has nothing to process. Total production amount is not ideal because of occurred blockage at RCY line. Total amount of produced castings was 5267 with 932 OK castings and 4335 NotOK castings.

Second optimization was done by addition of output conveyor to the front of first cooling tunnel to remove castings that have a suitable temperature. This conveyor will enable to supply FC line directly. Also step rate of conveyor between CL and FC was reduced by half to the 40 second step rate to ensure sufficient cooling time for castings. Production plan was modified by removing breaks at FC line with use of inverters.

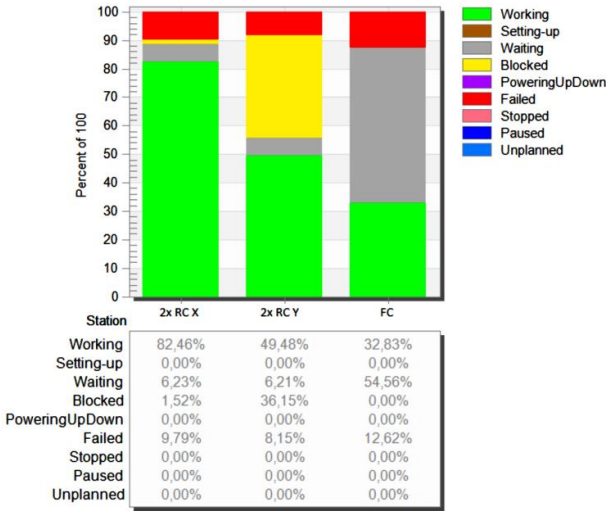

Fig. 8. Efficiency analysis with added conveyor
Obr. 8. Analýza efektívnosti pri pridaní dopravníka

It can be seen from Figure 8 that the blocking of the RCY casting line was reduced by half compared to variant 2. High blockage occurs when the FC line fails when the conveyor is filled. The efficiency of FC line has been increased compared to variant 2 due to increased throughput of the conveyor and due to removing the castings before cooling. Also, total production was increased to 6909 casting with 5042 Ok castings and 1867 NotOk castings.

CONCLUSION

The use of simulation as a tool that can transfer ideas into the real world is increasingly being used in Slovak companies. Many manufacturers have understood that it is better to develop a simulation model for the anticipated manufacturing process at the stage of project development, which reveals both the strengths and weaknesses of the project. By doing so, the original idea of the project can be further developed up to the final stage with recommendations to optimize the production process.

Based on the facts obtained about production process in the company, three simulations were conducted. First simulation represents real state of production line with two CL, second simulation represents future state of production with four CL and third simulation represents optimization for second simulation with conveyor addition. The simulation model shows that the current conveyor line will not be sufficient to expand production from two CL to four CL. We have found that the biggest problem is the cooling of castings during the finishing line where the castings remain on the conveyor for longer time. During failure, castings that are cooled on the upper floor and are blocked. After the fault has been removed, castings must pass through at least one cooling tunnel, even if their temperature is within the desired range. We removed this problem by adding a conveyor

in front of the first thermometer to measure the temperature before the first cooling tunnel, where the castings can be taken out if they are at a suitable temperature. The proposed solutions will find application in the final solution of the conveyor line by engaging four CL, increasing throughput and reducing CL blockage.

ACKNOWLEDGMENT

Contribution has been prepared within the solving of scientific grant project IPA 5/2019 project „Simulation of production processes with digital manufacturing tools".

LITERATURE

ALAVI, H., HABEK, P. 2016. Optimizing outcome in the university – industry technology transfer projects. Management Systems in Production Engineering. Vol. 22, 2016, No.2. pp. 94 – 100.

BAUER, W., SCHLUND, S., MARRENBACH, D., GANSCHAR, O. Industrie 4.0 – Volkswirtschaftliches Potenzialfür Deutschland. Studie. 2014. [online] [12.02.2019]. Available at: https://www.produktionsarbeit.de/content/dam/produktionsarbeit/de/documents/Studie-Industrie-4-0--Volkswirtschaftliches-Potential-fuer-Deutschland.pdf

GREGOR, M., KOSTURIAK, J., STRYCEK, P., REBETAK, J. 1992. Simulation of systems, Zilina, UNIZA. ISBN 80-7100-068-X15

KÓSA, L., KIŠEV, K., BALÁŽI, J., VACHO, L., OLEJÁR, M. 2019. Communication between a PLC and a Raspberry PI via openpowerlink. ACTA Facultatis Technicae, 24, 2019, pp. 17 – 26. ISSN 1336- 4472

NERADILOVA, H., FEDORKO, G. 2017. Simulation of the supply of workplaces by the AGV in the digital factory. TRANSCOM 2017: International scientific conference on sustainable, modern and safe transport. Procedia Engineering. 2017, pp. 638 – 643, DOI: 10.1016/j.proeng.2017.06.110.

POPOVICS, G., MONOSTORI, L., 2016 An approach to determine simulation model complexity. Procedia CIRP, Vol. 52, 2016, pp. 257–261. DOI: https://doi. org/10.1016/j.procir.2016.07.072

SIMANOVA L., GEJDOS, P. 2016. The process of monitoring the quality costs and their impact on improving the economic performance of the organization. Enterprise Management, Vol. 3, 2016, pp. 172 – 179.

SUJOVÁ, E., STŘIHAVKOVÁ, E., ČIERNA, H. 2018. An Analysis of the Assembly Line Modernization by Using Simulation Software. Manufacturing Technology. 18. pp. 839-845. DOI:10.21062/ujep/187.2018/a/1213-2489/MT/18/5/839.

SUJOVÁ, E., ČIERNA, H., ŻABIŃSKA, I. 2019. Application of Digitization Procedures of Production in Practice. Management Systems in Production Engineering. 27. pp. 23-28. DOI: 10.1515/mspe-2019-0004.

TPS. Tecnomatix Plant Simulation, [online] [09.07.2019]. Available at: http://4dsysco.com/siemens-plm/tecnomatix/tecnomatix-plant-simulation

Corresponding author:
Roman Bambura, +421 949 823 463, e-mail: bambura.r@gmail.com

VIBRATION MONITORING AND DIAGNOSTICS OF ROLLINGS BEARINGS

MONITOROVANIE VIBRÁCII A DIAGNOSTIKA VALIVÝCH LOŽÍSK

Silvia Kopčanová [a], Marián Kučera [b]

Department of Mechanics, Mechanical Engineering and Design, Faculty of Technology, Technical University in Zvolen, Študentská 26 960 01 Zvolen
email: [a] kopcanova15@gmail.com, [b] kucera@tuzvo.sk

ABSTRACT: Condition monitoring of machines is a very important part in the area of correct operation, because any failure or unplanned shutdown of the machine causes losses for production that need to be minimized. The article deals with vibration monitoring and diagnostics of rolling bearing that have been loaded in three modes. Describes the envelope method in vibrodiagnostics, measurement procedure and subsequent graphical comparison of measured results. Result of the measurement is that biggest mistake was in thirt regime (dry run) when was damaged inner race of the bearing.

Key words: load, diagnosis, failure, envelop analysis

ABSTRAKT: Monitorovanie stavu strojov je veľmi dôležitou súčasťou v oblasti správnej prevádzky, pretože každá porucha alebo neplánované odstavenie stroja spôsobuje straty na výrobe, ktoré je potrebné minimalizovať. Článok sa zaoberá monitorovaním vibrácií a diagnostikou valivých ložísk, ktoré boli zaťažené v troch režimoch. Popisuje obálkovú metódu vo vibrodiagnostike, postup merania a následné grafické porovnanie nameraných výsledkov. Výsledkom merania je, že najviac sa vibrácie prejavili v režime zaťaženom a chode ložiska na sucho, keď došlo k poškodeniu jeho vnútorného krúžku.

Kľúčové slová: zaťaženie, diagnostika, zlyhanie, obálková analýza

INTRODUCTION

A machine failure is a critical situation where the entire system that fails to build on the machine or its destruction can fail (Turis 2019). Therefore, it is important to pay attention to the area of equipment maintenance and its correct and timely diagnosis. Predictive maintenance is one of the main factors for maintaining and extending the life of equipment and components (Harvánek *et al*. 2019). Vibrodiagnostics is used as the most effective prevention in this area. Vibrodiagnostics consists of recording a time signal through sensors that are placed on a tracked object according to the appropriate standard and then analyzed and transformed into a frequency domain. In this part of the diagnostics there is an important step to the analysis of the results. Analysis and correct interpretation of

measured data play an important role in determining the actual condition of the equipment or its components. Many scientists around the world are addressing the areas of the right and most effective analysis, as the industry of diagnostics, prediction and maintenance has recently received increased attention as the shutdown of the machine is an undesirable phenomenon in the industry, generating considerable financial losses for the company.

Saruhan et. al. (2014) carried out the measurement of vibration of rolling element bearing (REB). For their experiment was used pair of bearing with one axis accelometers. Authors compared vibration analysis for four different defects states of REB (inner raceway defect, outer raceway defect, ball defect and combination of the bearing elements defect) with 2 load regime and two different speed. In their research presented, that the most effective techniques for condition monitoring of REB is vibration spectrum analysis.

Chebil et al. (2009) used a comparison of different techniques for the bearing monitoring. It was found that discrete wavelet transform based on time-frequency analysis achieved the best results.

Many of diagnosticians used for condition monitoring of bearings their characteristic defect frequencies through envelop analysis.

Nembhard et al. (2014) used for experiment multiparametrics diagnostics – connection of vibrodiagnostics and thermodiagnostic. They found out, that this method is more efficient for monitoring of machine. For the evaluation they used to Principal Component Analysis.

The paper deals with vibration monitoring of rolling bearing when the measurement rig is operated in three different regimes, which are describes in the next part of the article.

MATERIAL AND METHODS

For the experiment was used envelope analysis. This special envelope vibration acceleration methods are developed to accurately determine the current bearing condition. The advantage of envelope analysis is its speed with subsequent identification of the fault. It is intended for detection of bearing failure, when in subsequent connection with FFT analysis it locates the exact part of the bearing which is damaged (inner ring, outer ring, rolling element, cage).

The envelope analysis is evaluated in the resonance range between 5 - 20 kHz. Since each bearing portion has different relative velocities with respect to the shaft, the frequency at which these disturbances occur can be determined (Blata *et al*. 2017) This method consists in measuring the impulses that arise when the path is broken by the passage of the ball, the rollers or the engagement of the teeth. By rolling the damaged bearing element, impacts occur which cause increased vibration on the impact frequency. The signal is first fed to a filter (bandpass filter) that passes only high frequencies and removes most of the noise. After the guidance changes into so-called. Envelope (wrapped pulses). The energy is reduced, but the pulses are repeated at the same intervals as the frequency of the repetition of the signal does not change by filtering. We obtain the envelope spectrum using an FFT analyser that contains a component whose frequency indicates the kinematic bearing frequencies. The following relationships are used to calculate the kinematic (repetition) pulse frequency assuming pure rolling motion. (Helebrand 2005)

BPFO (Ball Pass Frequency – Inner Race) – frequency corresponding to inner ring damage

$$f = \frac{n}{2} f_r \left(1 - \frac{B_d}{P_d} cos\beta\right) \quad (1)$$

BPFI (Ball Pass Frequency – Inner Race) – frequency corresponding to inner ring damage

$$f = \frac{n}{2} f_r \left(1 + \frac{B_d}{P_d} cos\beta\right) \quad (2)$$

BSF (Ball Spin Frequency) frequency corresponding to ball spin or roller damage

$$f = \frac{P_d}{2B_d} f_r \left(\left(1 - \frac{B_d}{P_d} cos\beta\right)^2\right) \quad (3)$$

FTF (Fundamental Train Frequency) – damaging the cage

$$f = \frac{1}{2} f_r \left(1 + \frac{B_d}{P_d} cos\beta\right) \quad (4)$$

where: f – frequency [Hz],
B_d – diameter of rolling element [mm],
P_d – the middle diameter of bearing [mm],
n – the number of rolling element [-],
f_r – rotation frequency [Hz],
β – contact angle [°], (Ratman, C., el al., 2018)

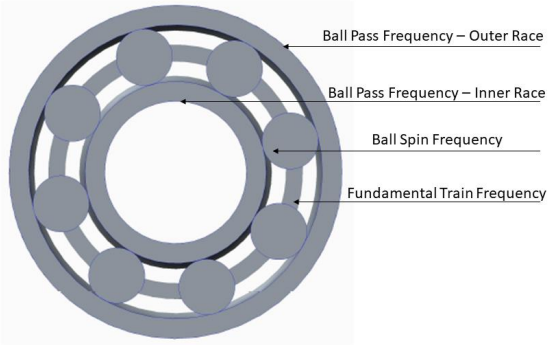

Fig. 1 Characteristic frequencies for the rolling bearing (Author, 2019)
Obr. 1 Charakteristické frekvencie pre guľkové ložiská

Experimental Rig

The experimental rig for the test is showed in Fig. 2. The test rig consists of a frame of the structure (8) made of H-profile steel with dimensions of 1200x300 mm. The shaft (6) is mounted on the structure, on which bearings (2, 5,12) are mounted in different distance. Type of bearings is UPC204. The bearings are fastened to the frame with screws. The mechanism is powered by an electric motor Siemens 0.25 kW, 50 Hz (7). A force transduc-

er (3) is attached to the second bearing from left (2). The values from the force transducer are transmitted via the electronic transducer EMS 169 (1) to the digital multimeter (4), through which the individual load is read. Signal of vibrations from bearings is measured (2) using AC102-1A accelerometers (10). The signal is evaluated by the Adash A4400-VA4 Pro Analyzer (9). The temperature is sensed by the Fluke Ti55 infrared camera (11).

In case of evaluation of measurements was used envelope′s method, which is efficient and often used in in diagnostic practice, because assuming broad spectrum analysis would be used, signal from parts of bearing should be lost in signal noise. For the purpose of temperature measurement of bearing was used infrared camera. Background of watched area had emissivity ε = 0,95 for the best results achieved.

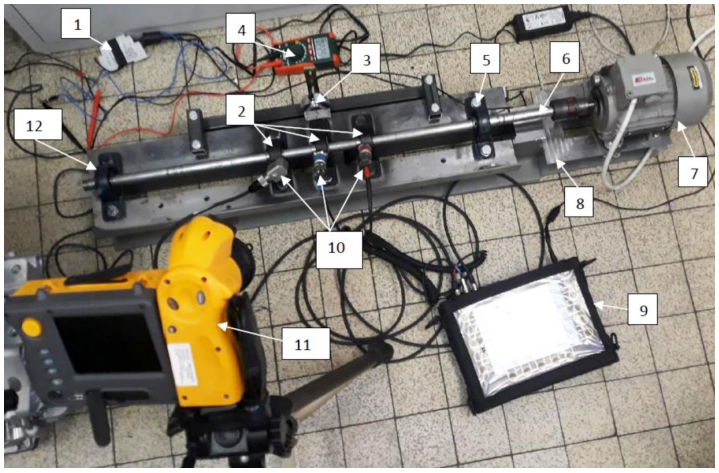

Fig. 2 Experimental rig (Author, 2019)
Obr. 2 Experimentálne zariadenie

Tab. 1 Bearing specification (ZVL Slovakia, 2019)
Tab. 1 Ložiskové špecifikácie (ZVL Slovakia, 2019)

Specification of Bearing UCP 6204			
Outer diameter[1)], D (mm)	47	Outer ring width[5)], B (mm)	14
Inner diameter[2)], d (mm)	20	Number of ball[6)], N_b	8
Pitch diameter[3)], d_p (mm)	33,4	Contact angle[7)], α (degree)	0
Ball diameter[4)], d_b (mm)	7,9		

[1)]vonkajší priemer, [2)]vnútorný priemer, [3)]priemer rozostupu, [4)]priemer guličky, [5)]vonkajšia šírka, [6)]počet guličiek, [7)]kontaktný uhol

RESULTS

The following steps were necessary to obtain the measurement results. Experiment was made with envelope method, where are showed characteristically frequency for rolling bearing type: 6204. In the first stage of the measurement, the experiments were made (Fig. 3). in an unloaded, fault-free condition when the nominal vibrations values were measured on bearing (Fig. 2) (2). The frequency of rotation was set to 50 Hz. In the next step, the monitored deposit was gradually loaded in the range of 0,2-1 kN. The frequency of rotation was set to 20 Hz and slightly damaged by insufficient lubrication. In the last part of the measurement, the bearing was loaded with 1 kN (Fig. 4) and damaged by dry operation (2).

Fig. 3 is a representation of the envelope spectrum on which different peeks appear, but at low acceleration values due to mechanical release of the bearing that has been released due to load.

Fig. 4 is a graph of envelope acceleration where the bearing was gradually loaded and slightly damaged by insufficient lubrication. Acceleration values have slightly increased, but the machine is still not in complete destruction. Fig. 5 is a vibration acceleration for an already damaged bearing, where the damage is already evident and according to the characteristic vibration we calculated according to the relation (4), where the result for the revolution frequency was 19 Hz. For ball bearings it can be said that there is a damaged cage on the bearing.

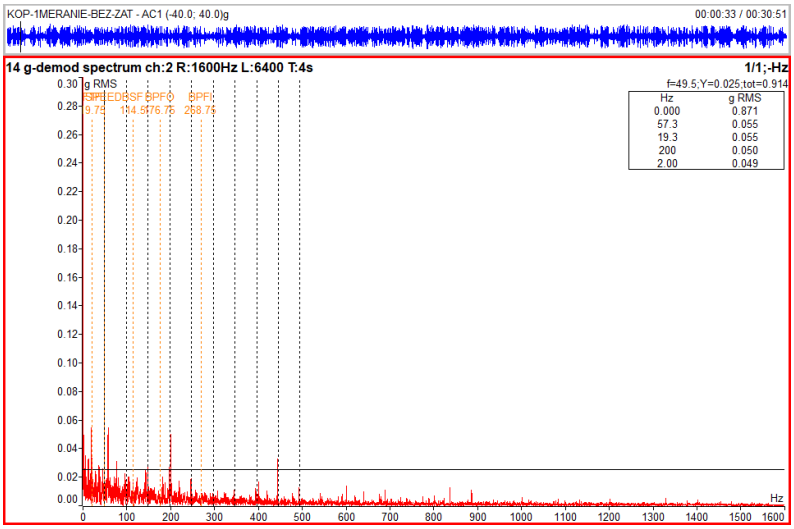

Fig. 3 Envelope spectrum in unloaded regime (50 Hz) (Author, 2019)
Obr. 3 Obálková analýza v nezaťaženom režime (50Hz) (Autor, 2019)

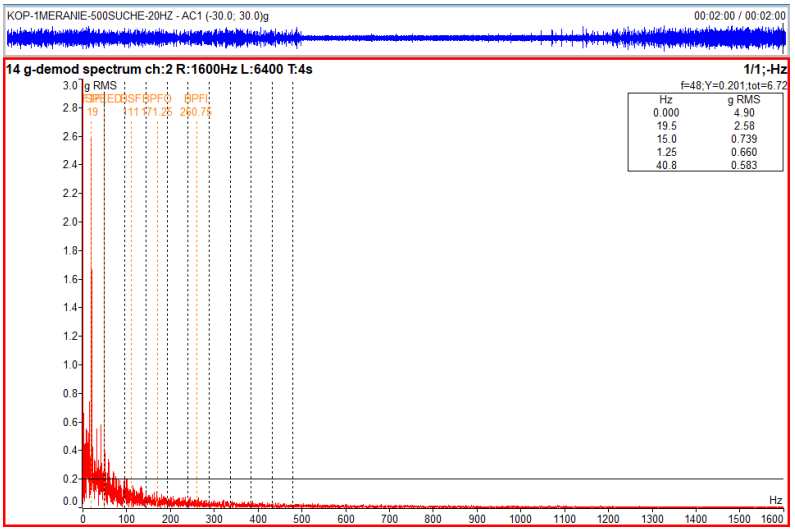

Fig. 4 Envelope spectrum where the bearing was gradually loaded (20 Hz) (Author, 2019)
Obr. 4 Obálková analýza, ložisko postupne zaťažované (20 Hz) (Autor, 2019)

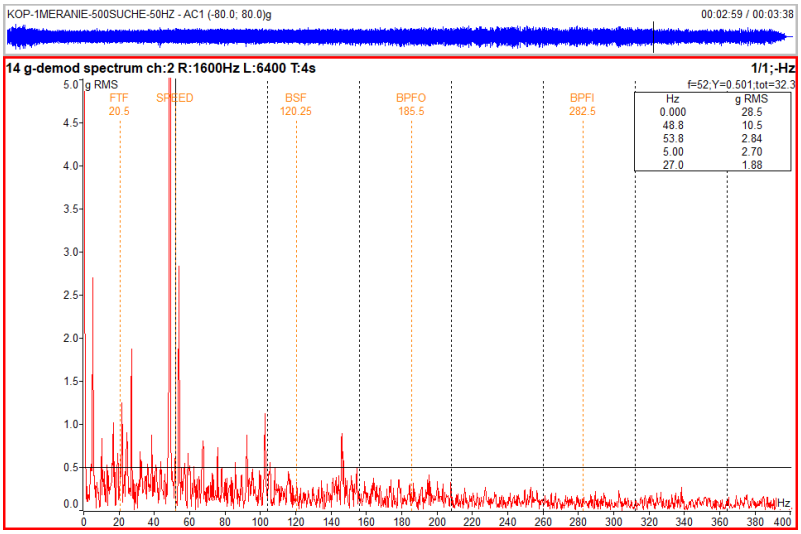

Fig. 5 Envelope spectrum in loaded and damage regime (50 Hz) (Author, 2019)
Obr. 5 Obálková analýza v zaťaženom režime a poškodené ložisko (50 Hz) (Autor, 2019)

DISCUSSION

With improving detection of fault diagnosis for shaft measured on the bearings deals Nembhard et. al. (2014). They used for monitoring single vibration sensor with simple

temperature sensor on each bearing. Experiment showed, that acquired data from the measurements of vibration and temperature gives better condition prognosis of machine when compared with vibration data alone.

Saruhan et. al. (2014) presented results of measurement of vibration of rolling element bearing (REB). For their experiment was used pair of bearing on which are placed one axis accelometers. Authors compared vibration analysis for four different defects states of REB (inner raceway defect, outer raceway defect, ball defect and combination of the bearing elements defect) with 2 load regime and two different speed. They found out that the most effective techniques for condition monitoring of REB is vibration spectrum analysis.

Chebil et al. (2009) compared differently techniques used for monitoring of bearing. It was found that discrete wavelet transform based on time-frequency analysis achieved the best results.

Many of diagnosticians used for condition monitoring of bearings their characteristic defect frequencies through envelop analysis, which was used also in our experiment. Our research in compared with another works showed useful of characteristics vibrations frequency, but for more exacting of measured is needed combine vibrodiagnostics with for example thermodiagnostics. It will be subject for our future research.

CONCLUSION

Today's machine diagnostics in technical practice should aim to bring diagnostic methods closer to manufacturing workers, to reduce the overall cost of machine maintenance and, last but not least, to ensure the safety and health of workers who are in close contact with these devices (Krajčovičová *et al*. 2015).

The paper deals with the diagnostics and behavior of the bearing in unloaded, gradually loaded and loaded and damaged mode. As can be seen from Figure (4), in a bearing in progressive mode, changes in vibration take place against the nominal value, but within the limits of a standard that determines the maximum vibration acceleration values. In the mode when the bearing was brought dry, it was damaged and, according to the characteristic vibration calculation, the main damage was on the inner cage of the bearing.

ACKNOWLEDGMENT

The article was created as part of the project "Progress and Application of Educational Methods in the Mechanics of Bodies" no. 015TU Z-4/2019 Cultural and Educational Grant Agency MŠVVaŠ SR.

REFERENCES

BLATA, J. ŠEDĚNKA, D., KAŠIAR, L., VOLNA, P. 2017. Examining the condition of the ball and the ball track on the heavy machine. In *Diagnostyka*. 18 (3), pp. 85-91. ISSN 1641-6414

HARVÁNEK, P., MELICHERČÍK, J., BERÁK, M., KOVÁČ, J. 2019. Termodiagnostika poruchy chladiaceho systému motorového vozidla. In *Mobilné energetické prostriedky - Hydraulika - Životné prostredie - Ergonómia mobilných strojov: vedecký recenzovaný zborník*. Zvolen: Technická univerzita vo Zvolene, 2019, s. 85--93. ISBN 978-80-228-3168-0.VEGA 1/0642/18.

CHARTE, D. 2015. Introduction to Portable Vibration Analysis. In Emerson process management. available online < https://www.slideshare.net >

CHEBIL, J., NOEL, G., MESBAH. M., DERICHE, M. 2009. Wavelet Decomposition for the Detection and Diagnosis of Faults in Rolling Element Bearings. In *Jordan Journal of Mechanical and Industrial Engineering*, vol. 3, no. 4, pp. 260-267. ISSN: 1995-6665

HELEBRANT, F., ZIEGLER, J. 2005. Technical diagnostics and reliability II. vibrodiagnostics (Technická diagnostika a spolehlivost II. Vibrodiagnostika). VSB TU Ostrava. 2005. 178 s. ISBN: 80-248-0650-9

KRAJČOVIČOVÁ, M., SVOREŇ, J. OSVALD, J. 2015. Transport and handling equipment (Dopravná a manipulačná technika). Zvolen: Technical University in Zvolen. 208 pp. ISBN 978-80-228-2669-3

NEMBHARD, A., SINHA, J., PINKERTON, J., ELBHBAH, K. 2014. Combined vibration and thermal analysis for the condition monitoring of rotating machinery. In *Structural Health Monitoring*, Vol. 13 no. 3, pp. 281-295. ISSN: 1741-3168

RATNAM, C. JASMIN, N., RAO, V. RAO, K. 2018. A Comparative Experimental Study on Fault Diagnosis of Rolling Element Bearing Using Acoustic Emission and Soft Computing Techniques. In *Tribology in Industry*. Vol. 40, No. 3 (2018) 501-513. DOI: 10.24874/ti.2018.40.03.15

SARUHAN, H., SARIDEMIR, S., QICEK, A., UYGUR, I. 2014. Vibration Analysis of Rolling Element Bearings Defects. In *Journal of applied research and technology*, vol. 12 no. 3, pp. 384-395. ISSN: 1665-6423

TURIS, J. 2019. Predikčná tribodiagnostika. In *Mobilné energetické prostriedky - Hydraulika - Životné prostredie – Ergonómia mobilných strojov: vedecký recenzovaný zborník*. Zvolen: Technická univerzita vo Zvolene, 2019, s. 241–250. ISBN 978-80-228-3168-0. VEGA 1/0155/18; KEGA 015TU Z-4/2019.

WANG, F., et al. 2017. Condition monitoring and fault diagnosis methods for low-speed and heavy-load slewing bearings: a literature review. In *Journal of Vibroengineering*. Vol. 19. Issue 5. ISSN 1392-8716

Contribution has been prepared within the solving of scientific grant project „Progress and Application of Educational Methods in the Mechanics of Bodies“ no. 015TU Z-4/2019 Cultural and Educational Grant Agency MŠVVaŠ SR.

Corresponding author:
Silvia Kopčanová, 0905 350 881, kopcanova15@gmail.com

INFLUENCE OF FEED RATE AND CUTTING SPEED OF MILLING ON FINAL SURFACE QUALITY AFTER PLANE MILLING SPRUCE WOOD

VPLYV POSUVNEJ A REZNEJ RÝCHLOSTI PROCESU FRÉZOVANIA NA VÝSLEDNÚ KVALITU OPRACOVANIA TERMICKY MODIFIKOVANÉHO SMREKOVÉHO DREVA

Michal Korčok[1 a)], Peter Koleda[1 b)], Štefan Barcík[1 c)], Vlado Goglia[2], Roman Bambura[3]

[1]Department of Manufacturing and Automation Technology, Faculty of Technology, Technical University in Zvolen, Študentská 26, 960 53 Zvolen, Slovak Republic
e-mail: [a)] korcokmichal@gmail.com, [b)] peter.koleda@tuzvo.sk, [c)] barcik@tuzvo.sk
[2]Institute for process Techniques, Facultys of Forestry, University in Zagreb, Svetosimunska 25,10000 Zagreb,Croatia, e-mail: vgoglia51@gmail.com.
[3]Department of Manufacturing Technologies and Quality Management, Faculty of Technology, Technical University in Zvolen, Študentská 26, 960 53 Zvolen, Slovak Republic, e-mail: bambura.r@gmail.com

ABSTRACT: The article deals with examination of feed rate and cutting speed influence on final surface quality of natural and thermally treated spruce wood during face milling. Technical parameters for feed rate were v_f = 6 m.min^{-1}, 10 m.min^{-1}, 15 m.min^{-1} and cutting speed v_c = 20 m.s^{-1}, 40 m.s^{-1}, 60 m.s^{-1} for final quality surface treatment (R_a - mean surface arithmetic deviation). Three types of milling heads with angular geometry γ = 15°, 20°, 30° and three types of blades were used in the experiment (HSS 18% W with AlTiCrN coating, tool steel cutter 19 573 induction hardened, steel knife MAXIMUM SPECIAL 55). The material used in the experiment was spruce, which was naturally and thermally modified at T: 160 °C, 180 °C, 200 °C, 220 °C. The final quality of surface was measured using contactless method by device LPM - 4, which works on a principle of laser profilometry. The best quality (lowest roughness) was achieved when milling the sample treated at temperature of 160 °C at feed rate of 6 m.min^{-1} on the contrary, the worst measured data (highest roughness) were in the heat treatment of 220 °C with a feed rate of 15 m.min^{-1}. Regarding to cutting speed, the best quality was achieved when milling the sample treated at 160 °C and of cutting speed 60 m.s^{-1}, the worst quality was achieved when milling the sample treated at 220 °C at speed of 20 m.s^{-1}.

Key words: quality surface, feed rate, cutting speed, thermowood, Thermal modification

ABSTRAKT: Predložený článok sa zaoberá posúdením vplyvov podávacej a reznej rýchlosti na výslednú kvalitu opracovania pri frézovaní prírodného a tepelne upraveného smrekového dreva. Technické parametre pre podávaciu rýchlosť boli v_f = 6 m.min^{-1}, 10 m.min^{-1}, 15 m.min^{-1} a reznú rýchlosť v_c = 20 m.s^{-1}, 40 m.s^{-1}, 60 m.s^{-1} na výslednú kvalitu

opracovania povrchu (Ra - stredná aritmetická odchýlka povrchu). Pri experimente boli použité 3 typy frézovacích hláv s uhlovou geometriou γ = 15°, 20°, 30° a tri typy nožov (HSS 18% W s povlakom AlTiCrN, nôž z nástrojovej ocele 19 573 indukčne kalený, nôž z ocele MAXIMUM SPECIAL 55). Materiál použitý v experimente bol smrek, ktorý bol v prírodnom stave a tepelne modifikovanom pri teplotách T: 160 °C, 180 °C, 200 °C, 220 °C. Meranie údajov sa realizovalo bezkontaktnou metódou, pomocou laserového profilometra LMP – 4. Najlepšie namerané údaje pri opracovaní povrchu sme namerali pri posuvnej rýchlosti 6 $m.min^{-1}$ s tepelnou úpravou 160 °C naopak najhoršie namerané údaje boli pri tepelnej uprave 220 °C s posuvnou rýchlosťou 15 $m.min^{-1}$. Pri reznej rýchlosti sa najnižšia drsnosť povrchu namerala pri tepelnej úprave 160 °C a reznej rýchlosti 60 $m.s^{-1}$ naopak najhoršiu kvalitu povrchu sa namerala pri reznej rýchlosti 20 $m.s^{-1}$ a tepelnej úprave 220 °C.

Kľúčové slová: podávacia rýchlosť, rezná rýchlosť, thermowood, tepelná úprava, kvalita opracovania

INTRODUCTION

Wood is considered to be one of the most promising raw materials, and it is also seen as the load-bearing material of the future (Bekhta *et al*. 2014; Gaff 2014; Gottlöber *et al*. 2016). It is one of the oldest used materials (Prokeš 1982). Even with the development of new types of materials, wood has still not been replaced because of its valuable properties. Today, wood is extensively used in the construction industry, the chemical processing industry, and the production of wood-based materials.

Research regarding the heat treatment of wood has increased significantly in recent years as a result of the ongoing search to improve wood properties, along with the desire to take advantage of this technique in order to employ wood in outdoor applications. Many aspects of heat-treated wood, such as dimensional stability, durability, mechanical properties, equilibrium moisture content, mass loss, wettability, color change, chemical modifications, and others (Esteves and Pereira 2009) have been studied for various wood species. However, only limited studies have looked at wood machinability and the resulting wood quality (de Moura and Brito 2008; Budakci *et al*. 2013; Tu *et al*. 2014; Kubs *et al*. 2016).

Heat treatment, which is based on the basic idea of the heat treatment of the wooden material at the temperatures above 150 °C at which chemical reactions accelerate, leads to permanent changes in the chemical composition of the polymer compounds of the cell wall. Meanwhile, resistance against biological degradation is provided without any spoiling in the structure of the wood (Johansson 2005). According to (Enjily and Jones 2006), heat treatment modifies the molecular structure of the wooden material so that a product with low equilibrium moisture content and reduced dimensional changes is obtained (Enjily and Jones 2006).

With the ever-increasing consumption of thermally modified wood, it comes into contact with the most basic wood machining operations, including milling. Milling is the machining of material with a rotating tool (milling head and milling cutter) in order to remove material. The material is milled to obtain a high-quality surface as well as exact dimensions of the workpiece, which is important for further processing (rotary, planar, or

shaped surfaces) (Welzbacher *et al*. 2011; Kvietková 2015a). This process of machining is characterized by being a chip-forming process in which the chip thickness changes from minimum to maximum, or vice versa (Lisičan 1996; Bekéš et al. 1999).

In order to complete the final product, the wood can be processed using various methods. Each product has different surface quality requirements given by its function and appearance. Each surface of the product represents the output of a certain fabrication process (Gáborík *et al*. 2017).

Each process step leaves expected irregularities on the surface. These irregularities may affect the required function of such surfaces. The irregularities can be evaluated with respect to both their macro- and microgeometry concerns (Dubovská 2000). Both macro- and microscopic irregularities appearing on the wood surface mean very small deviations from the optimum flat surface. The wood surface is the area separating the wood substance from its environment (Požgaj 1997). For real wood surfaces, the effects of the working tool on the surface geometry shall always be taken into account (Liptáková and Kúdela 2000). The wood surface geometry results from its anatomic structure and treatment method (Barcík and Gašparík 2014).

As far as the process is concerned, major attention should be paid to veneer surface roughness. Sawn and milled surfaces of pieces are subjected to further surface treatments within the manufacturing process (varnishing, polishing, etc.) (Schulz *et al*. 2012), and such operations are affected by roughness. Surface roughness monitoring is the most usual method for the surface quality evaluation. Surface roughness is a geometric feature given by the material type and its treatment method. Suitable features and parameters of surface roughness criteria are measured as follows:

R_a = arithmetic mean deviation of the evaluated profile;

R_z = profile maximum height

Surface quality is achieved by treatment with appropriate tools, thereby removing wood surface irregularities (Kvietková *et al*. 2015a, 2015b). The most usual wood finishing methods are grinding and, to a lesser extent, milling. The disadvantages of grinding are its lengthiness and dust generation. Therefore, new methods of wood surface roughness reduction are found within mechanical and/or thermomechanical smoothing (e.g., pressing), which eliminate these disadvantages (Gáborík and Dudas 2008; Gáborík and Žitný 2010). The grinding process can be improved by moistening the surface between the grinding steps, using water with approximately 10% urea-formaldehyde based glue.

The aim of the paper is to assess the effect of feed and cutting speed of thermally modified spruce wood on the quality of the finish surface. Quality of surface is quantified by surface roughness.

MATERIALS AND METHODS

Samples from spruce (*Picea abies*), the average age of which was 107 years, were used for the experiment. The wood for the experiment was extracted from the locality Vlčí jarok, 450 m. n. m. (Budča, Slovak Republic). Samples for the experiment were cut and processed to the following dimensions: 700 mm x 110 mm x 20 mm. Thermal treatment of samples was realized by ThermoWood® technology at ČZU in Kostelec nad Černými

lesy, where the samples were adjusted to temperatures of 160, 180, 200 and 220 °C. All technological conditions for production of samples for the experiment are described in (Hrčková *et al*., 2018). Similarly, the determination of density for spruce wood is also described in (Hrčková *et al*., 2018). The technical conditions for the experiment were the same as in (Koleda *et al*., 2018) but extended by three types of knives. The first type of knife was HSS steel with 18% W and coated with AlTiCrN (a). The second type of knife was made of tool steel 19 573 (STN 41 9573), which was induction hardened (b) and the last type of knife was made of steel MAXIMUM SPECIAL 55: 1985/5 (c).

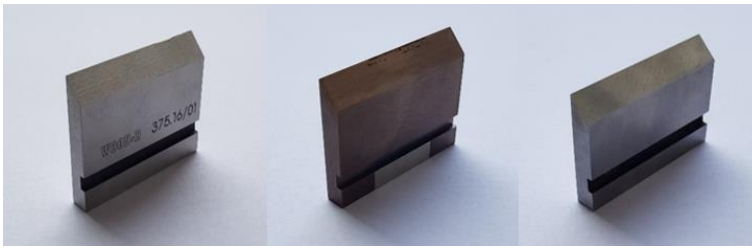

a **b** **c**

Fig. 1 Milling knives
Obr. 1 Frézovacie nože

The milling knife a (Fig. 1 a) was coated by the PVD (Physical Vapor Deposition) method, while the knife b and c (Fig. 1 b and Fig. 1 c) had no additional surface treatment. The process of applying the knife coating was carried out in the company WOOD – B, s.r.o. in Nové Zámky, Slovakia. The type b knife (Fig. 1 b) was inductively hardened in the laboratories of the National Academy of Sciences (Institute of Physics and Technology), based in Minsk (Belarus). Before the experimental measurement, a hardness measurement was performed on all knives, which was carried out at TU in Zvolen. Hardness was measured on a Škoda RB1 hardness tester (120° diamond cone, measuring range 20 ÷ 67 HRC) (Fig. 2).

Fig. 2 Hardness tester Škoda RB1
Obr. 2 Tvrdomer Škoda RB1

During the measurement, 3 injection places were selected along the front cutting edge. Specifications of used knives with measured hardness values are given in Tab. 1.

Table 1 Used milling knives and their measured hardness
Tabuľka 1 Použité frézovacie nože a ich nameraná tvrdosť

	knife A	knife B	knife C
Edit type	multilayer AlTiCrN	induction hardened	–
Application temperature	(450 ÷ 500) °C	800 °C	–
Hardness of the milling knife	62 HRC	63 HRC	64 HRC

Measurement of roughness of processed samples as a quality parameter was realized by contactless method using laser profilometer LMP - 4, which evaluated the monitored parameter Ra (mean arithmetic deviation of roughness profile). The technical parameters of the machine, the course of measurement and also the data processing itself are described in the article Korčok et al. (2018).

RESULTS AND DISCUSSION

Influence of feed rate

A multi-factor analysis of variance for the dependence of feed rate versus surface roughness is shown in Fig. 3 and the analysis of feed rate variation versus surface roughness is shown in Fig. 4. From the multi-factor analysis of variance we can see that the greatest surface roughness was measured at wood treated at temperaure of 220 °C at feed rate of 15 m.min^{-1}. Conversely, the best surface quality (the lowest roughness) was measured at the heat treatment of 160 °C at a feed rate of 6 m.min $^{-1}$.

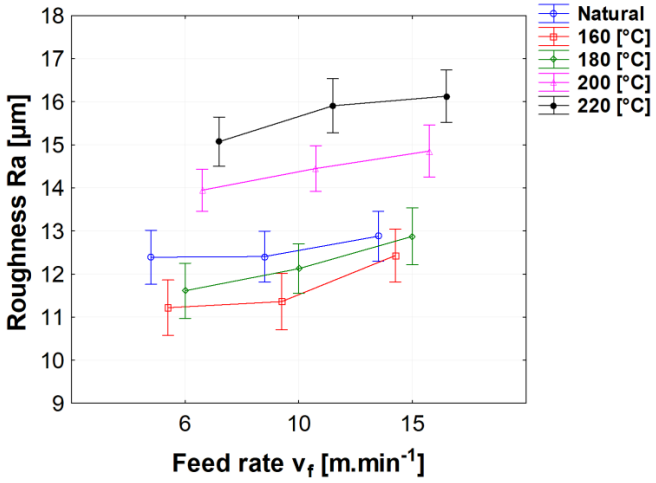

Fig. 3 Multifactor analysis of variance for the dependence of surface roughness on feed rate
Obr. 3 Viacfaktorová analýza rozptylu závislosti drsnosti povrchu na posuvnej rýchlosti

Influence of cutting speed

The multi-factor analysis of variance for the dependence of cutting speed versus surface roughness is shown in Fig. 4. It can be seen that the best surface finish was achieved at 160 °C. In this sample, it can be seen that for both cutting speeds 20 and 40 $m.s^{-1}$ the surface roughness is almost identical. The worst machining quality was measured for a sample with the heat treatment at 220 °C and the cutting speed of 20 $m.s^{-1}$.

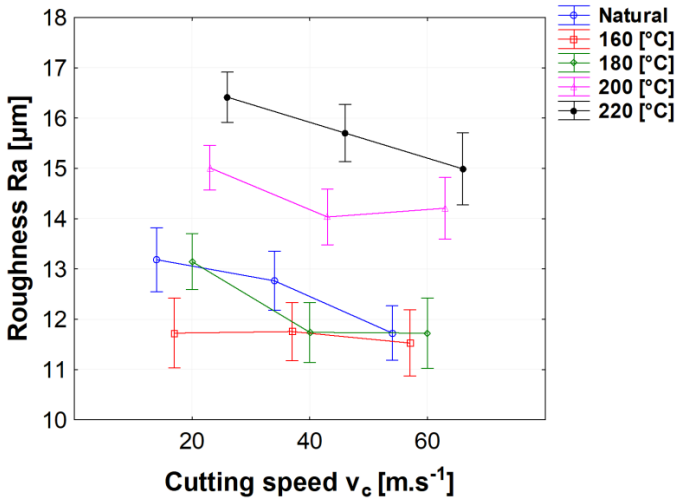

Fig. 4 Multifactor analysis of variance for the dependence of surface roughness on cutting speed
Obr. 4 Viacfaktorová analýza rozptylu závislosti drsnosti povrchu na reznej rýchlosti

Presented paper deals with the optimization of technical parameters (cutting speed and feed rate) in dependence on the investigated parameter - Ra (surface roughness), which was measured on treated and untreated spruce samples. Samples for the experimental part were plane milled on the lower spindle mill and the surface roughness was then measured using a LMP - 4 laser profilometer. Our experiment on the roughness of heat treated wood can be compared with Kaplan et al. 2018, which dealt in his article with oak wood. In the presented article he confirmed that the gradual increase of the cutting speed also gradually improves the quality of the machined surface, which was also shown in the experiment. Similarly, the influence of feed rate on the quality of machining has identical, but it should be noted that the technical parameters and the method of measuring surface roughness was not identical with our experiment. Kvietková et al. 2015b, examined the effect of heat treatment on the final quality of beech wood processing. Their experiment also confirmed the phenomenon, as in our article, where the gradual increase in cutting speed decreases the roughness of the machined surface. The same applies to the feed rate, where with the gradual increase of feed rate the surface roughness increased, but it should be noted that the authors made measurements using the contact method and had different technical parameters for milling. Currently, the authors investigate the effects of the duration of heat

treatment on the surface roughness of various tree species, which will be the subject of further publication.

CONCLUSIONS

From the experimental results we can clearly confirm that with increased feed rate the surface roughness gradually increased. The best machining quality was achieved at a feed rate of 6 $m.min^{-1}$, while the worst was achieved at 15 $m.min^{-1}$. The biggest increase was measured at feed rate of 10 $m.min^{-1}$.

Experimental measurement confirmed a phenomenon which states that as the cutting speed gradually increased the better surface finish with less surface roughness is achieved. This statement is confirmed for sample with a thermal treatment at 220 °C with natural wood. This was confirmed for almost all the samples used in the experiment except for the sample that was thermally treated at 160 °C, where at a cutting speed of 60 $m.s^{-1}$ the surface roughness increased compared to the roughness we achieved for the cutting speed of 40 $m.s^{-1}$. This phenomenon may have been caused by poor processing of the sample. The best surface roughness for all samples used in experiment was achieved at cutting speed of 60 $m.s^{-1}$.

ACKNOWLEDGEMENTS

The paper was written within the project: VEGA 1/0315/17, "Research of relevant properties of thermally modified wood at contact effects in the machining process with the prediction of obtaining an optimal surface" the project of Internal Project Agency No. 2/2019 "Impact of selected technological, tool and material factors on the surface finish quality and energetic intensity at plane milling of thermally modified spruce wood" and with the support of project APVV 17/0456 "Thermal modification of wood with water vapor for purposeful and stable change of wood color".

REFERENCES CITED

BARCÍK, Š., GAŠPARÍK, M. 2014. Effect of tool and milling parameters on the size distribution of splinters of planed native and thermally modified beech wood. In *BioResources*, vol. 9, no. 1, pp 1346-1360, DOI: 10.15376/biores.9.1.1346-1360.

BEKÉŠ, J., HRUBEC, J., KICKO, J., LIPA, Z. 1999. Teória Obrábania [Theory of Machining], Slovenská Technická Univerzita, Bratislava, Slovakia.

BEKHTA, P., PROSZYK, S., KRYSTOFIAK, T., MAMONOVA, M., PINKOWSKI, G., LIS, B. 2014. Effect of thermomechanical densification on surface roughness of wood veneers. In *Material Science and Engineering*, vol. 9, no. 4, pp 233-245. DOI: 10.1080/17480272.2014.923042.

BUDAKÇI, M., ILÇE, A. C., GÜRLEYEN, T., UTAR, M. 2013. Determination of the surface roughness of heat-treated wood materials planed by the cutters of a horizontal milling machine. In *BioResources*, vol. 8, no. 3, pp 3189-3199. DOI: 10.15376/biores.8.3.3189-3199.

de MOURA, L. F., BRITO, J. O. 2008. Effect of thermal treatment on machining properties of Eucalyptus grandis and Pinus Caribaea var. hondurensis woods. *Proceedings of the 51st International Convention of Society of Wood Science and Technology*, Conceptión, Chile, 10-12 November. Paper WS-18, pp. 1-9.

DUBOVSKÁ, R. 2000. Niektoré poznatky o kvantifikácii drsnosti pri obrábaní dreva, [Some knowledge of quantifying roughness in woodcutting]. *Procesy Trieskového A Beztrieskového Obrábania Dreva*, Zvolen, Slovakia, pp. 43-47 (in Slovak).

ENJILY, V., JONES, D. 2006. The potential for modified materials in the panel products industry. *Wood Resources and Panel Properties Conference*, COST Action E44/E49, 12-14 June, Valencia, Spain.

ESTEVES, B., PEREIRA, H. M. 2009. Wood modification by heat treatment: A review. In *BioResources*, vol. 4, no. 1, pp 370-404. DOI: 10.15376/biores.4.1.370-404

GÁBORÍK, J., DUDAS, J. 2008. Thermo-mechanical smoothing of wood. In *Annals of Warsaw University of Life Sciences –SGGW, Forestry and Wood Technology*, vol. 65, pp 49-54.

GÁBORÍK, J., ŽITNÝ, M. 2010. Quality changes of aspen and beech surface after smoothing by rotary tool. In *Acta facultatis xylologiae Zvolen*, TU vo Zolene, pp. 41- 46.

GÁBORÍK, J., GAFF, M., RUMAN, D., GAŠPARÍK, M., SVOBODA, T., VOKATY, V., SÍKORA, A. 2017. Quality of the surface of aspen wood after pressing. In *BioResources*, vol. 12, no. 1, pp 82-94. DOI: 10.15376/biores.12.1.82-94

GAFF, M. 2014. Three-dimensional pneumatic molding of veneers. In *BioResources*, vol. 9, no. 3, pp 5676-5687. DOI: 10.15376/biores.9.3.5676-5687

GOTTLÖBER, CH., WAGENFÜHR, A., RÖBENACK, K., AHMED, D. ECKHARDT, S. 2016. Strategies, concepts and approaches to avoid cuttermarks on wooden workpiece surfaces. In *Wood Material Science and Engineering*, vol. 11, no. 3, pp 147-155. DOI: 10.1080 / 17480272.2015.1133701

HRČKOVÁ, M., KOLEDA, P., KOLEDA, P., BARCÍK, Š., ŠTEFKOVÁ, J. 2018. Color change of selected wood species affected by thermal treatment and sanding. In *BioResources*, vol. 13, no. 4, pp 8956-8975. DOI: 10.15376/biores.13.4.8956-8975

JOHANSSON, D. 2005. Strength and Colour Response of Solid Wood to Heat Treatment, Licentiate thesis, Luleå Teknoloji University, Skellefteå, Sweden.

KAPLAN, L., KVIETKOVÁ, M., SEDLECKÝ, M. 2018. Effect of the interaction between thermal modification temperature and cutting parameters on the quality of oak wood. In *BioResources*, vol. 13, no. 1, pp 1251-1264. DOI: 10.15376/biores.13.1.1251-1264

KOLEDA, P., BARCÍK, Š., NOCIAROVÁ, A. 2018. Effect of technological parameters of machining on energy efficiency in face milling of heat-treated oak wood. In *BioResources*, vol. 13, no. 3, pp 6133-6146. DOI: 10.15376/biores.13.3.6133-6146

KORČOK, M., KOLEDA, P., BARCÍK, Š., VANČO, M. 2018. Effects of technical and technological parameters on the surface quality when milling thermally modified European oak wood. In *BioResources*, vol. 13, no. 4, pp 8569-8577. DOI: 10.15376/biores,13.4.8569-8577

KUBS, J., GAFF, M., BARCIK, S. 2016. Factors affecting the consumption of energy during the milling of thermally modified and unmodified beech wood. In *BioResources*, vol. 11, no. 1, pp 736-747. DOI: 10.15376/biores.11.1.736-747

KVIETKOVÁ, M., BARCÍK, Š., ALÁČ, P. 2015a. Impact of angle geometry of tool on granulometric composition of particles during the flat milling of thermally modified beech. In *Wood Research*, vol. 60, no. 1, pp. 137-146.

KVIETKOVÁ, M., GAŠPARÍK, M., GAFF, M. 2015b. Effect of thermal treatment on surface quality of beech wood after plane milling. In *BioResources*, vol. 10, no. 3, pp 4226-4238. DOI: 10.15376/biores.10.3.4226-4238

LIPTÁKOVÁ, E., KÚDELA, J. 2000. The surface properties of beech wood in different ways mechanical machining. *Procesy trieskového a beztrieskového obrábania dreva*, TU Zvolen, pp. 107-115.

LISIČAN, J. 1996. Teória a Technika Spracovania Dreva [Theory and Technique of Wood Processing], Matcentrum, Zvolen, Slovakia.

POŽGAJ, A. 1997. Štruktúra a Vlastnosti Dreva [Wood Structure and Properties], Príroda, Bratislava, Slovakia, 486 p. (in Slovak).
PROKEŠ, S. 1982. Obrábění Dřeva a Nových Hmot ze Dřeva (Woodworking and New Materials from Wood). SNTL – Nakladatelství Technické Literatury, Prague, Czech Republic.
SCHULZ, T., SCHEIDING, W., FISCHER, M. 2012. Sperrholz und Sperrholzformteile aus thermisch modifizierten Furnieren. In *Holztechnologie*, vol. 53, pp 14-24.
TU, D., LIAO, L., YUN, H., ZHOU, Q., CAO, X., HUANG, J. 2014. Effects of heat treatment on the machining properties of Eucalyptus urophylla x E. camaldulensis. In *BioResources*, vol. 9, no. 2, pp 2847-2855. DOI: 10.15376/biores.9.2.2847-2855
WELZBACHER, C. R., RASSAM, G., TALAEI, A., BRISCHKE, C. 2011. Microstructure, strenght and structural integrity of heat-treated beech and spruce wood. In *Material Science and Engineering*, vol. 6, no. 4, pp 219-227. DOI: 10.1080/17480272.2011.622411

Corresponding author:
Michal Korčok, +421 907 950 774, korcokmichal@gmail.com

INVESTIGATION OF ADHESION AND WEAR OF ZRC COATING ON WOODCUTTING TOOLS

VÝSKUM ADHÉZIE A OPOTREBENIA ZRC POVLAKOV DREVOREZNÝCH NÁSTROJOV

Valery Zhylinski[1 a)], Vadzim Chayeuski[1 b)], Andrey Kuleshov[2], Peter Koleda[3 a)], Štefan Barcík[3 b)]

[1]Belarussian State Technological University, 220006, Belarus, Minsk, Sverdlov St. 13a, email: [a)] zhilinski@yandex.ru, [b)] chayeuski@belstu.by
[2]Department of Solid State Physics. Belarusian State University, Nezavisimosti ave. 4, 220030, Minsk, Republic of Belarus, e-mail: kuleshak@bsu.by
[3]Department of Manufacturing and Automation Technology, Faculty of Technology, Technical University in Zvolen, Študentská 26, 960 53 Zvolen, Slovak Republic, e-mail: [a)] peter.koleda@tuzvo.sk [b)] barcik@tuzvo.sk

ABSTRACT: the investigation of adhesion of ZrC / Ni-P-UDD coating on hard alloy knives has been cared out in the present work. The Ni-P sublayers with ultradisperse diamonds (UDD) were electroplated on blades of hard knives (T03SMG hard alloy). The ZrC-coatings were deposited by the PVD technique after electroplating. The value of the critical load on the scratch track of the ZrC--Ni-P-UDD coating was 26 N. It had been found that the durability period of woodcutting tools with the ZrC-Ni-UDD coatings was higher in 2,5–2,6 times in compared with durability period of the bare tools during the pilot milling tests of laminated chipboards.

Key words: coatings, milling tool, knives, durability period, wear

ABSTRAKT: v tejto práci bolo overené priľnutie povlaku ZrC / Ni-P-UDD na nože z tvrdej zliatiny. Ni-P subvrstvy s ultradisperznými diamantmi (UDD) sa galvanicky nanášali na ostrie nožov (tvrdá zliatina T03SMG). Po galvanickom pokovovaní boli povlaky ZrC nanesené technikou PVD. Hodnota kritického zaťaženia na oterovej línii povlaku ZrC-Ni-P-UDD bola 26 N. Zistilo sa, že trvanlivosť nástrojov na rezanie dreva s povlakmi ZrC-Ni-UDD bola vyššia 2,5 – 2,6-krát v porovnaní s dobou trvanlivosti pôvodných nástrojov počas pilotných testov frézovania laminovaných drevotrieskových dosiek.

Kľúčové slova: povlaky, frézovacie nástroje, nože, trvanlivosť, opotrebenie

INTRODUCTION

Nowadays high demand for quality of wood products makes it necessary for researchers to create new ideas and approaches to production of cutting tool elements. One of the most common types of tool materials for woodworking CNC machines are hard alloys based on tungsten carbide (WC) and cobalt. The cutting elements from hard alloys

are widely used by such well-known companies as Leitz, TIGRA, Faba, LEUCO, and KANEFUSA. Different types of chemical wear (corrosion and oxidation) of these tools are proved to play a significant role in destruction of cutting edge during processing of plate wooden materials. This leads to pulling out of grain from the surface of tungsten carbide cutting element. Woodcutting tool with application of synthetic diamond (UDD) is offered as technological novelty by foreign companies. It has been known that an application of hard ceramics-like coatings, such as TiC, ZrN, ZrC, MoN coatings, synthesized by the physical vapour deposition (PVD) or chemical vapour deposition (CVD) methods, is widely used for strengthening of surface layers of the cutting tools. The PVD and CVD coatings, which possess outstanding high hardness, wear resistance, chemical stability and low friction coefficient, are produced from carbide and nitride composites. The multi-layered coatings of CrZrN, Ti-(TiAl)N, TiCrN, (Ti-Zr-Nb)N synthesized by the PVD process are the basic of superior mechanical and tribological properties of hard alloy tools. Thereby, the lifetime of hard alloy tools can be considerably improved by the use of Ni and Cr electroplatings as sublayers for PVD ceramics-like coatings. The cutting tools with double layer of ZrN coating / Ni-Co electroplating on hard alloy knives showed the increase of their durability period during the milling of laminated chipboards.

The aim of this work is the investigation of adhesion of ZrC / Ni-P-UDD coating on hard alloy knives and analyzation of the phase and elemental composition ZrC/ Ni-P-UDD coatings on the surface of hard alloy.

MATERIALS AND METHODS

The substrates were knives made from T03SMG (hard alloy) of company TIGRA (Germany). The Ni-P-UDD coatings were deposited from the Wots electrolyte with NaH_2PO_2 at a current density of 4 A/dm^2 and temperature of 50°C. The electrolyte composition was consisted of $NiSO_4 \cdot 7H_2O$ (250 g/dm^3), $NiCl_6 \cdot 6H_2O$ (50 g/dm^3), H_3BO_3 (30 g/dm^3), NaH_2PO_2 (30 g/dm^3). The UDD particles with a size of 4-6 nm were homogenized by magnetic stirrer in suspension of 2–5 g/dm^3 into Wots electrolyte during electrochemical deposition of Ni-P-UDD coatings. The ZrC-coatings were fabricated by vacuum-arc PVD method with use zirconium cathodes and the Bulat unit.

The microstructure of coatings was analysed by the scanning electron microscopy (SEM) and energy-dispersive X-ray spectroscopy (EDS) with the use of Hitachi S-4800 electron microscope. The adhesion of the coatings was assessed a micro-scratch tester with the maximum load of 150 N. The speed of the tester indenter, which had a conical-shaped diamond tip with curvature radius of $0.5 \cdot 10^{-3}$ m, was $0.83 \cdot 10^{-4}$ m/s. The loading rate was 42 N/s. Fields of scratch track were studied with use of the optical and Hitachi S-4800 electron microscope.

RESULTS AND DISCUSSION

Microstructural analysis and surface morphology

The microstructure of the Ni-P-UDD coatings was shown in Fig. 1. The morphology was formed by globular clusters. This fact may indicate that the UDD particles had been centres of nickel crystallization.

Figure 1 revealed that carbon presented in the Ni-P-UDD layer and formed the agglomerates with a size of 0.7–2.5 μm. The EDS spectrum of the Ni-P- UDD coatings (Fig. 1) showed that the Ni-P-UDD layer did not mix with the hard alloy substrate.

The surface morphology of the ZrC coating was shown as rough. The surface had patterns with pits, pores and dots (particles). These aspects were characterized the arc PVD deposition of ZrC. This is a result of the ejection of small liquid drops of Zr due to the high current densities in the arc evaporation process.

The elemental composition showed EDS maps of the element distribution within the cross-section of the ZrC/Ni-P-UDD coating on the knife (Fig. 1) indicated on the presence of phosphor in the Ni-P-UDD layer. The release of phosphor has been caused by the electrochemical reduction of phosphor during the electrochemical deposition of Ni. The nickel-phosphor phase of Ni-P-UDD coating could interact with the metal cobalt and it could form the continuous solid solutions with higher adhesion.

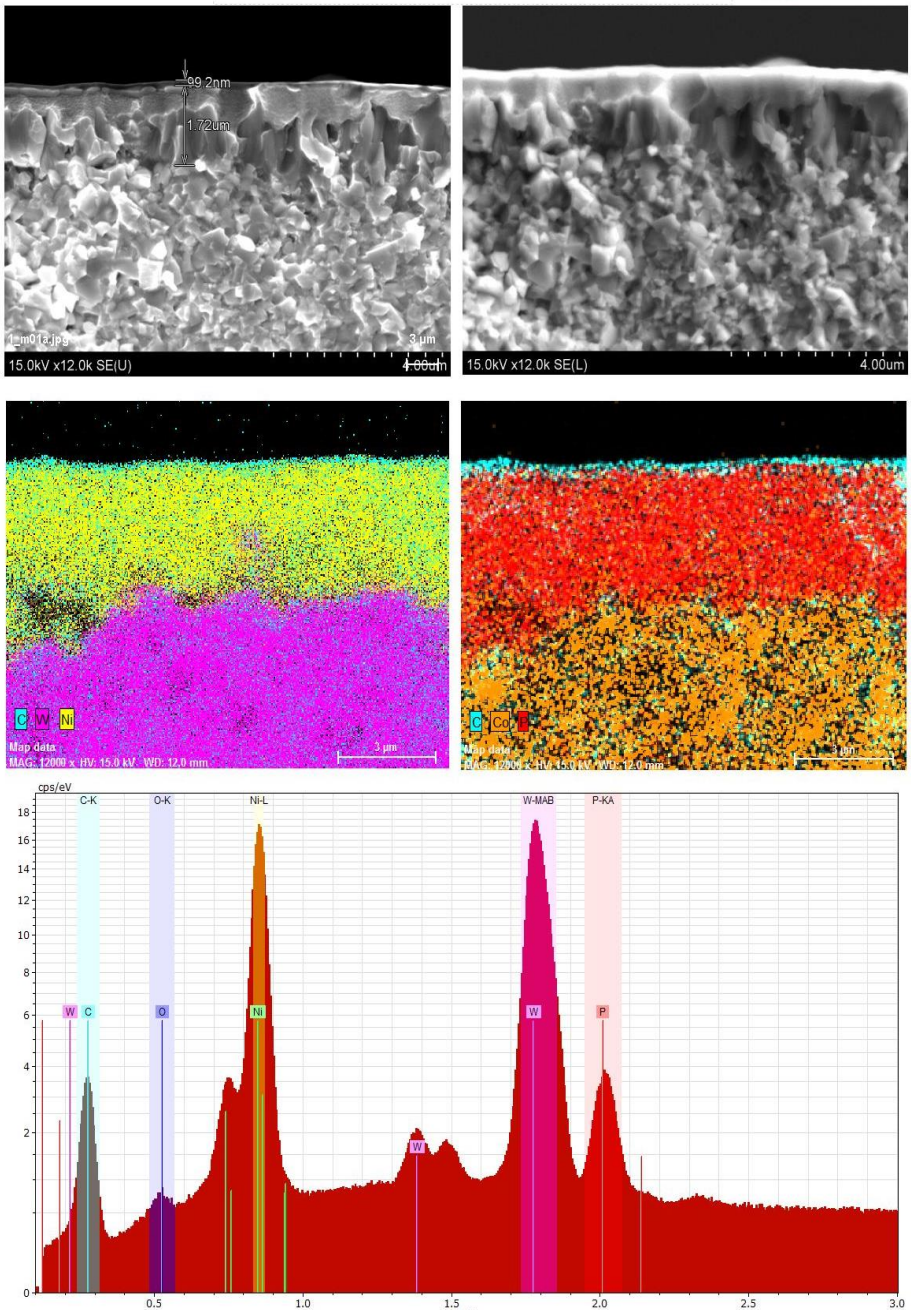

Fig. 1 Microstructure and chemical composition of the ZrC / Ni-P-UDD coating in spectroscopy diagram

Obr. 1 Mikroštruktúra a chemické zloženie povlaku ZrC / Ni-P-UDD v spektroskopickom diagrame

Scratch test analysis and pilot tests

The coating is destructed when the load has reached 26 ± 1 N, according to the obtained experimental data of the tribological tests of the ZrC/Ni-UDD coating on the Scratch Tester.

As a result, the indenter with further increase of the load begins to slide on the surface of the carbide WC-Co base. The obtained high value (Fig. 2) of the critical loads proves high adhesion of the Ni-UDD layer to the hard alloy substrate. The Ni-UDD layers are promising material for the industrial application in formation of multilayer coating with higher strength of the adhesion

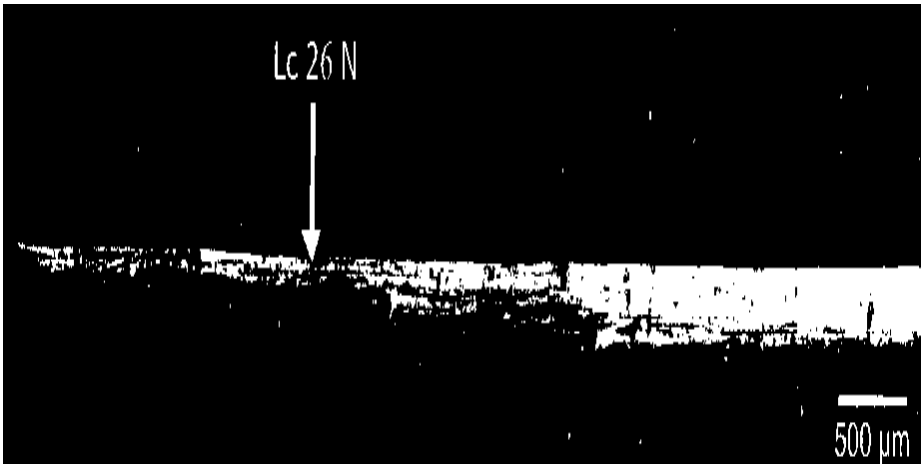

Fig. 2 Optical image of the scratch track on the ZrC/Ni-P-UDD coating
Obr. 2 Optický obraz oterovej stopy na povlaku ZrC / Ni-P-UDD

The width and shape of the cohesive path onto ZrC/Ni-P-UDD coating show non-uniformities at the beginning of scratch track that can be assigned to the surface roughness (Fig. 2). Besides, there are some delaminated coating inside the scratch channel onto ZrC/Ni-P-UDD coating. The crack formation inside of the scratch channel has indicated of coating damage, which progressive under loading of the diamond stylus. The width of the scratch channel is considerably wider than the width of the path onto ZrC/Ni-P-UDD coating at the beginning (Fig. 2), and it will achieve the maximum at the end of the scratch test (26 N).

Pilot tests of laminated chipboards

The unique structure of the ZrC/Ni-P-UDD coatings with their high strength of adhesion is used to increase the durability period of woodcutting tools for the milling of chipboard by CNC machines. Figure 3 shows the SEM images of a cross-section of the knife-edge after the pilot cutting tests of laminated chipboards. There is a significant dulling of the edge after the cutting tests.

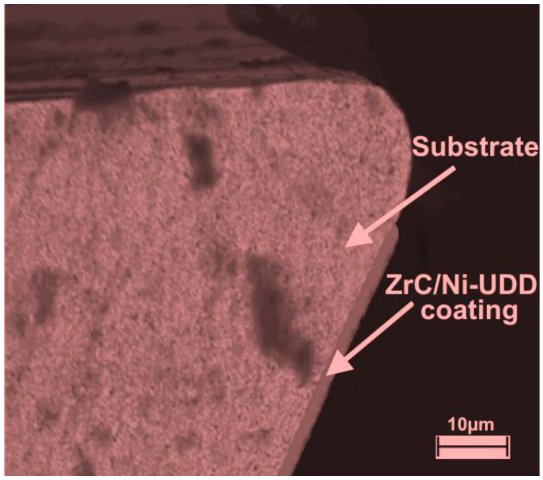

Fig. 3 SEM image of the knife edge with the ZrC/Ni-P-UDD coating after the pilot cutting tests of laminated chipboards
Obr. 3 Obraz SEM okraja noža s povlakom ZrC / Ni-P-UDD po pilotných testoch rezania laminovaných drevotrieskových dosiek

The estimation of knives after the pilot cutting tests of laminated boards shows that the volumetric wear of the knife with ZrC/Ni-P-UDD coating reduces in 2.5-2.6 times in compared with the volumetric wear of the knife without coating.

CONCLUSION

Thus, the electrochemical deposition of Ni-P sublayer with ultradisperse diamonds on hard alloy knives has allowed forming the higher adhesion of ZrC layer in multilayer coating of ZrC/Ni-UDD. The value of the critical load on the scratch track of the ZrC-Ni-P-UDD coating was 26 N. The pilot cutting tests of the knife with ZrC/Ni-P-UDD coating has proved the increase of durability period in 2.5–2.6 times than this value of the knife without coating.

Thus, the unique structure of the ZrC/Ni-P-UDD coatings with their high strength of adhesion may be used to increase the durability period of woodcutting tools for the milling of chipboard by CNC machines.

ACKNOWLEDGEMENT

Article was written as part of the project VEGA 1/0315/2017: Research of relevant properties of thermally modified wood at a contact effects in the machining process with the prediction of obtaining an optimal surface

REFERENCES

BERESNEV, V.M. et al. 2014. Tribotechnical Properties of the Coatings (Ti-Zr-Nb)N. In *J. Nano-Electron. Phys.*, Vol. 6, No. 4, pp. 4011-4015.

BURKAT, G.K., DOLMATOV, V.Yu. 2004. Application of ultrafine-dispersed diamonds in electroplating. In *Phys. Solid State*, Vol. 46, No. 4, pp. 703-710.

EGASHIRA, K. et al. 2011. Fabrication and cutting performance of cemented tungsten carbide micro-cutting tools. In *Precis. Eng.*, Vol. 35, No. 4, pp. 547-553

GRIGORIEV, S.N. et al. 2017. Comparative analysis of cutting properties and nature of wear of carbide cutting tools with multi-layered nano-structured and gradient coatings produced by using of various deposition methods. In *Int. J. Adv. Manuf. Technol.*, Vol. 90, No. 9-12, pp. 3421-3435.

CHAYEUSKI, V.V. et al. 2018. Characteristics of ZrC/Ni-UDD coatings for a tungsten carbide cutting tool. In *Appl. Surf. Sc.*, No. 446, pp. 18-26.

CHAYEUSKI, V. et al. 2016. Influence of high energy treatment on wear of edges knives of wood-cutting tool. In *MM Sci. J.*, Vol 6, pp. 1519-1523.

CHAYEUSKI, V.V. et al. 2019. Structural and Mechanical Properties of the ZrC/Ni-Nanodiamond Coating Synthesized by the PVD and Electroplating Processes for the Cutting Knifes. In *J. of Materi Eng and Perform*, Vol. 28, Issue 3, pp. 1278–1285.

KIM, Hoe-Kun et al. 2015. The effects of the H/E ratio of various Cr–N interlayers on the adhesion strength of CrZrN coatings on tungsten carbide substrates. In *Surf. Coat. Technol*., Vol. 284, pp. 230-234.

KONONOV, A.G. et al. 2015. Thermal stability of chromium coatings modified with nano-sized oxygen-containing additives. In *Mechanics of Machines, Mechanisms and Materials*, 2015, Vol. 4, pp. 353-357.

KULESHOV, A.K. et al. 2011. Properties of coatings based on Cr, Ti, Mo nitrides with embedded metals deposited on cutting tools. In *J. Friction and Wear*, Vol. 32, No. 3, pp. 192-198.

KULESHOV, A.K. et al. 2014. Effect of ZrN and Mo–N Coatings and Sulfacyanization on Wear of Wood-Cutting Knives. In *J. Frict. Wear*, Vol. 35, No. 3, pp. 201-209.

KUMAR, T. S et al. 2014. Metallurgical Characteristics of TiAlN/AlCrN Coating Synthesized by the PVD Process on a Cutting Insert. In *J. Mat. Eng. Perf*., Vol. 23, No. 8, pp. 2877-2884.

MA, G. et al. 2015. The friction coefficient evolution of a TiN coated contact during sliding wear. In *Appl. Surf. Sci.*, Vol. 345, pp. 109-115.

MATEI, A.A. et al. 2015. Structural characterization and adhesion appraisal of TiN and TiCN coatings deposited by CAE-PVD technique on a new carbide composite cutting tool. In *J. Adhesion Sci. Tech.*, Vol. 29, No.23, pp. 2576-2589.

PALOMAR, F.E. et al. 2010. Coatings made of tungsten carbide and tantalum carbide for machining tools. In *Vacuum*, Vol. 84, pp. 1236-1239.

TILLMANN, W., MOMENI, S. 2016. Tribological development of TiCN coatings by adjusting the flowing rate of reactive gases. In *J. Phys. Chem. Solids*, Vol. 90, pp. 45-53.

Contact address:

Assoc. prof. Ing. Valery Zhylinski, PhD, Belarussian State Technological University, 220006, Belarus, Minsk, Sverdlov St. 13a, email: zhilinski@yandex.ru

TECHNICAL-TECHNOLOGICAL CHARACTERISTICS OF THE THERMAL PROCESS OF COLOR MODIFICATION OF BIRCH WOOD WITH SATURATED WATER STEAM

TECHNICKÉ A TECHNOLOGICKÉ CHARAKTERISTIKY PROCESU TERMICKEJ MODIFIKÁCIE FARBY BREZOVÉHO DREVA SÝTOU VODNOU PAROU

Ladislav Dzurenda

Faculty of Wood Sciences and Technology, Technical University in Zvolen, 960 01 Zvolen, Slovakia, dzurenda@tuzvo.sk

ABSTRACT: The aim of this work is to present the technical-technological characteristics of the process of modification of the color of birch timber, thickness h ≤ 40 mm with water vapor for 3 modes with temperatures I = 105 ± 2.5 °C, tII = 125 ± 2.5 °C and tIII = 135 ± 2.5 °C for τ = 7.5 hr. Based on the targeted experimental work and the subsequent analyzes, the following are defined for the individual modes of thermal modification of birch wood color:
– the density of thermally modified birch wood by saturated steam,
– acidity values of thermally modified birch wood saturated with water vapor,
– coordinates of thermally modified birch wood in color space CIE L * a * b *,
– range of total color differences ΔE * thermally modified birch wood,
– norms of heat consumption per 1 m^3 of thermal modification of color of birch wood,
– consumption norms for saturated water vapor per m^3 of thermal modification of birch wood color with saturated steam.

Keywords: birch wood, the CIE–L*a*b*colour space, thermal treatment, saturated water steam, technical and technological parameters.

ABSTRAKT: Cieľom práce je prezentácia technicko–technologických charakteristík procesu modifikácie farby brezového reziva hrúbky h ≤ 40 mm sýtou vodnou parou pre 3 režimy s teplotami t_I = 105±2.5°C, t_{II} = 125±2.5°C a t_{III} = 135±2.5°C po dobu τ = 7,5 hod.
Na základe cielených experimentálnych prác a následne vykonaných analýz, sú pre jednotlivé režimy termickej modifikácie farby brezováho dreva sýtou vodnou parou stanovené:
– hodnoty hustoty termicky modifikovaného brezového dreva sýtou vodnou parou,
– hodnoty acidity termicky modifikovaného brezového dreva sýtou vodnou parou,
– súradnice termicky modifikovaného brezového dreva vo farebnom priestore CIE L*a*b*,
– škála celkových farebných diferencií ΔE*termicky modifikovaného brezového dreva,
– normatívy spotreby tepla na 1 m^3 termickej modifikácie farby brezového dreva sýtou vodnou parou.
– normatívy spotreby sýtej vodnej pary na 1 m^3 termickej modifikácie farby brezového dreva sýtou vodnou parou.

Kľúčové slová: breza, farebný priestor CIE-L*a*b*, termická úprava, sýta vodná para, technické a technologické parametre.

INTRODUCTION

Wood colour is one of the most important macroscopic features differentiating the appearance of individual wood species. Wood colouring is caused, besides basic chemical components: cellulose, hemicelluloses, and lignin, by accessory substances such as dye, tanning agent, resins located in cell walls and lumens.

Timber placed in the environment of hot water, saturated water steam or saturated humid air is getting warmer and its physical, mechanical and chemical properties changes. Mentioned facts are used in technology of steam bending and boiling during veneers and plywood, bent furniture or pressed wood manufacturing processes (Kollmann & Gote 1968; Nikolov *et al*. 1980; Sergovsky & Rasev 1987; Lawnniczak 1995; Trebula 1996; Deliiski 2003).

Thermal treatment processes of wood with saturated water steam, in addition to specific physico-mechanical changes of wood, are accompanied by chemical reactions such as partial hydrolysis and extraction leading to a colour change as well (Melcer *et al*. 1989; Bučko 1995; Kačík 2001; Geffert *et al*. 2017). In the past, colour modification, especially wood darkening, was used to remove undesirable differences in colour of lighter sapwood and darker heartwood, or to remove wood stains resulting from steaming or moulding. Recently, the research has been aimed at the colour change of specific wood species to more or less distinctive hues or imitation of the exotic wood species (Tolvaj *et al*. 2009; Dzurenda 2014; Barcik *et al*. 2015; Baranski *et al*. 2017; Hadjiski & Deliiski 2016, Dzurenda 2018).

The aim of the thesis is to determine the technical and technological characteristics of thermal modification of birch wood color in the form of sawn timber with thicknesstimber $h \leq 40$ mm by saturated water vapor with temperature modes: $t_I = 105 \pm 2.5$ ° C, $t_{II} = 125 \pm 2.5$ ° C and $t_{III} = 135 \pm 2.5$ ° C time $\tau = 7.5$ hours.

MATERIALS AND METHODS

Birch wood in a form of sawn timber with thickness h = 40 and the moisture content of $w_p = 56.8 \pm 5.3$ % was thermally treated with saturated water steam in the pressure autoclave: APDZ 240 (Himmasch AD, Haskovo, Bulgaria) in the company Sundermann Ltd. Banská Štiavnica. Mode of colour modification of birch sawn timber with saturated water steam is shown in Fig.1. and the technical parameters of each mode are given in tab. 1.

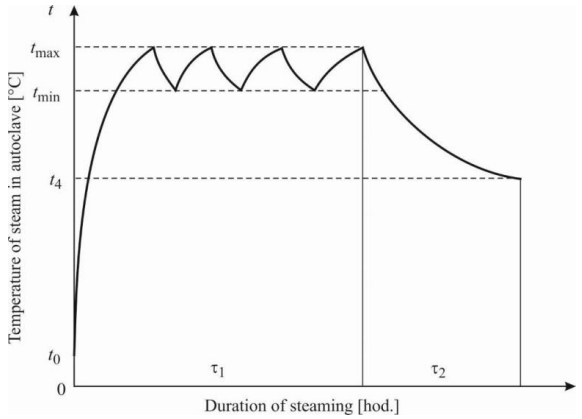

Fig. 1. Mode of color modification of birch wood with saturated water steam.
Obr. 1. Režim pre modifikáciu farby brezového dreva sýtou vodnou parou.

Table 1. Modes of color modification of birch wood with saturated water steam
Tabuľka 1. Režimy farebnej modifikácie brezového dreva sýtou vodnou parou

Modes	Temperature of the saturated water steam, °C			Duration technological process of thermal treatment of wood τ, h		
	t_{min}	t_{max}	t_4	τ_1–stage I	τ_2–stage II	Total $\tau_1 + \tau_2$
Mode I.	102.5	107.5	100	6.0	1.5	7.5
Mode II.	122.5	127.5	100			
Mode III.	132.5	137.5	100			

The density of wood in a dry state was determined in accordance with STN 49 0108:1993 Wood – Determinination of density. Wood density from the measured weights of samples and their volumes was calculated using the equation:

$$\rho_0 = \frac{m_0}{V_0} \qquad [kg \cdot m^{-3}] \tag{1}$$

where: m_0 – weight of the dry sample [kg],
V_0 – volume of the dry sample [m^3].

The pH value of wet wood was measured on samples of 75 pieces of timber before the thermal process, as well as after its termination and cooling of the wood. Forasmuch as the diameter of sensor head of the potentiometer used to measure pH is d = 10 mm and it cannot be placed (immersed) into the solid material, the hole with the diameter of 12 mm was formed in the place of measurement with the accu drilling machine. Sawdust resulting from drilling was poured into the hole and the sensor head LanceFET+H 22704-010 of the pH meter SENTRON SI 6OO was inserted into wet sawdust.

Subsequently, thermally colored modified birch timber by individual modes as well as thermally untreated timber was dried to a moisture content of w = 12 ± 0.5% in a conven-

tional hot air dryer: KAD 1x6 (KATRES s.r.o). Longitudinal and transverse manipulations were made woodturning blanks with the dimensions: 40 x 80 x 600 mm. Surfaces and edges were processed using Swivel spindle milling machine FS 200.

Color Reader CR-10 (Konica Minolta, Japan) was used to assess wood colour of birch sawn timber in the CIE-L*a*b*colour space. The light source D65 with lit area of 8mm was used.

The brightness values L * and chromatic coordinates a *, b * of the color space CIE-L* a* b* were measured on the set n = 45 birch blanks of thermally untreated birch wood, n = 66 birch blanks of thermally treated wood with mode I., n = 68 birch blanks from thermally treated wood with water vapor mode II. and n = 65 birch blanks from thermally treated wood with water vapor saturation mode III.

Color coordinates of thermally untreated as well as treated birch wood are introduced using a formula $x = \bar{x} \pm s_x$, it means using the average measured value and standard deviation. The extent of variation of set values in the CIE-L* a* b* colour space of thermally untreated as well as treated birch wood is determined by the coefficient of variation.

Total color difference ΔE* is determined according to following formula, in accordance with the standard ISO 11 664-4 as the result of the difference in the colour coordinates ΔL*, Δa*, Δb* set following the surface measurements of thermally untreated as well as treated birch timber

$$\Delta E^* = \sqrt{\left(L_2^* - L_1^*\right)^2 + \left(a_2^* - a_1^*\right)^2 + \left(b_2^* - b_1^*\right)^2} \tag{2}$$

where: L^*_1, a^*_1, b^*_1 coordinate values in the wood color space of dried, milled thermally un modified birch wood,

L^*_2, a^*_2, b^*_2 coordinate values in the wood color space of dried, milled thermally modified birch wood.

Rate of change in the wood colour and hues during the processes of thermal treatment following the total colour difference ΔE* can be classified according to the chart mentioned by the authors: Cividini et al.(2007) shown in Tab.2.

Table 2. Classification of total colour difference ΔE*
Tabuľka 2. Klasifikácia celkovej farebnej zmeny ΔE*

0.2 < ΔE*	Not visible difference
0.2 < ΔE* < 2	Small diference
2 < ΔE* < 3	Color difference visible with high quality screen
3 < ΔE* < 6	Color difference visible with medium quality screen
6 < ΔE* < 12	High color difference
ΔE* > 12	Difference colours

Energy consumption of the technological process of birch sawn timber color modification is presented through the heat consumption standard Q_{TFS} and saturated water steam consumption per 1 m^3 of wood. Heat consumption standard of colour modification of 1 m^3

wood is according to the research of *Dzurenda (2016)* described by the formula:

$$Q_{ha} = \frac{Q_{hw} + Q_{hf} + Q_{hil} + Q_{he} + Q_{hfv} + Q_{hew}}{V_w}, \quad (\text{MJ/m}^3) \tag{3}$$

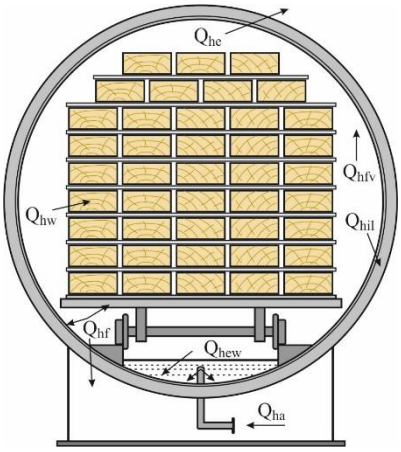

Fig. 2. The structural model of the heat distribution in the autoclave in the process of modifying the color of the wood with saturated water steam.
Obr. 2. Štruktúrny model distribúcie tepla v autokláve v procese modifikácie farby dreva nasýtenou vodnou parou.

where: Q_{hf} – heat necessary to heat the construction material of the autoclave, MJ;
Q_{hw} – heat necessary for heating colour modification wood, MJ;
Q_{hil} – heat necessary to heat the autoclave's insulation, MJ;
Q_{he} – heat necessary to cover heat losses from the surface of the pressure autoclave, MJ;
Q_{hfv} – heat extracted by condensate from the pressure autoclave, MJ;
Q_{hew} – heat extracted by saturated steam after opening the autoclave, MJ;
V_w – volume of the colour modification wood in the pressure autoclave, m³;

The consumption of saturated water steam necessary for colour modification of 1m³ of birch sawn timber is determined using the formula:

$$m'' = \frac{Q_{ha}}{h'' - h'} \quad (\text{kg/m}^3) \tag{4}$$

where: Q_{ha} – heat consumption standard to modify 1 m³ of birch sawn timber, kJ/m³;
h'' – enthalpy of saturated water steam at the temperature t_{max}, kJ/kg;
h' – enthalpy of saturated water at the temperature t_4, kJ/kg.

RESULTS AND DISCUSSION

The colour of wood of *Betula pendula Roth.* is according to the authors: Perelygin (1965), Makoviny (2010), Klement et al. (2010) pale white-brown. The authors: Babiak et al. (2004), describe the color of birch wood using coordinates in the CIE-L* a* b* colour space: L* = 78,07; a* = 5,92; b* = 20,02. Mentioned statements are confirmed by our measurements as well. According to the results, the coordinates of birch wood on the planed surface at birch wood moisture w ≈ 12% in the CIE-L* a* b* colour space are: L * = 82.7 ± 1.3; a * = 6.7 ± 0.6; b * = 19.8 ± 0.9.

The results of laboratory work determining the density of both thermally untreated and thermally treated birch wood by individual modes in the dry state are shown in Table 3.

Table 3. The density of the dry untreated and thermally treated birch wood.
Tabuľka 3. Hustoty suchého termicky neupravovaného i upravovaného brezového dreva.

Thermal Modification Modes	Basic statistical characteristics of the density of wood in a dry state			
	ρ_0 [kg·m^{-3}]	s [kg·m^{-3}]	v_x [%]	n [-]
Untreated wood	704.0	61.1	8.6	17
Modification Mode I.	696.0	55.0	7.9	18
Modification Mode II.	678.0	60.1	8.8	16
Modification Mode III.	675.0	67.6	10.0	17

The density of dry birch wood decreases as a result of thermal treatment. The density drop is from $\Delta\rho_0$ = 1.15 % by heat treatment by mode I. after $\Delta\rho_0$ = 4.29 % for heat treatment by mode III.

Acidity of wet thermally untreated birch wood at a w ≈ 53.9% humidity is pH = 5.3 ± 0.2.

The measured values acidity of wet thermally modified birch different modes for cooling are shown in Table. 4.

Table 4. Measured values of moisture and acidity of thermally modified birch wood.
Tabuľka 4. Namerané hodnoty vlhkosti a acidity tepelne modifikovaného dreva brezy.

Modes	The temperature of the saturated water vapor	Wood moisture content	pH value
Mode I.	t_I = 105 ± 2.5 °C	w ≈ 45,5 %	pH = 4,6 ± 0,2
Mode II.	t_{II} = 125 ± 2.5 °C	w ≈ 43,8 %	pH = 3,7 ± 0,3
Mode III.	t_{III} = 135 ± 2.5 °C	w ≈ 46,5 %	pH = 3,3 ± 0,2

Measured pH values of birch in the process of heat treatment confirm the knowledge about the hydrolysis of polysaccharides in wet wood during the application of heat. Products of hydrolysis and extraction after wood boiling or other heat treatment processes mentioned in works: Melcer et al (1989), Kačík (2001), Laurova et al. (2004), Samešova el al. (2018) were quantified using the hydromodulus or created condensate. Measuring the pH value of wet wood using the potentiometer SENTRON SI 600 with the sensor head LanceFET+H 22704-010 can be considered unique. This way, wood hydrolysis and its ef-

fect on the wood colour change can be monitored. Following the measured values of acidity of wet wood resulting from the given modes of heat treatment of birch wood, the fact that the temperature affects the hydrolysis of hemicelluloses and the change in the chromophore system of wood more significantly than the time of heat treatment process can be stated.

The colour of dried planed, thermally untreated birch wood and the hue resulting from the thermal treatment with saturated water steam are shown in Fig. 2.

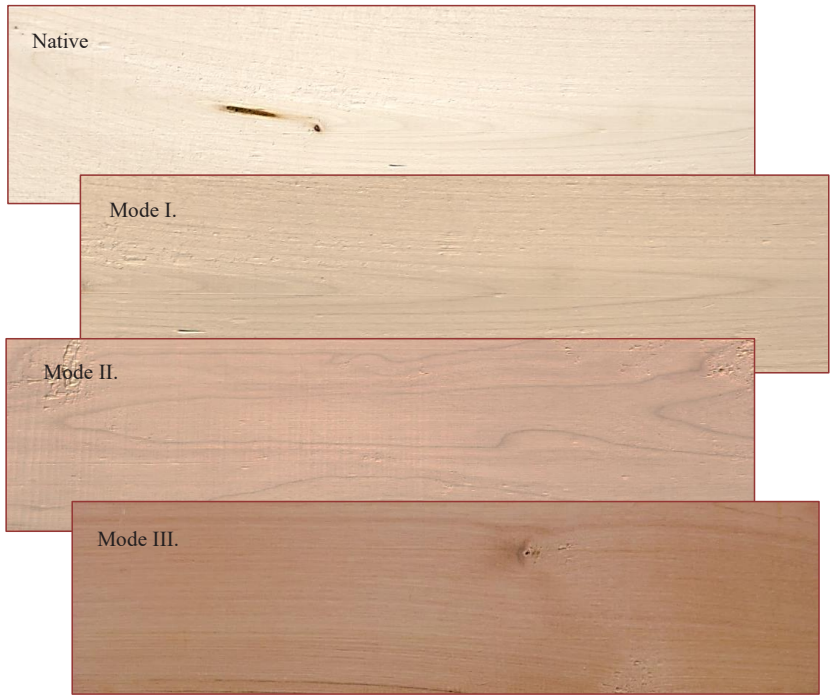

Fig. 3. View of birch wood before and after heat treatment by individual modes.
Obr. 3. Pohľad na brezové drevo pred a po tepelnom spracovaní jednotlivými režimami.

The original pale white-brown color of birch wood changes to brown colored shades in the thermal treatment process. As the temperature of the saturated water vapor increases, the shade of the birch wood darkens.

Based on the visual control of the color of the wood on the surfaces and the side surfaces of the birch blanks as well as the measurement of the values on the individual color coordinates, it can be stated that the birch wood is uniformly colored throughout the volume. This fact makes it possible to use thermally modified sawmill assortments for the production of lamellas for the production of floorings, respectively other 3D woodworking without worrying about the uneven color of the wood after its cross-section.

Coordinates in the CIE-L*a*b* colour space describing the colour of wood before and after thermal treatment on dried and planed surface are mentioned in Tab. 5.

Table 5 Coordinates in the CIE-L*a*b* colour space of birch wood before and after thermal treatment with saturated water steam.
Tabuľka 5 Súradnice farieb brezového dreva vo farebnom priestore CIE-L*a*b* pred a po tepelnom spracovaní nasýtenou vodnou parou.

Birch		Coordinates		
		L*	a*	b*
Native wood – thermally untreated	number of measurements [-]	45	45	45
	Average coordinate value [-]	82,7	6.7	19.8
	Standard deviation [-]	1.3	0.6	0.9
	Coefficient of variation [%]	1.5	8.8	4.5
Wood after heat treatment with mode I.	number of measurements [-]	66	66	66
	Average coordinate value [-]	75.7	10.6	21.2
	Standard deviation [-]	1.2	0.7	0.8
	Coefficient of variation [%]	1.5	6.6	3.8
Wood after heat treatment with mode II.	number of measurements [-]	68	68	68
	Average coordinate value [-]	67.3	11.9	18.5
	Standard deviation [-]	1.2	0.7	0.7
	Coefficient of variation [%]	1.7	5.9	3.8
Wood after heat treatment with mode III.	number of measurements [-]	65	65	65
	Average coordinate value [-]	56.8	12.4	18.3
	Standard deviation [-]	1.1	0.6	0.4
	Coefficient of variation [%]	1.9	4.8	2.2

The rate of change of values ΔL*, Δa*, Δb* for individual coordinates of the colour space of birch wood resulting from the heat treatment process with saturated water steam is shown in bar graph in Figure 4.

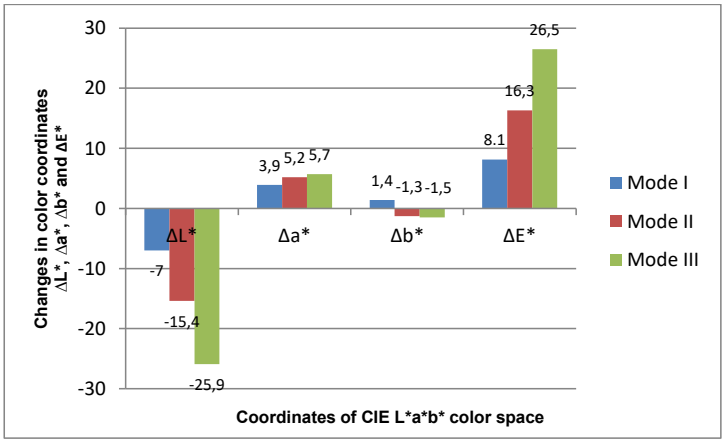

Fig. 4. The change of ΔL*, Δa*, Δb* values of the CIE-L*a* b* colour space of the thermally treated birch wood resulting from the colour modification modes I., II., III. and total color difference ΔE*.
Obr. 4. Zmeny **ΔL*, Δa*, Δb*** na súradniciach farebného priestoru CIE-L* a* b* v procese tepelného spracovania brezového dreva režimami I., II., III. a celková farebná diferencia **Δ**E *.

The biggest changes in the individual coordinates in the color space CIE L*a*b* are at the coordinates of the lightness As the temperature of the saturated water vapor increases, the lightness difference ΔL * increases, too. While in mode I. with a saturated water temperature t = 105 ± 2.5 ° C the decrease in lightness is ΔL* = -7.0, so in the process of thermal modification of birch wood color by mode III. with a temperature of t = 135 ± 2.5 ° C, the decrease in lightness is almost 4 times.

Changes in chromatic coordinates of red color a* and yellow colors b* are not as pronounced. While, at the coordinate of the red color, the values increase from Δa* = 3.9 to Δa* = 5.7, the values yellow color oscillates around Δb* = ± 1.5 to the yellow coordinates.

Total colour differences of the birch wood ΔE* resulting from the heat treatment processes by saturated water steam in at the temperature interval t = 105 °C ÷ 137 °C ranges from the values of ΔE* = 8.1 ÷ 26.5. Within the colorimetric classification of the colour changes shown in Tab. 2, achieved hues can be defined into the category of visible and great color changes. The pale brown shade of birch wood acquired by the thermal modification I mode with a total color difference of ΔE* = 8.1 belongs to the category of visible changes in color shades to the naked eye. Color changes of birch wood achieved by modes II. and III. with color difference values: E* = 16.3 ÷ 26.5 ranges birch wood to the category of large variations in brown color shades.

Dependence of the growth of the total colour differences ΔE* of thermally treated birch wood on the temperature of saturated water steam in the CIE-L* a* b* colour space is consistent with the knowledge of wood colour changes during the heat treatment processes described by the authors: Molnar & Tolvaj (2002), Dzurenda (2014, 2018), as well as of high temperature drying in the environment of superheated water steam Klement & Marko (2009); Baranski et al. (2017), or heat processes in the production of thermowood Barcik et al.(2015).

From the aspect of the operational efficiency of the process of thermal modification of the color of the wood by the water vapor saturation, the question of the energy intensity of the technological process is not negligible. Heat consumption of the heat balance of the technological process for individual modes of color modification of birch timber thickness h = 40 mm with moisture content w ≈ 56% and initial wood temperature t_d ≈ 15° C in pressure autoclave APDZ 240, for capacity autoclave V_D = 16 m^3, Table 6.

Table 6. Heat consumption for technological process of color modification of birch wood in the form of sawn timber h = 40 mm in autoclave AZDZ 240.
Tabuľka 6. Spotreba tepla pre technologický proces farebnej modifikácie brezového reziva h = 40 mm v autokláve AZDZ 240.

Name of the heat consumption item	Symbol	Mode I.		Mode II.		Mode III.	
		MJ	[%]	MJ	[%]	MJ	[%]
Heating colour homogenised wood	Q_{hw}	3 500.1	69.2	4339.9	71.2	4 770.7	71.9
Heating the autoclave‘s construction material	Q_{hf}	540.0	10.6	540.0	8.8	540.0	8.2
Heating the autoclave‘s insulation	Q_{hil}	84.4	1,7	101.7	1.6	110.4	1,7
Heat losses of the pressure autoclave	Q_{he}	90.4	1.8	106.0	1.7	112.9	1.7
Heat losses from extracted steam	Q_{hfv}	54.9	1.1	54.9	0.9	54.9	0.8
Heat losses from extracted condensate	Q_{hfw}	791.9	15.6	955.9	15.8	1039.8	15.7

Table 7 shows the normative values of heat consumption and the consumption of saturated water vapor of the pressure autoclave APDZ 240 for individual modes of wood color modification 1 m3 of birch timber thickness h = 40 mm.

Table 7. The consumption heat and the consumption of saturated water steam autoclave APDZ 240 for modification modes 1 m^3 birch sawn timber thickness h = 40 mm
Tabuľka 7. Spotreby tepla a sýtej vodnej pary tlakového autoklávu APDZ 240 pre jednotlivé režimy farebnej modifikácie dreva pre 1 m^3 brezového reziva hrúbky h = 40 mm

Modes	Normative value of heat consumption MJ/m^3	Consumption of saturated water vapor kg/m^3
Mode I.	Q_{ha} = 316.3	m″ = 143.7
Mode II.	Q_{ha} = 381.2	m″ = 173.3
Mode III.	Q_{ha} = 414.3	m″ = 188.3

The heat consumption per 1m^3 of thermally colored wood, depending on the temperature of the saturated steam in the process, is in the range of: Q_{ha} = 316.3–414.3 MJ/m^3.

The stated values of heat consumption compared to the values of heat consumption in the process of wood vapor at atmospheric pressure in the steam chambers, or thermal treatment of veneer prisms in pools, as described by (Trebula 1986; Dzurenda & Deliiski 2010,2011) are significantly lower.

Mentioned statement results not only from 3–4 shorter time of the technological process, as well as by the fact that 2/3 to 3/4 of the applied heat is directly used for heating the wood to the required technological temperature Dzurenda (2017).

The negative fact of the technological process of color modification of wood with saturated steam is the fact that said technological process is a typical discontinuous process characterized by uneven heat consumption Figure 5.

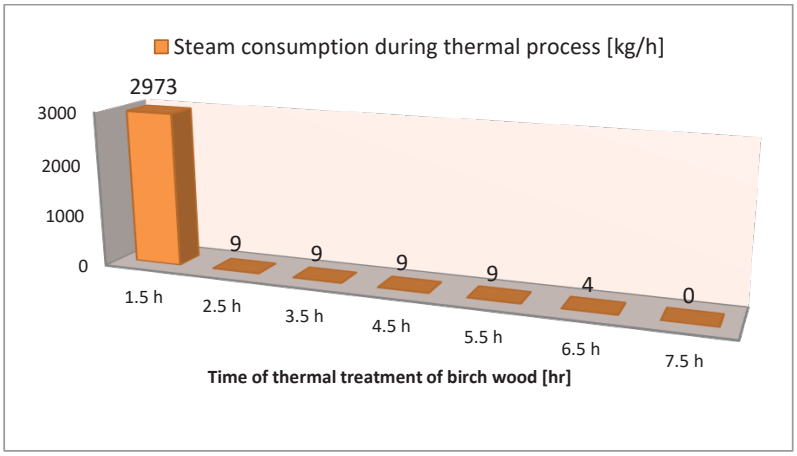

Fig. 5. The consumption of saturated water vapor in proces modification of color V = 16 m^3 of birch sawn timber h = 40 mm according to mode III. in APDZ 240 autoclave.
Obr. 5. Spotreba nasýtenej vodnej pary v procese úpravy farby V = 16 m^3 brezového reziva h = 40 mm podľa režimu III. v autokláve APDZ 240.

Following the analysis of the heat consumptions during the technological process, the highest heat consumption is at the beginning of the process at the time $\tau_o \approx 1.5$ hours when the heat of the condensing water steam is used to heat modified wood and the autoclave as well can be stated. Subsequently, the heat of condensing saturated water steam is used to cover heat losses of the autoclave. During the II. phase of the technological process τ_2 saturated water steam does not enter the autoclave. Heat losses of the autoclave are covered by the heat from isochoric cooling of saturated steam in the autoclave and the heat from cooling process of autoclave construction material. For mode III. thermal modification of birch timber color h = 40 mm saturated water vapor with temperature t = 137 °C, the course of steam consumption during the technological process time is displayed.

CONCLUSION

On the basis of targeted experimental work and subsequent analyzes, the paper presents the technical and technological characteristics of the process of modification of the color of birch timber, thickness $h \leq 40$ mm by saturation water vapor modes with temperatures $t_I = 105 \pm 2.5$°C, $t_{II} = 125 \pm 2.5$°C a $t_{III} = 135 \pm 2.5$°C for $\tau = 7.5$ hours.

- The density of dry birch wood decreased due to thermal modification from $\rho_0 = 704{,}0 \pm 40{,}6$ kg.m^{-3} to $\rho_0 = 696{,}0 \pm 55{,}0$ kg.m^{-3} after thermal treatment by mode I. and to $\rho_0 = 675{,}0 \pm 67{,}6$ kg.m^{-3} after thermal treatment with mode III.
- The wet birch wood by thermal process mode I. changes acid from pH = 5.3 to pH = 4.6, mode II. to pH = 3.7 and Mode III. to pH = 3.3.II. na pH = 3.7 a režimom III. na pH = 3.3.
- The color of birch wood has changed from a light white to brown color by a thermal process. As increasesthe temperature of the saturated vapor water the birch wood darkens and brown.The color shade of thermally treated wood by mode I. in the color space CIE–L * a * b * is identified by the coordinates: L * = 75.7 ± 1.2; a * = 10.6 ± 0.7; b * = 21.2 ± 0.8, mode II. coordinates: L * = 67.3 ± 1.2; a * = 11.9 ± 0.7; b * = 18.5 ± 0.7 and mode III. coordinates: L * = 56.8 ± 1.1; a * = 12.4 ± 0.6; b * = 18.3 ± 0.4.
- The scale of total color differences ΔE * of thermally modified birch wood by individual regimes is in the interlude values ΔE * = 8.1–26.5, ie in terms of categorization of color changes reported by Cividini et al. (2007) birch thermally modified wood belongs to the category of visible and large color changes.
- Heat consumption per m^3 of thermal modification of birch wood color in APDZ 240 autoclave for mode I. is $Q_{ha} = 316.3$ MJ.m^{-3}, for mode II. is $Q_{ha} = 316.3$ MJ.m^{-3} and for mode III. is $Q_{ha} = 316.3$ MJ.m^{-3}.

The new color shades of birch wood, achieved by the process of thermal modification of wood color by water vapor, without major changes in the mechanical properties of wood, extend the possibilities of wider use of birch wood in the building-joinery, construction-artistic and design areas.

ACKONWLEDGEMENT

This experimental research was prepared within the grant project: *APVV-17-0456 „Termická modifikácia dreva sýtou vodnou parou za účelom cielenej a stabilnej zmeny farby drevnej hmoty"* as the result of work of author and the considerable assistance of the APVV agency.

REFERENCES

BABIAK, M., KUBOVSKÝ, I., MAMOŇOVÁ, M. 2004. Farebný priestor vybraných domácich drevín. In: *Interaction of wood with various Forms of Energy*. Technická univerzita Zvolen, pp. 113 – 117.

BARAŃSKI, J., KLEMENT, I., VILKOVSKÁ, T., KONOPKA, A. 2017. High Temperature Drying Process of Beech Wood (Fagus sylvatica L.) with Different Zones of Sapwood and Red False Heartwood. In: *BioResources* 12(1), 1861-1870. DOI:10.15376/biores.12.1.1761-1870.

BARCIK, Š., GAŠPARÍK, M., RAZUMOV, E.Y. 2015. Effect of thermal modification on the colour changes of oak wood. In: *Wood Research*. 60 (3):385-396.

BUČKO, J. 1995. Hydrolýzne procesy. Zvolen: Vydavateľstvo TU Zvolen, 116 p.

CIVIDINI, R., TRAVAN, L., ALLEGRETTI, O. 2007. White beech: A tricky problem in drying process. In: *International Scientific Conference on Hardwood processing*. September 24-25-26, 2007 Quebec City, Canada.

DELIISKI, N. 2003. Modelirane i technologii za proparvane na drvesiny materiali v avtoklavi. DSc. Thesis, University of Forestry, Sofia, 358 p.

DZURENDA, L., DELIISKI, N. 2010. Tepelné procesy v technológiách spracovania dreva. Zvolen: Vydavatelstvo TU vo Zvolene, 274 p.

DZURENDA, L., DELIISKI, N. 2011. Matematický model pre stanovenie normatívu spotreby tepla na plastifikáciu preglejkárenských výrezov a priziem v bazénoch pre termickú úpravu dreva In: Acta Facultatis Xylologiae Zvolen. 2011, 53(2):25-36, ISSN 1336-3824.

DZURENDA, L. 2014. Sfarbenie bukového dreva v procese termickej úpravy sýtou vodnou parou. In: Acta facultatis xylologiae Zvolen, 56 (1):13 – 22.

DZURENDA, L. 2016: Numeric Model of the Normative Consumption of Heat for the Colour Homogenisation of Wood in Pressure Autoclaves. In: AIP Conf. Proc. 1745, 020008-1–020008-7; (2016), doi: 10.1063/1.4953702

DZURENDA, L. 2017: The Effect of Saturated Steam Vapor Temperature on Heat Consumption in the Process of Color Modification of Acacia Wood. In: AIP Conf. Proc. 1889, 020006-1–020006-5; (2016), doi: 10.1063/1.5004340

DZURENDA, L. 2018. The Shades of Color of Quercus robur L. Wood Obtained through the Processes of Thermal Treatment with Saturated Water Vapor. In: *BioResouces* 13(1), 1525–1533; doi: 10.1063/biores 13.1.1525-1533.

GEFFERT, A., VÝBOHOVÁ, E., GEFFERTOVÁ, J. 2017. Characterization of the changes of colour and some wood components on the surface of steamed beech wood. In: Acta facultatis xylologiae Zvolen, 59 (1):49 – 57, ISSN 1366-3824, doi: 10.17423/afx.2017.59.1.05.

HADJISKI, M., DELIISKI, N. 2016. Advanced Control of the Wood Thermal Treatment Processing. In: Cybernetics and Information Technologies. Bulgarian Academy of Sciences 16(2):176-197.

ISO 11 664-4:2008 Colorimetry-Part 4: CIE 1976 L*a*b* Colour space.

KAČIK, F. 2001. Tvorba a chemické zloženie hydrolyzátov v systéme drevo-voda-teplo. Zvolen: TU Zvolen, 75 p.

KLEMENT, I., MARKO, P. 2009. Colour changes of beech wood (Fagus sylvatica L.) during high temperature drying process. In: *Wood research* 54 (3): 45-54.
KLEMENT, I., RÉH, R., DETVAJ, J. 2010. Základné charakteristiky lesných drevín – spracovanie drevnej suroviny v odvetví spracovania dreva. NLC Zvolen, 82 p .
KOLLMANN, F., GOTE, W. A. 1968. Principles of Wood Sciences and Technology, Vol. 1. Solid Wood, Springer Verlag: Berlin – Heidelberg–New York, 592 p.
LAUROVA, M., MAMONOVA, M., KUČEROVA, V. 2004. Proces parciálnej hydrolýzy bukového dreva (Fagus sylvatica L.) parením a varením. Zvolen: TU Zvolen. 58 p.
LAWNICZAK, M. 1995. Zarys hydrotermicznej i plastycznej obróbki drewna. Czesc I. – Warzenie i parzenie drewna. Poznan, 149 p.
MAKOVÍNY, I. 2010. Úžitkové vlastnosti a použitie rôznych druhov dreva. Zvolen: Technická univerzita Zvolen, 104 p.
MELCER, I., MELCEROVÁ, A., SOLÁR, R., KAČÍK, F. 1989. Chemizmus hydrotermickej úpravy listnatých drevín. Zvolen: Vysoká škola lesnícka a drevárska, 2/1989, 76 pp.
MOLNAR, S., TOLVAJ, L. 2002: Colour homogenisation of different wood species by steaming. In: Interaction of wood with various Forms of Energy. Technical university in Zvolen, p. 119−122.
NIKOLOV, S., RAJCHEV, A., DELIISKI, N. 1980. Proparvane na drvesinata. Sofia: Zemizdat, 174 p.
PERELYGIN, L., M. 1965. Náuka o dreve, Bratislava: SVTL, 444 p.
SAMEŠOVÁ, D., DZURENDA, L., JURKOVIČ, P. 2018. Kontaminácia kondenzátu produktmi hydrolýzy a extrakcie v termickom procese farebnej modifikácie roztrúsenopórovitých listnatých drevín. In: *Trieskové a beztrieskové obrábanie dreva*, 11(1): 235–239. ISSN 2453-904X
SERGOVSKIJ, P. S., RASEV, A. I. 1987. Gidrotermičeskaja obrabotka i konservirovanije drevesiny. Lesnaja promyšlennost, Moskva, 360 p.
STN 49 0108:1993 Drevo – Zisťovanie hustoty.
TOLVAJ, L., NEMETH, R., VARGA, D., MOLNAR, S. 2009. Colour homogenisation of beech wood by steam treatment. In: *Drewno*. 52 (181): 5-17.
TREBULA, P. 1996. Sušenie a hydrotermická úprava dreva. Zvolen: TU Zvolen, 255 p.

Contact address:
Ladislav Dzurenda, Faculty of Wood Sciences and Technology, Technical University in Zvolen, 960 01 Zvolen, Slovakia, dzurenda@tuzvo.sk

THE CHANGE OF ACIDITY AND COLOR OF BIRCH WOOD IN THE PROCESS OF THERMAL MODIFICATION

ZMENA ACIDITY A FARBY BREZOVÉHO DREVA POČAS TERMICKEJ MODIFIKÁCIE

Michal Dudiak [a)], **Anton Geffert** [b)], **Jarmila Geffertová** [c)]

Technical university of Zvolen, Faculty of Wood Sciences and Technology, T. G. Masaryka 24 960 01 Zvolen [a)] xdudiak@is.tuzvo.sk; [b)] geffert@tuzvo.sk; [c)] geffertova@tuzvo.sk

ABSTRACT: The aim of this paper is to determine the dependence of changing the acidity and color of birch wood in the process of thermal modification of color with saturated water steam in the pressure autoclave by the temperature of water steam t = t = 105 °C, 125 °C, 135 °C and the time duration τ = 3, 6, 9, 12 hours. The thermal modification was performed on woodturning blanks with the dimensions of 32 x 90 x 600 mm, where after the treatment process the surface of blanks was technologically processed and then was evaluated the color in each mode and modification time in the CIE-L*a*b* color space. By increasing the temperature and the modification time, occurs a more significant change of values in the luminance (L *) and color coordinate (a *, b *) while the uniform brown color shade is across the whole volume of wood. The brightness of the birch wood described by coordinate L* was from the range 83.7 to 53.5. The values of color coordinate a* were from the range 6.8 to 12.5 and the color coordinate b * from the range 19.8 to 21.1.
In the process of thermal modification occurs a various chemical change in the wood which are mostly catalyzed by acetic or formic acid that are cleaved from acetyl functional groups of hemicelluloses. By the process of partial hydrolysis of carbohydrates and lignin or by extraction of the accompanying wood components occurs the change of pH value of birch wood between 5.3 and 3.2 by the humidity of w ≈ 45%. The measurement of pH change of birch wood in individual modes and times of thermal modification was performed by pH meter SI 600 with needle probe LanceFET + H from SENTRON.

Keywords: wood acidity, silver birch, thermal modification, saturated water steam, CIE-L*a*b* color space

ABSTRAKT: Táto práca je zameraná na stanovenie závislosti zmeny acidity a farby brezového dreva v procese termickej modifikácie farby sýtou vodnou parou v tlakovom autokláve pri teplotách sýtej vodnej pary t = 105 °C, 125 °C, 135 °C a časoch τ = 3, 6, 9, 12 hodín. Termická modifikácia bola vykonávaná na brezových prírezoch s rozmermi 32 x 90 x 600 mm, kde po procese úpravy bol povrch prírezov technologicky opracovaný a následne vyhodnotená farba v jednotlivých režimoch a časoch modifikácie vo farebnom priestore CIE-L*a*b*. Zvyšovaním teploty a času modifikácie dochádza ku výraznejším zmenám hodnôt na súradnici svetlosti (L*) a farebných súradniciach (a*, b*), pričom jednotný hnedý farebný odtieň je v celom objeme dreva. Svetlosť brezového dreva popísaná súradnicou L* bola v rozpätí 83,7 – 53,5. Hodnoty na farebnej súradnici a* boli od 6,8 do 12,5 a farebnej súradnici b* v rozpätí 19,8 – 21,1.

V procese termickej modifikácie dochádza v dreve k rôznym chemickým zmenám, ktoré sú vo väčšine prípadov katalyzované kyselinou octovou či mravčou, odštepovanou z acetylových funkčných skupín hemicelulóz. Procesom parciálnej hydrolýzy sacharidov a lignínu, či extrakciou sprievodných zložiek dreva, dochádza k zmene hodnoty pH brezového dreva v rozpätí 5,3 – 3,2 pri vlhkosti w ≈ 45 %. Meranie zmeny pH brezového dreva v jednotlivých režimoch a časoch termickej modifikácie bolo vykonávané pH-metrom SI 600 s vpichovou sondou LanceFET+H od firmy SENTRON.

Kľúčové slová: acidita dreva, breza biela, termická modifikácia, sýta vodná para, farebný priestor CIE-L*a*b*

INTRODUCTION

Raw wet wood is composed of natural ingredients: cellulose, hemicellulose, lignin, small accessory substances containing: glycosides, fats, waxes, resins, dyes, anorganic substances and bound water in cell walls with free water in the lumen. Water in wet wood is solution of sugars and minerals carried by the root system during the growth tree from the land, and also organic acids in the case of thermal modification of wet wood. (Čudinov & Stepanov 1968; Deliiski 1990).

The influence of saturated water steam on wood changes its chemical composition and structure at various levels, as a result of which the mechanical, physical and chemical properties of the modified wood are changing. Many changes and reactions occurring in wood during the thermal modification are beneficial in terms of better utilization of such modified wood. On the other hand there are unwanted phenomena, which cause deterioration of mechanical or physical properties of wood (Kačík 2001; Solar 2004; Dzurenda & Deliiski 2012).

The effect of water steam on wood in relation to irreversible chemical changes in wood can be divided into autocatalytic hydrolytic reactions of the main wood components (carbohydrates, lignin) and their interactions, as well as the extraction of accessory substances in the wood. The result of hydrolytic reactions is the formation of oligomeric and monomeric carbohydrate units, which are subject to further changes catalyzed by weak organic acids (acetic, formic), which arise in the process of thermal modification by cleavage of functional groups from hemicelluloses. Various dehydration, condensation or oxidation reactions of carbohydrates and their products are one of the causes of increased acidity of wood in the thermal process (Fengel & Wegener 1984; Kačík 1997).

The change of color caused by the thermal treatment of wood with saturated water steam is one of the changes which is linked to changes in the chemical structure of the wood. This change of color has an important role in the further processing of wood, because the color shade is unified and the imitation of the color of other trees is possible. (Tolvaj et al. 2009; Barcik et al. 2015; Dzurenda 2018). One way of measuring or objectively quantifying the color of wood is to express it using the CIE-L*a* b* color space coordinates. The color coordination system is based on the measurement of three parameters: brightness L* from 100 for white to 0 for black, chromatic coordinate a* to determine the shade between red (+a*), green (-a*) and chromatic coordinate b* determining the shade between yellow (+b*), blue (-b*) according to ISO 7724.

The aim of this work is to determine changes in acidity and color of birch wood due to thermal modification with saturated water steam in order to unify color shade at temperatures t = 105 °C, 125 °C, 135 °C and time τ = 3, 6, 9, 12 hours.

MATERIALS AND METHODS

Raw blanks sawed from trunks of birch wood with dimensions of 32 x 90 x 600 mm and humidity w > 45% were thermally modified with saturated steam to change the color in the APDZ 240 pressure autoclave at company Sundermann s.r.o. Banská Štiavnica shown in Figure 1.

Fig. 1 A pressure autoclave APDZ 240
Obr. 1 Tlakový autokláv APDZ 240

The technological process of birch wood thermal treatment was carried out in three independent modes, with the sampling after 3, 6, 9 and 12 hours. A uniform process of thermal modification of birch wood with saturated water steam for all modes is shown in Figure 2, where the temperature changes occurred during the modification in each mode.

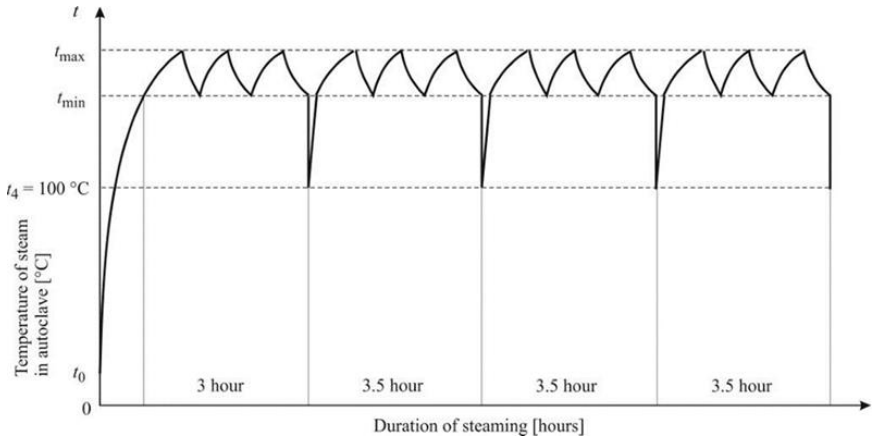

Fig. 2 Mode of modification of birch wood with saturated water steam.
Obr. 2 Režim modifikácie brezového dreva sýtou vodnou parou.

Table 1 shows the temperature and time parameters in each mode during the thermal modification of birch wood.

Table 1 Modes of color modifications of birch wood by saturated water steam.
Tabuľka 1 Režimy farebnej brezového dreva sýtou vodnou parou

Mode	t_{min}	t_{max}	t_4	Sampling at the time of thermal modification of wood color			
Mode I.	102,5	107,5	100	τ_1 = 3 h	τ_2 = 6 h (+ 0.5 h [a])	τ_3 = 9 h (+ 1.0 h [a])	τ_4 = 12 h (+ 1.5 h [a])
Mode II.	122,5	127,5	100				
Mode III.	132,5	137,5	100				

Remark: [a] technological pause

The moisture, pH and color of the blanks were measured before the birch wood thermal modification process, as well as after sampling at different times and thermal modification modes. The moisture of the blanks has an important role during the measurement of wood pH. To reach good contact of the potentiometer probe of the pH meter, the moisture of the samples must be above the saturation point of fibers (w > BNV). The humidity of the wood was measured with an FMD6 resistance hygrometer at the pH measurement point of the birch wood sample, to eliminate the dried samples.

The pH measurement of the thermally modified and native samples of birch wood was performed by the direct method, by pH meter SI 600 with penetration probe LanceFET + H from SENTRON (Steel tipped probe for penetration 2270-010 and measurement of non-liquids) shown in Figure 3. All measurements were carried out 3 times at the center of the blank thickness and 100 mm from the blank face. The pH meter probe is not designed to measure pH in solids but only semi-solids, for that reason, a 12 mm hole was drilled using a cordless drill and the wet sawdust obtained was pushed back into the drilled hole using a glass rod. A pH-meter penetration electrode was inserted into the prepared sawdust chamber. After contact of the probe with wet sawdust and after stabilization the pH changes were monitored at 15-second intervals for 7 minutes.

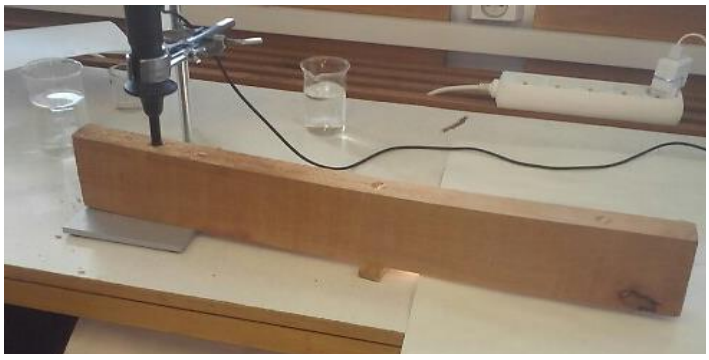

Fig. 3 Direct pH measurement of birch wood
Obr. 3 Priame meranie pH brezového dreva

After pH measurements, all thermally modified, as well as native birch wood blanks were soft-mode dried in a KAD 1x6 convection oven (KATRES s.r.o.) at Sundermann s.r.o. to humidity w = 12 ± 1%. Thus dried birch blanks were machined four times on a planer-thickness mill.

The color of the birch wood was evaluated in the CIE-L*a*b* color space with a Color-reader CR-10 colorimeter (Konica Minolta, Japan). There was used a D65 light source and the diameter of the optical scanning aperture was 8 mm.

A color measurement was performed on the treated samples of native and thermally modified birch wood, where the lightness of the sample L* and the color coordinates a*, b* were evaluated. Six measurements were performed on each sample, of which 3 measurements were performed at the center and 100 mm from the edge to the height of the blank, and 3 measurements were performed at the center and 100 mm from the edge to the width of the blank. Color measurement was performed on 6 samples at each mode and at each time of modification. The color values of the samples are given in Table 3 in the form of a record as the mean value ± the standard deviation of the measurement.

From the difference in the color coordinates ΔL*, Δa*, Δb*, determined by measuring the color of the wood surface of both the thermally modified and native birch blanks, was determined the total color difference ΔE according to the following equation ISO 11 664-4:

$$\Delta E^* = \sqrt{\left(L_2^* - L_1^*\right)^2 + \left(a_2^* - a_1^*\right)^2 + \left(b_2^* - b_1^*\right)^2} \quad (1)$$

Where: L^*_1, a^*_1, b^*_1 values at the coordinates of the color space of the dried surface, machined and thermally unmodified (native) birch wood.

L^*_2, a^*_2, b^*_2 values at the coordinates of the color space of the dried surface, machined and thermally modified birch wood.

A scale (Table 2) proposed by the authors (Allegretti et al. 2009) was used to assess the degree of change in color and color shades of wood obtained in the hydrothermal and thermal treatment processes.

Table 2 Classification of the total color difference ΔE*.
Tabuľka 2 Klasifikácia celkovej farebnej diferencie ΔE*.

0.2 < ΔE*	Not visible difference
0.2 < ΔE* < 2	Small difference
2 < ΔE* < 3	Color difference visible with high quality screen
3 < ΔE* < 6	Color difference visible with medium quality screen
6 < ΔE* < 12	High color difference
ΔE* > 12	Different colors

RESULTS

Acidity of wet, thermally unmodified birch wood by Solár (2004); Kacik et al. (2007), has a pH from 4.8 to 5.5. The pH values of the birch wood measured by the direct method at a humidity w ≈ 53.9% were 5.3 ± 0.2.

The color of natural birch wood is described by Babiak et al. (2004) in the CIE-L * a * b * coordinate system with L* = 78.07; a* = 5.92; b* = 20.02. Our measured values of native birch wood at coordinates L*, a*, b* at humidity w ≈ 12% are: L* = 83.7 ± 1.3; a* = 6.8 ± 0.6; b* = 19.8 ± 0.9.

The measured pH values of wet, thermally modified birch wood, as well as values of the CIE-L * and * b * coordinate system, which are describing the color of the birch wood after machining the blank surface, are shown in Table 3. The measured values are shown using the program STATISTICA 12 in Figure 4-8.

Table 3 Moisture, pH and color coordinate values L*, a*, b* of birch wood in the process of thermal modification of birch wood.
Tabuľka 3 Hodnoty vlhkosti, pH a farebných súradníc L*, a*, b* brezového dreva v procese termickej modifikácie brezového dreva.

Temperature of saturated water steam	Wood moisture	Time of thermal modification of birch wood color			
		3 hours	6 hours	9 hours	12 hours
t_I = 105 ± 2.5 °C	w ≈ 45,5 %	pH = 4,9 ± 0,1	pH = 4,7 ± 0,1	pH = 4,6 ± 0,2	pH = 4,4 ± 0,3
	w ≈ 11,5 %	L* = 80.7 ± 1.2	L* = 75.8 ± 1.2	L* = 74.7 ± 0.8	L* = 71.3 ± 1.2
		a* = 8.5 ± 0.8	a* = 10.7 ± 0.7	a* = 10.5 ± 0.7	a* = 10.5 ± 0.8
		b* = 19.2 ± 0.6	b* = 21.1 ± 0.5	b* = 21.4 ± 0.6	b* = 19.8 ± 0.4
		ΔE* = 3.5	ΔE* = 8.9	ΔE* = 9.8	ΔE* = 12.9
t_{II} = 125 ± 2.5 °C	W ≈ 43,8 %	pH = 3,9 ± 0,1	pH = 3,8 ± 0,2	pH = 3,7 ± 0,3	pH = 3,6 ± 0,2
	w ≈ 11,8 %	L* = 73.9 ± 1.1	L* = 66.6 ± 1.2	L* = 64.3 ± 1.2	L* = 63.8 ± 1.2
		a* = 10.3 ± 0.8	a* = 11.9 ± 0.7	a* = 12.5 ± 0.7	a* = 12.2 ± 0.8
		b* = 19.8 ± 0.9	b* = 18.9 ± 0.5	b* = 18.5 ± 0.5	b* = 19.8 ± 0.4
		ΔE* = 10.4	ΔE* = 18.8	ΔE* = 20.2	ΔE* = 20.6
t_{III} = 135 ± 2.5 °C	W ≈ 46,5 %	pH = 3,6 ± 0,1	pH = 3,4 ± 0,2	pH = 3,2 ± 0,1	pH = 3,2 ± 0,1
	w ≈ 11,7 %	L* = 65.1 ± 1.9	L* = 59.9 ± 1.5	L* = 55.6 ± 0.9	L* = 53.5 ± 0.7
		a* = 11.6 ± 0.6	a* = 12.5 ± 0.4	a* = 12.5 ± 0.3	a* = 12.1 ± 0.4
		b* = 18.7 ± 0.6	b* = 19.4 ± 0.5	b* = 19.5 ± 0.6	b* = 18.8 ± 0.4
		ΔE* = 19.2	ΔE* = 24.4	ΔE* = 28.8	ΔE* = 30.6

The dependence of pH changes of birch wood in the process of thermal modification in the temperature range from t = 105 °C to t = 135 °C with time from τ = 0 to τ = 12 hours is shown in Figure 4.

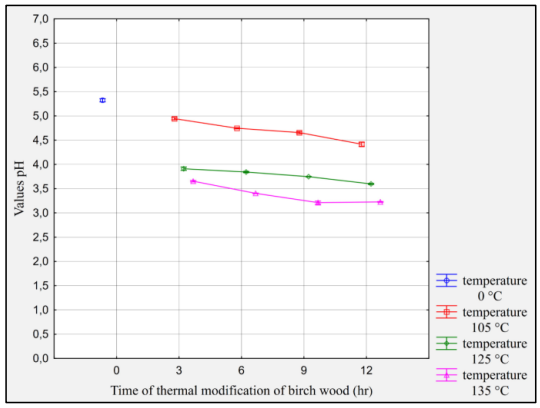

Fig. 4 The dependence of pH change of birch wood on temperature and time in thermal modification process
Obr. 4 Závislosť zmeny hodnoty pH brezového dreva na teplote a čase v procese termickej modifikácie

Changes in thermally modified birch wood at lightness coordinate L*, as well as changes at chromatic coordinates of red a* and yellow b*, at temperatures tI = 105 ° C, tII = 125 ° C, tIII = 135 ° C and time 0, 3, 6, 9, 12 hours are shown in Figure 5-7.

The overall color change is shown in Figure 8 through the color difference ΔE * at temperatures tI = 105 ° C, tII = 125 ° C, tIII = 135 ° C and time 3, 6, 9, 12 hours in the process of thermal modification of birch wood.

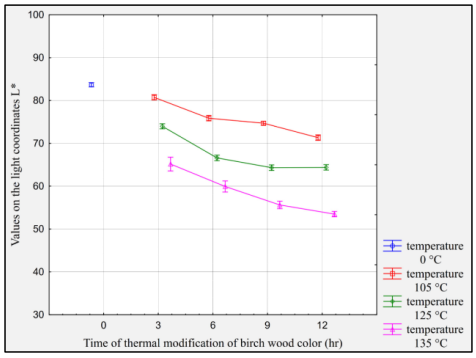

Fig. 5 The dependence L* coordinate on temperature and modification time
Obr. 5 Závislosť súradnice svetlosti L* na teplote a čase modifikácie

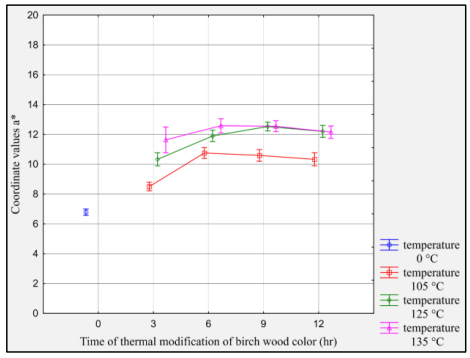

Fig. 6 The dependence color coordinate a*on temperature and modification time
Obr. 6 Závislosť farebnej súradnice a* na teplote a čase modifikácie

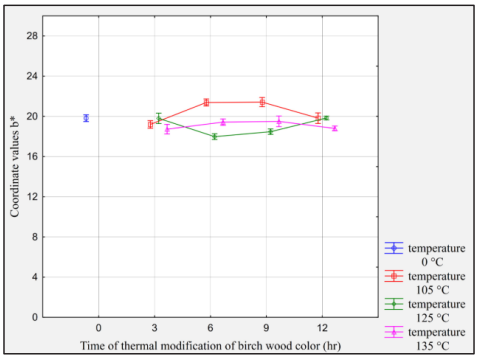

Fig. 7 The dependence color coordinate a*on temperature and modification time
Obr. 7 Závislosť farebnej súradnice a* na teplote a čase modifikácie

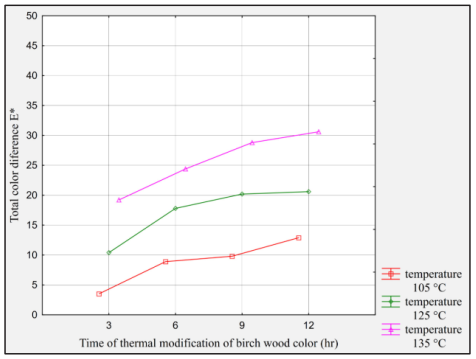

Fig. 8 The dependence total color difference E* on temperature and time of modification
Obr. 8 Závislosť celkovej farebnej diferencie* na teplote a čase modifikácie

DISCUSSION

In the process of thermal modification of birch wood by saturated water steam a decrease in the pH value of wood due to time and temperature was demonstrated. This decrease of values by increasing temperature and time is confirmed by already known knowledge about hydrolysis processes of saccharides in wet wood, the process of which is mainly temperature-related.

From the course of dependencies (Figure 4) it can be concluded that the acidity was increased together with increasing steaming temperature. The greatest decrease in pH was measured after the first three hours of steaming and the pH of the wood fell from the original 5.3 by 8% at a steaming temperature of 105 °C, by 26% at 125 °C and by 32% at 135 °C. With increasing steaming time, the decrease of pH was already more moderate. The lowest pH values were determined after 12 hours of steaming, when the pH value decreased by 17% at 125 °C, by 30% at 135 °C and by about 40% at 135 °C.

The increase of acidity (decrease of pH values) can be attributed in the early stages of hydrothermal activity to an increase in the concentration of acetic and formic acid released from the acetyl and formyl groups of hemicelluloses (Kačík 2001).

The measured acidity values of wet birch wood achieved by the thermal treatment modes indicate that the temperature factor has a greater influence on the magnitude of the hydrolysis of hemicelluloses than the time of the thermal process.

During steaming, the wood changes color. Their intensity is determined by the conditions of hydrothermal treatment and the type of wood. The change of color is related to the formation of new chromophores due to chemical changes in lignin and to the reactions of degradation products of polysaccharides and extractives (Solar 1997).

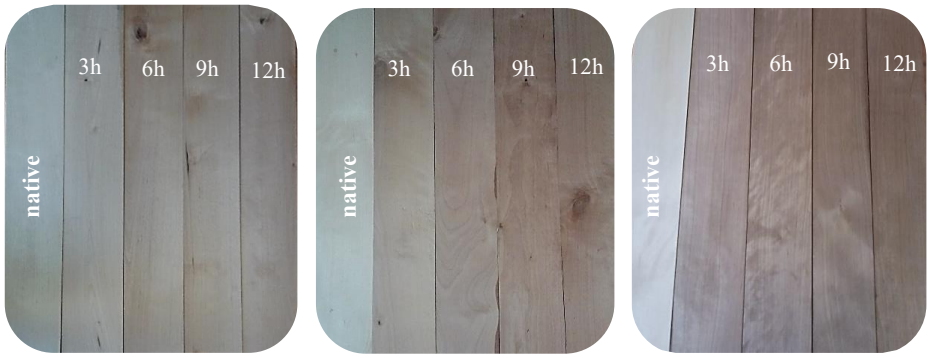

Fig. 9 Color changes of birch wood by steaming at 105–135 °C
Obr. 9 Zmeny farby brezového dreva parením pri 105–135 °C

The color of birch wood in the process of steam-saturated thermal treatment changes from a light white-brown color to a pale-brown color at a temperature t = 105 ± 2.5 °C and a thermal modification time τ = 6 – 12 hours; through brown shades attained at t = 125 ± 2.5 °C for 6 to 12 hours; to brown coloring of birch wood at t = 135 ± 2.5 °C for τ = 9 – 12 hours of color modification.

For objective measurement of birch wood color changes in each steaming mode, the surface color of the samples was measured with the Color Reader CR-10 colorimeter and it was evaluated in the CIE-L* a* b* color space via L*, a*, and b* coordinate changes. The measurement results are shown in Figures 5 to 8.

During hydrothermal treatment there was a significant decrease in L* brightness depending on the steaming conditions. At the lowest steaming temperature (105 °C) after 12 hours the lightness of the wood surface decreased by 14.8%, at 125 °C by 23.8% and at 135 °C by up to 36.1%.

The values of the green-red coordinate a* had an upward trend in the first six hours with a shift to the red area of the coordinate system. In the next period, the values of the coordinate α* were stabilized. The effect of temperature was reflected in an increase in the values of coordinate a*, with the lowest values measured at 105 °C. At a temperature of 125 °C and 135 °C at 9 and 12 hours, the values of coordinate a * were equalized.

The process of changes in the blue-yellow coordinate b* due to time at individual temperatures is not unambiguous. The b* coordinate at 105 °C and 135 °C at 3, 6, 9 hours shifted to the yellow area of the color space, and after 12 hours of steaming a decrease to the blue area was noted. This is probably related to chemical changes that are the subject of further research.

The significant influence of temperature and time of hydrothermal treatment on total color difference values *(DE*)* can be clearly stated. At the lowest steaming temperature (105 °C) after 3 hours, a value of *DE** was calculated to 3.5, which is the classification for IV. degree of color change classification according to Allegretti et al. 2009; ‚Color difference visible with medium quality screen' (Table 2). After 12 hours *DE** was 12.9 which is classified as "different colors".

At a steaming temperature of 125 °C after 3 hours *DE** value was calculated to 10.4 („high color difference“) and more than 12 „different colors“ were calculated at intervals of 6, 9 and 12 hours. The maximum *DE** (20.6) was calculated after 12 hours of steaming. At a steaming temperature of 135 °C, the total color difference over the whole-time range observed was „different colors“ with a maximum of 30.6 at 12 hours.

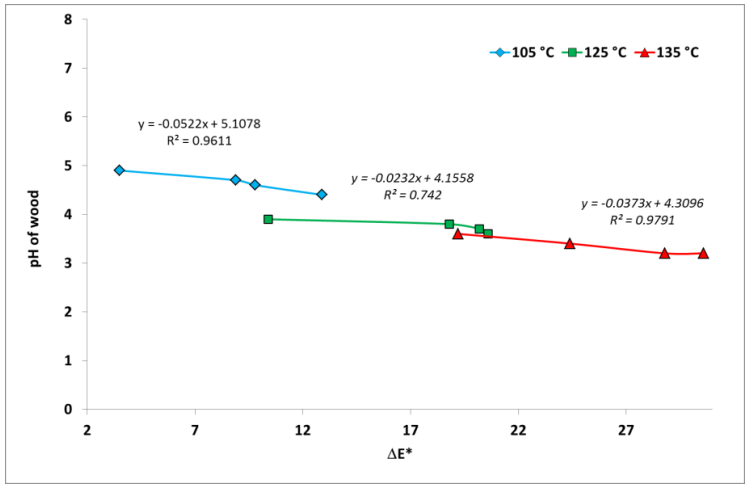

Fig. 10 pH dependence of birch wood on its total color difference E * and temperature
Obr. 10 Závislosť pH brezového dreva na jeho celkovej farebnej diferencii E* a teplote

Figure 10 shows the dependence of wood pH and *D*E *, which confirms that the decrease in pH as a result of ongoing chemical changes (release of acidic components and formation of secondary chromophoric systems) affects the color changes of wood as a function of temperature and time of hydrothermal treatment.

By visual inspection of the thermally modified wood at a temperature t = 105 ± 2.5 °C and a time τ = 3 hours in the center of the split birch blank, it can be said that the thermally modified wood is uniformly colored throughout the cross-section of the blank. On this basis it can be stated that the wood modified in this way can be used for production of various assortment of furniture, toys, but also 3D products with uniform color shade.

The achieved color changes in the process of thermal modification of birch wood with saturated water steam in individual modes and times are in the first mode at temperature t = 105 ± 2.5 °C with the naked eye very low, where at higher times and temperatures in mode I., II. and III. they achieve even more or less rich brown color shades.

CONCLUSION

On the basis of the work carried out the experiment can be said that the during process of the thermal modification of the birch wood with saturated water steam at T = 105 ° C

and a time of 3 hours it was achieved the desired effect of color tone unification of the entire cross section of the blank of birch.

Native, but also saturated steam-modified birch blanks were modified to change and unify the color shade. These color changes achieved in each mode over time were measured and evaluated using the CIEL-L* a* b* color space coordinate system.

Thus, modified color birch wood, which is environmentally friendly and healthy, expands the possibilities of its processing in construction and carpentry. For example: manufacture of flooring, wall coverings, furniture made of solid wood, toys or other decorative materials in the home.

In the process of thermal modification, there are changes in the properties of wood, which are accompanied by partial hydrolysis of carbohydrates, lignin and which are autocatalyzed with acetic acid. During partial hydrolysis there is an overall change in the acidity of the modified wood. The acidity of the birch wood was determined by a direct pH measurement method and it has been shown that the acidity of the wood with decreasing temperature and increasing time has a decreasing tendency, so transition to more acidic areas. Acidity of birch wood in mode III. (t =135 °C, τ = 12 hours) was expressed as pH = 3.2. Such acidic pH values of the wood affect the woodcutting tool by which the wood is machined which may be deteriorated or wear of the cutting edge, which affects the quality of the machined surface.

ACKNOWLEDGMENT

The contribution was prepared within the project agency IPA TUZVO, which contributed significantly to the creation of this contribution through the project: IPA TUZVO 15/2019.

We also thank the APVV grant agency, which also helped to create this contribution within the APVV grant project 17-0456.

REFERENCES

ALLEGRETTI, O., TRAVAN, L., CIVIDINI, R. 2009. Drying Techniques to obtain White Beech. In *Quality control for wood and wood products.* EDG Wood Drying Seminar, Bled, pp. 7–12.

BABIAK, M., KUBOVSKÝ, I., MAMOŇOVÁ, M. 2004. Color space of selected local woods. In: *Interaction of wood with various Forms of Energy*. Technical university in Zvolen

BARCÍK, Š., GAŠPARÍK, M., RAZUMOV, E.Y. 2015. Effect of thermal modification on the colour changes of oak wood. In: *Wood Research*. No.60 vol. 3. pp. 385-396.

BUČKO, J. 1995. *Hydrolýzne procesy.* Technical university in Zvolen, Slovakia. p. 116. ISBN 80-228-0462-2

ČUDINOV, B. S., STEPANOV, V. L. 1968. Phasenzusammensetzung der Wassers in gefrorenem Holz. In *Holztechnologie*. no. 9, vol. 1, pp. 14 – 18.

DELIISKI, N. 1990. Mathematische beschreibung der spezifischen wärmekapazität des aufgetautent and gefrorenen Holzes. In *Fundamental Reserch of Wood*. Warszawa. pp. 229 – 233.

DELIISKI, N., DZURENDA, L. 2010. Modeling of heat processes in wood processing technologies. Avangard Prima, Sofia. Bulgaria.

DZURENDA, L., DELIISKI, N. 2012. Convective drying of beech lumber without color changes of wood. In. *Drvna industrija*. no. 63 vol.2. pp. 95 – 103.

DZURENDA, L. 2018. The Effect of Moisture Content of Black Locust Wood on the Heating in the Saturated Water Steam during the Process of Colour Modification, In: *MATEC Web of Conferences 168*, 06004
FENGEL, D., WEGENER, G. 1989. Wood: Chemistry, Ultrastructure, Reactions; Walter de Gruyter: Berlin, Germany. p. 613.
GEFFERT, A., VÝBOHOVÁ, E., GEFFERTOVÁ, J. 2017. Characterization of the changes of colour and some wood components on the surface of steamed beech wood. In: *Acta facultatis xylologiae Zvolen.* No. 59 vol. 1. pp. 49 – 57, ISSN 1366-3824, doi: 10.17423/afx.2017.59.1.05.
GEFFERT, A., GEFFERTOVÁ, J., DUDIAK, M., 2019. Direct Method of Measuring the pH Value of Wood. *Forests* 2019, Volume 10, Issue 10, 852. ISSN 1999-4907, doi: 10.3390/f10100852
GRAY, V.R. 1958. The acidity of wood. *Journal of the Indstitute of Wood Science*. No 1.pp. 58 – 64.
KAČÍK, F. 1997. *Vplyv teploty a vlhkosti na zmeny sacharidov dreva*. Technical university in Zvolen. p. 69.
KAČÍK, F. 2001. *Tvorba a chemické zloženie hydrolyzátov v systéme drevo-voda-teplo.* Zvolen, TU vo Zvolene. p. 75. ISBN 80-228-1098-3
KAČÍK, F., VÝBOHOVÁ, E., KAČÍKOVÁ, D. 2007. Volatile compounds arising at hydrolysis of birch wood. In *Acta Facultatis Xylologiae, Zvolen*. No. 2. pp. 39 – 46.
KOLLMANN, F., GOTE, W. A. 1968. Principles of Wood Sciences and Technology. Solid Wood, Springer Verlag: Berlin – Heidelberg - New York. Vol. 1. p. 592 .
MOLNAR, S., TOLVAJ, L. 2002. Colour homogenisation of different wood species by steaming. In: *Interaction of wood with various Forms of Energy*. Technical university in Zvolen, Slovakia.
PONCSAK, S., KOCAEFE, D., BOUZARA, M. AND PICHETTE, A. 2006. Effect of high temperature treatment on the mechanical properties of birch (Betula pendula). Wood Science and Technology. No. 40 vol. 8. pp. 647 – 663.
SHULGA, G., VITOLINA, S., SHAKELS, V., BELKOVA, L., CAZACU, G., VASILE, C., NITA, L. 2012. Lignin separated from the hydrolyzate of hydrothermal teatment of birch wood and its surface properties. Latvia – Romania, Cellulose Chem. Technol. No.46 vol. 5-6. pp. 307 – 318.
SOLÁR, R. 1997. *Zmeny lignínu v procesoch hydrotermickej úpravy dreva.* VŠ 1/1997/A. 1.vyd. Zvolen: TU vo Zvolene, 1997. 57 s. ISBN 80-228-0599-8.
SOLÁR, R. 2004. *Chémia dreva.* Zvolen, TU vo Zvolene. p. 101. ISBN 80-228-1420-2
SUBRAMANIAN, R., SOMASEKHARAN, K. 2009. Acidity of Wood. *Holzforschung - International Journal of the Biology, Chemistry, Physics and Technology of Wood*. No. 37 vol. 3. pp. 117 – 120. doi:10.1515/hfsg.1983.37.3.117
TOLVAJ, L., NEMETH, R., VARGA, D., MOLNAR, S. 2009. Colour homogenisation of beech wood by steam treatment. In: *Drewno*. No. 52 vol. 181. pp. 5 – 17.

Corresponding author:
Michal Dudiak, Tel; +421-45-520-6367, e-mail; xdudiak@is.tuzvo.sk

AN INFLUENCE OF SPATIAL ORIENTATION OF A HEATED SMOOTH AND TRAPEZOIDAL SURFACE ON HEAT TRANSFER COEFFICIENTS

VPLYV PRIESTOROVEJ ORIENTÁCIE OHRIEVANEJ HLADKEJ A LICHOBEŽNÍKOVEJ PLOCHY NA SÚČINITELE PRESTUPU TEPLA

Zuzana Brodnianská

Department of Environmental and Forestry Machinery, Faculty of Technology, Technical University in Zvolen, Studentska 26, 960 01, Zvolen, Slovak Republic, zuzana.brodnianska@tuzvo.sk

ABSTRACT: The paper is focused on visualization of temperature fields in the vicinity of the heated heat exchange surfaces in free air convection. A temperature fields in the vicinity of the heated smooth and shaped heat exchange surface are visualized by a contacless optical method. Local and mean heat transfer coefficients are evaluated from the holographic interferogram images. The local heat transfer coefficients, α_x, are determined by the temperature derivative for different spatial orientations and surface temperatures of the heat exchange surfaces, 0º, 45º and 90º, respectively 313 K to 333 K. The mean heat transfer coefficients and heat flux densities, α_m and q_m, showed the highest values for a smooth and trapezoidal surface at a 90º inclination. The highest value of the mean heat transfer coefficient and heat flux density is achieved by the trapezoidal surface at a 90° inclination angle, at a surface temperature of 333 K (α_m = 6.95 W/m^2.K; q_m = 264.10 W/m^2). The increase in α_m and q_m was 21.3 % compared to the smooth surface.

Keywords: Heat transfer coefficient, Convection, Temperature, Heat exchange surface, Interferogram

ABSTRAKT: Príspevok je zameraný na vizualizáciu teplotných polí v okolí ohrievaných teplovýmenných plôch pri prirodzenej konvekcii vzduchu. Teplotné polia v okolí ohriatej hladkej a tvarovanej plochy sú vizualizované bezkontaknou optickou metódou. Z výsledných obrazov holografických interferogramov sú vyhodnocované lokálne a stredné súčinitele prestupu tepla. Lokálne súčinitele prestupu tepla α_x sú určené deriváciou teplôt pre rôzne priestorové orientácie teplovýmenných plôch (0º, 45º, 90º) a rôzne povrchové teploty v rozsahu 313 K až 333 K. Najvyššie hodnoty stredného súčiniteľa prestupu tepla a hustoty tepelného toku dosahovala lichobežníková plocha pri sklone 90º, pri povrchovej teplote 333 K (α_m = 6,95 W/m^2.K; q_m = 264,10 W/m^2). V porovnaní s hladkou plochou dosahoval nárast α_m a q_m o 21,3 %.

Kľúčové slová: súčiniteľ prestupu tepla, konvekcia, teplota, teplovýmenná plocha, interferogram

INTRODUCTION

The heat transfer parameters from the heated heat exchange surfaces in free air convection are necessary for designing various types of plate heat exchangers and heating bodies, finned surfaces of cooling elements in electrical engineering, finned surfaces of engines, etc. The study of heat transfer in the vicinity of the heated smooth and shaped heat exchange surfaces with different spatial orientation in free convection of air was studied by several world authors.

Author (Pavelek 2001) dealt with the interferometric research of heat transfer in free air convection in a set of the heated vertical plates with constant surface temperatures. He described the conclusions for optimum design of heat exchangers in a vertical plate system with maximum heat flow densities. Authors (Ambrosini *et al*. 2003) investigated heat transfer on smooth and finned heat exchange surfaces in free convection using optical methods (Schlieren method and holographic interferometry). Subsequently, authors (Ambrosini and Tanda 2006) used these optical methods for experimental research of the vertical smooth and grooved channels. They obtained temperature distributions and local heat transfer coefficients in the examined area.

Authors (Martynenko and Khramtsov 2005) processed heat transfer data in free convection using various optical visualization methods in the book. They performed calculations under various boundary and input conditions. Some calculations specifically applied to technical applications. The work of (Lu *et al.* 2010) presents experimental research of heat transfer in free air convection in three rectangular channels with different gap distances. The use of fins can significantly increase the heat transfer from the surface of the conductive material.

In the scientific monograph (Černecký *et al*. 2012) the authors dealt with the optimization of the shape of heat exchange surfaces of the heat exchangers even in the case of free air convection in the vicinity of the vertical different shaped surfaces. In addition to holographic interferometry, they also used thermal imaging techniques for visualization. Authors (Igaz and Černecký 2014) presented in the monograph the possibilities of increasing the heat transfer efficiency in free convection from a heated heat exchange surface at its various profiles. Their results indicate that the heat transfer efficiency of the heat exchange surface is strongly influenced by surface profiling. Higher heat flux densities have been achieved for profiles with a more rugged surface.

Authors (Roeleveld and Naylor 2014) visualized the free air convection in a heated vertical channel using a Mach-Zehnder interferometer. The buoyancy inside the channel influenced the flow. The experimentally obtained flow and temperature fields were used for numerical modeling. The Rayleigh number varied from 5 to 215. Authors (Lewandowski *et al.* 2014) visualized the temperature fields in the vicinity of the vertical heated surface using a thermal imaging camera. In order to visualize the temperature fields in ambient air, not only on the surface, they used a plastic mesh that emitted infrared radiation after heating with hot air. The mesh was placed perpendicular to the heated surface. They obtained temperature gradients and their distribution on the surface and calculated local heat transfer coefficients and local Nusselt numbers. In the paper (Brodnianská and Černecký 2016) the authors focused on visualization of temperature fields in the vicinity of the vertical profiled heated surfaces. They compared the triangular profile with the trapezoidal profile and analyzed holographic interferograms to determine the values of the

heat transfer coefficients along the shaped heated surfaces. Holographic interferometry method was used for visualization of temperature fields. Experimentally obtained temperature fields were supplemented with CFD simulations.

Presented paper is focused on evaluation of local heat transfer coefficients, α_x, in the vicinity of the heated smooth and trapezoidal surface using temperature derivation method. Temperature fields are visualized by holographic interferometry without disturbing the research area. Local and mean heat transfer parameters for three different spatial orientations of heat exchange surfaces in free air convection were evaluated from interferogram images. The research of temperature fields was carried out for different surface temperatures of the heat exchange surfaces in the range of 313 K to 333 K.

DETERMINATION OF THE HEAT TRANSFER COEFFICIENTS BY TEMPERATURE DERIVATIVES

Different fluid density caused by different temperatures in the vicinity of the heated surface causes buoyancy forces, which moves the warmer liquid upwards and the colder liquid flows into its place (Lenhard *et al.* 2009). As the air flows along the heated surface, there is a local heat transfer coefficient α_x between the surface T_{sx} and the fluid T_a at the local point x. The value of the local heat transfer coefficient α_x depends on several factors (for example, temperature difference between surface and fluid, fluid flow rate, fluid type, shape and surface roughness). Figure 1 shows the shape of the temperature profile in the thermal boundary layer with local thickness h_{TBL} (Brodnianská 2013).

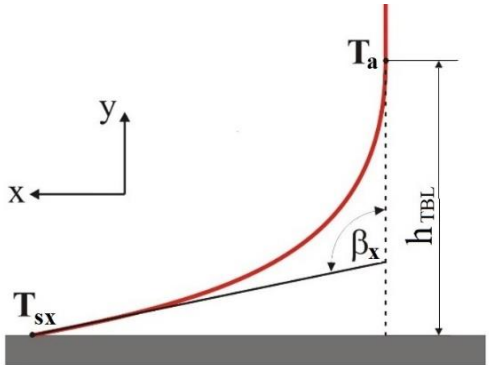

Fig. 1 The temperature profile in the thermal boundary layer along the heat exchange surface
T_s – surface temperature of heat exchange surface, T_a – temperature of ambient air,
h_{TBL} – thickness of thermal boundary layer
Obr. 1 Teplotný profil v teplotnej medznej vrstve pozdĺž teplovýmennej plochy
T_s – povrchová teplota teplovýmennej plochy, T_a – teplota okolitého vzduchu,
h_{TBL} – hrúbka teplotnej medznej vrstvy

The calculation of the local heat transfer coefficient is based on the equation (Pavelek, 2001):

$$\alpha_x = -\lambda_a \cdot \left(\frac{dT}{dy}\right)_x \cdot \frac{1}{T_{sx} - T_a} \tag{1}$$

where λ_a – thermal conductivity coefficient of ambient air [W/m.K],
T_{sx} – surface temperature of heat exchange surface at location *x* [K],
T_a – temperature of ambient air [K].

From the shape of the temperature profile it is possible to determine the temperature difference and the temperature derivative using the angle β_x, which creates the tangent to the temperature profile at the surface with the *y*-axis (Fig. 1).

Values of the local heat transfer coefficients can be obtained in several ways (for example, from refractive index derivatives, from interference order derivatives, from temperature derivatives, from temperature boundary layer thicknesses). In this paper the temperature derivative was used.

For the derivative of the surface temperature in the direction perpendicular to the surface, the equation is (Pavelek 2001):

$$\left(\frac{dT}{dy}\right)_x = tg\beta_x \tag{2}$$

The equation for calculating the local value of the heat transfer coefficient was obtained by substituting formula (2) to formula (1):

$$\alpha_x = -\lambda_a \cdot tg\beta_x \cdot \frac{1}{T_{sx} - T_a} \tag{3}$$

In interferometric heat transfer research, it is preferred to calculate the heat transfer coefficients by means of temperature derivative. From the holographic interferogram images, a detailed temperature distribution in the fluid, in our case in the air, can be obtained (Božek and Pivarčiová 2012).

The mean heat transfer coefficients α_m were obtained as:

$$\alpha_m = \frac{1}{L} \cdot \int_0^L \alpha_x \cdot dx \tag{4}$$

where *L* – length of the heated surface [m].

The mean heat flux densities q_m of a heated surfaces were obtained as:

$$q_m = \alpha_m \cdot (T_s - T_a) \tag{5}$$

EXPERIMENTAL RESEARCH

The smooth and trapezoidal heat exchange surfaces with dimensions of 200×200 mm were used for the research. The geometric parameters of the trapezoidal profile are shown in Fig. 2. Heat exchange surfaces were made of duralumin material (aluminum, copper and magnesium alloy) with a thermal conductivity coefficient of 238 W/m.K. Heat exchange surfaces (2) were heated electrically by means of a resistive heater (3) with temperature controller (5). The heater was mounted in a construction fixture (1) that allowed the heat exchange surfaces to be set to a position 45° and 90° (Fig. 3). The laser beam (6) passed through the test section, depending on the objective diameter (80 mm).

Heat exchange surfaces (2) were heated to constant temperatures of T_s = 313 K, 318 K, 323 K, 328 K and 333 K. The thermocouples types K (NiCr-Ni) ZA 9020-FS with accuracy

±0.05 K were used for surface and ambient air temperature measurement. Temperature sensors were connected to Datalogger Almemo 2290-8 in order to make records (Koleda *et al.,* 2017).

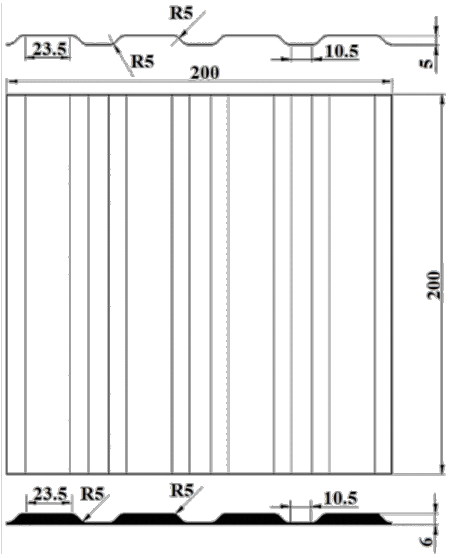

Fig. 2 Geometric parameters of heated trapezoidal surface
Obr. 2 Geometrické parametre ohriatej lichobežníkovej plochy

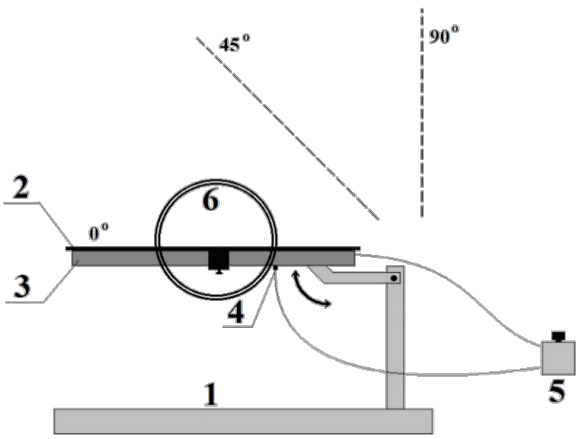

Fig. 3 The experimental scheme of the installed smooth heat exchange surface and laser beam passed through the test section, 1 – construction fixture, 2 – heat exchange surface, 3 – resistive heater, 4 – temperature sensor, 5 – temperature controller, 6 – laser beam
Obr. 3 Experimentálna schéma osadenej teplovýmennej plochy a prechod laserového žiarenia meracím úsekom, 1 – konštrukčný prípravok, 2 – teplovýmenná plocha, 3 – odporové vyhrievacie teleso, 4 – snímač teploty, 5 – regulátor teploty, 6 – laserové žiarenie

The distribution of the temperature fields in the vicinity of the heat exchange surfaces was visualized by real-time holographic interferometry. For this purpose, a holographic variant of a Mach-Zehnder interferometer with a helium-neon laser was arranged. Local and mean heat transfer parameters from heated surfaces to ambient air were evaluated by quantitative analysis of holographic interferograms.

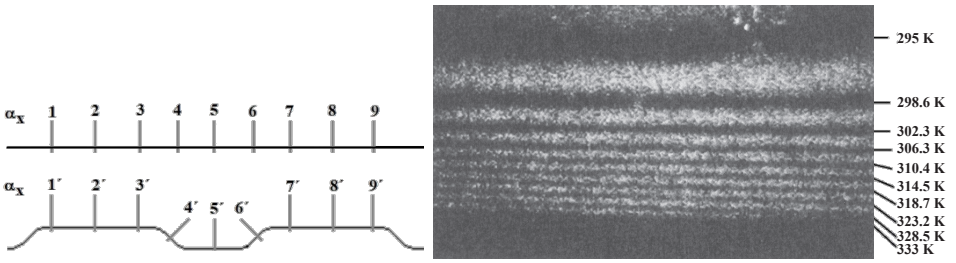

a) b)

Fig. 4 Indication of local sections and temperature distribution by interference fringes
a) local sections to evaluate the local heat transfer coefficients for smooth and trapezoidal surface, b) temperature distribution in the vicinity of the smooth heated surface
Obr. 4 Naznačenie lokálnych rezov a rozloženie teplôt formou interferenčných prúžkov
a) lokálne rezy pre vyhodnotenie lokálnych súčiniteľov prestupu tepla pre hladkú a lichobežníkovú plochu, b) rozloženie teplôt v okolí hladkej ohriatej plochy

Interferograms were adjusted for brightness and contrast before evaluation (Koleda and Hrčková, 2017). Subsequently, the distances of the interference fringes from the surface were determined in the individual sections perpendicular to the heated surface (Fig. 4a).

Individual interference fringes were assigned temperature in the direction away from the heated surface at surface temperature 333 K: 328.5 K; 323.2 K; 318.7 K; 314.5 K; 310.4 K; 306.3 K; 302.3 K; 298.6 K and 295 K (Fig. 4b). Using the temperature derivative method, the local heat transfer coefficients, α_x, in individual sections were calculated using formula (3).

RESULTS AND DISCUSSION

From the holographic interferogram images were calculated isotherms in the vicinity of the heated smooth and trapezoidal surfaces with a change in surface temperature. The Fig. 5 showed interferograms of temperature fields in the vicinity of the heated smooth surface with a surface temperature of 333 K and with change of spatial orientation. The Fig. 6 showed interferograms of temperature fields in the vicinity of the heated trapezoidal surface with a surface temperature 333 K and with change of spatial orientation. The aim was to determine the effect of spatial orientation and shape of heated surface on the heat transfer parameters.

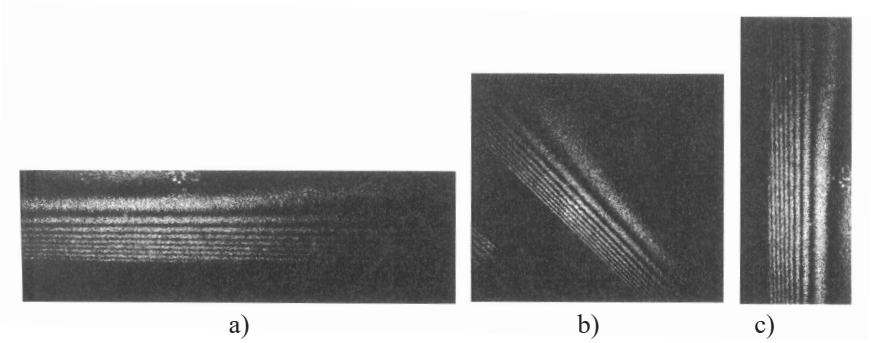

Fig. 5 The holographic interferograms of the smooth heated surface in different spatial orientation at surface temperature 333 K
a) 0° angle of inclination, b) 45° angle of inclination, c) 90° angle of inclination
Obr. 5 Holografické interferogramy hladkej ohriatej plochy pri rôznej priestorovej orientácii a povrchovej teplote 333 K
a) uhol sklonu 0°, b) uhol sklonu 45°, c) uhol skonu 90°

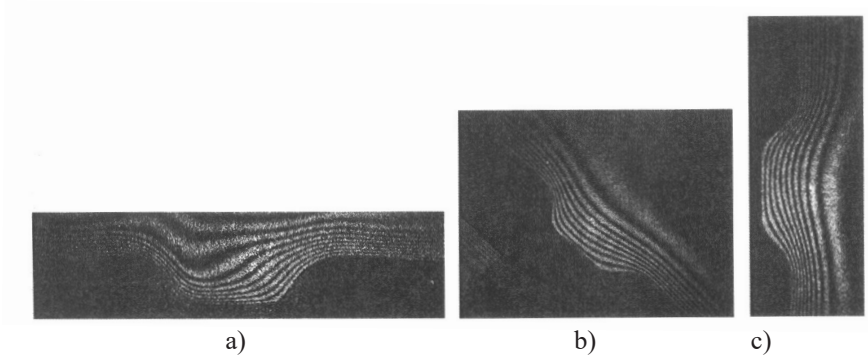

Fig. 6 The holographic interferograms of the trapezoidal heated surface in different spatial orientation at surface temperature 333 K
a) 0° angle of inclination, b) 45° angle of inclination, c) 90° angle of inclination
Obr. 6 Holografické interferogramy lichobežníkovej ohriatej plochy pri rôznej priestorovej orientácii a povrchovej teplote 333 K
a) uhol sklonu 0°, b) uhol sklonu 45°, c) uhol skonu 90°

As the surface temperature of the heated surfaces increases, the number and density of the interference fringes increases. An interference fringes represent the course of isotherms in the vicinity of the heated surfaces. At a vertical position of the smooth and trapezoidal surface, free convection causes a reduction in the thickness of the thermal boundary layer and this affects the resulting mean heat transfer coefficients.

Table 1 The influence of spatial orientation of the smooth heated surface on mean heat transfer parameters
Tabuľka 1 Vplyv priestorovej orientácie hladkej ohriatej plochy na stredné parametre prestupu tepla

Angle of inclination[1)]	T_s [K]	T_a [K]	α_m [W/m^2.K]	q_m [W/m^2]
0º	313	295	3.54	67.32
45º	313	295	3.95	71.10
90º	313	295	4.72	84.96
0º	318	295	3.96	91.08
45º	318	295	4.29	98.67
90º	318	295	4.95	113.85
0º	323	295	4.08	114.24
45º	323	295	4.58	128.24
90º	323	295	5.29	148.12
0º	328	295	4.52	149.16
45º	328	295	5.03	165.99
90º	328	295	5.60	184.80
0º	333	295	4.89	185.82
45º	333	295	5.21	197.98
90º	333	295	5.73	217.74

[1)]Uhol sklonu

Table 2 The influence of spatial orientation of the trapezoidal heated surface on mean heat transfer parameters
Tabuľka 2 Vplyv priestorovej orientácie lichobežníkovej ohriatej plochy na stredné parametre prestupu tepla

Angle of inclination[1)]	T_s [K]	T_a [K]	α_m [W/m^2.K]	q_m [W/m^2]
0º	313	295	3.88	69.84
45º	313	295	4.38	78.84
90º	313	295	5.13	92.34
0º	318	295	4.56	104.88
45º	318	295	5.02	115.46
90º	318	295	5.60	128.80
0º	323	295	5.16	144.48
45º	323	295	5.52	154.56
90º	323	295	5.95	166.60
0º	328	295	5.89	194.37
45º	328	295	6.13	202.29
90º	328	295	6.57	216.81
0º	333	295	6.09	231.42
45º	333	295	6.52	247.76
90º	333	295	6.95	264.10

[1)]Uhol sklonu

From the distribution of the interference fringes, local heat transfer coefficients along the heated surfaces were evaluated using formula (3). Subsequently, the mean heat transfer coefficients and mean heat flux densities were calculated using formula (4, 5) for the smooth heated surfaces (Table 1) and the trapezoidal surfaces (Table 2).

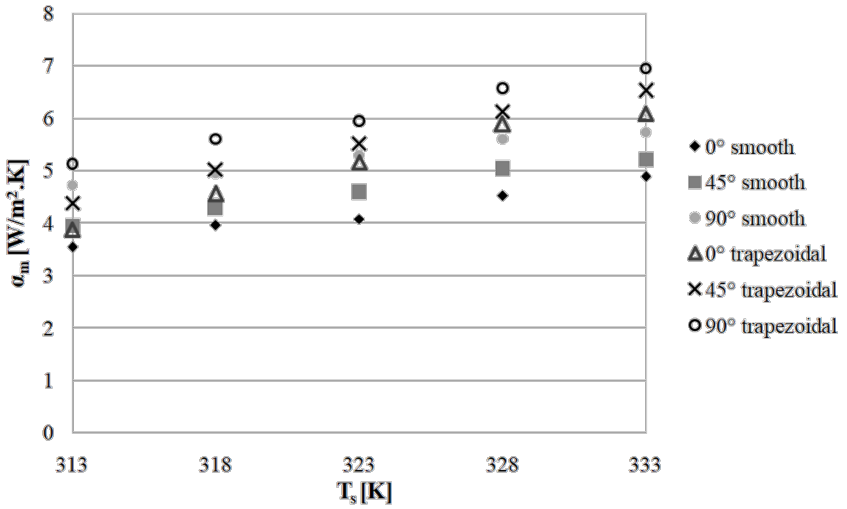

Fig. 7 The course of mean heat transfer coefficient depending on the surface temperature of smooth and trapezoidal surfaces
Obr. 7 Priebeh stredného súčiniteľa prestupu tepla v závislosti na povrchovej teplote hladkých a lichobežníkových plôch

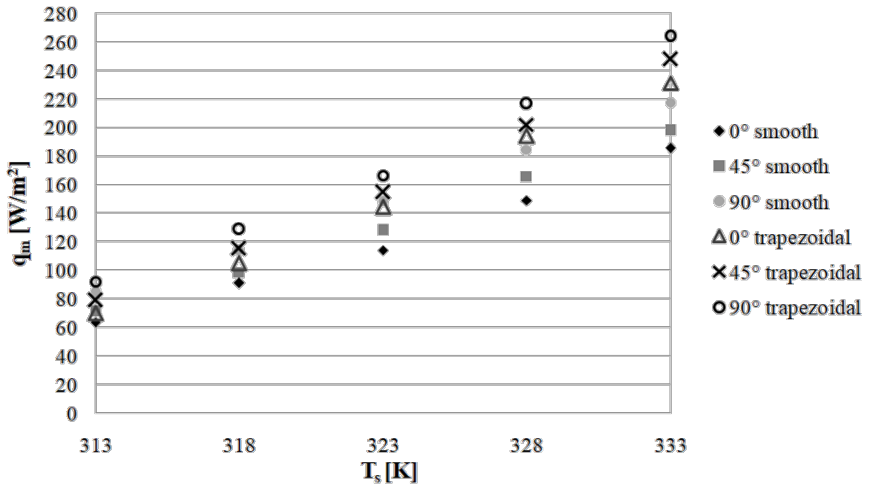

Fig. 8 The course of heat flux density depending on the surface temperature of smooth and trapezoidal surfaces
Obr. 8 Priebeh hustoty tepelného toku v závislosti na povrchovej teplote hladkých a lichobežníkových plôch

The results of the experiment show that spatial orientation and shape of the heat exchange surface have a significant effect on the mean heat transfer parameters. From the course in Fig. 7 and Fig. 8, we can observe a gradual increase in mean heat transfer coefficients and heat flux densities with an increase in the surface temperature of the smooth and trapezoidal surface. Changing the angle of inclination from 0° to 90° caused an increase in values α_m and q_m.

In terms of comparing the smooth and trapezoidal surfaces, the more intense heat transfer achieved the trapezoidal surfaces ranging from 8.7 % to 30.3 % compared to the smooth surface as the surface temperature increased. The most intense heat transfer (α_m = 6.95 W/m^2.K) is achieved by the trapezoidal surface at a 90° inclination angle and at a surface temperature of 333 K. This surface also achieves the highest heat flux density (q_m = 264.10 W/m^2). The trapezoidal surface at an inclination angle of 90° and at a surface temperature of 333 K achieves an α_m and q_m values of 21.3 % higher compared to the smooth surface.

The heat flux density of the smooth and trapezoidal surfaces increased with an increase in the temperature difference between the surface temperature T_s and the ambient air temperature T_a. The heat flux density of the smooth surface increased by 223.4 % and the trapezoidal surface by 278.2 % as the surface temperature increased from 313 K to 333 K.

By suitable inclination of the heated surface, the heat transfer from the surface to the ambient air can be intensified. The resulting heat flux density is influenced not only by the mean heat transfer coefficient, but also by the temperature difference between the surface temperature and the ambient temperature of air.

CONCLUSION

The paper is focused on the research of the influence of profiling and spatial orientation of the heated surfaces on heat transfer in free convection. Measurement of heat transfer parameters on the smooth and trapezoidal heated surface while changing their spatial orientation (0°, 45°, 90°) and their surface temperature (313 K to 333 K) was realized.

A Mach-Zehnder interferometer was set to visualize the temperature fields in the vicinity of the heated surfaces. Local and mean heat transfer coefficients and heat flux densities were evaluated from holographic interferogram images. The results show that the profiling, spatial orientation and temperature difference significantly influence the heat transfer from a heated surface to the ambient air in free convection.

The highest value of the mean heat transfer coefficient and heat flux density is achieved by the trapezoidal surface at a 90° inclination angle, at a surface temperature of 333 K (α_m = 6.95 W/m^2.K; q_m = 264.10 W/m^2). The trapezoidal surface at an inclination angle of 90° and at a surface temperature of 333 K achieves an α_m and q_m values of 21.3 % higher compared to the smooth surface.

As the surface temperature and the angle of inclination of the heated surface increase, the heat transfer coefficient values increase. Accordingly, as the temperature difference T_s-T_a and the mean heat transfer coefficient α_m increase, the heat flux density q_m of the smooth and trapezoidal surfaces increases.

LITERATURE

AMBROSINI, D., PAOLETTI, D., TANDA, G., GALLI, G. 2003. Optical investigations of natural convection in vertical channels. *7th International symposium on fluid control, measurement and visualization,* Italy: Sorrento, 2003, 10 p.

AMBROSINI, D., TANDA, G. 2006. Comparative measurements of natural convection heat transfer in channels by holographic interferometry and schlieren. In *European Journal of Physics*, vol. 27, no. 1, pp. 159 – 172. DOI: 10.1088/0143-0807/27/1/016.

BOŽEK, P., PIVARČIOVÁ, E. 2012. Registration of holographic images based on integral transformation. In *Computing and Informatics*, vol. 31, pp. 1369-1383. ISSN 2585-8807.

BRODNIANSKÁ, Z. 2013. *Výskum prenosových javov* v *tepelných procesoch holografickou interferometriou*. Dizertačná práca. Zvolen: Technická univerzita vo Zvolene, 2013. 150 s.

BRODNIANSKÁ, Z., ČERNECKÝ, J. 2016. The impact of the shaped vertical heated surfaces on the values of the heat transfer coefficients. In *JP Journal of Heat and Mass Transfer*, vol. 13, no. 4, pp. 575-588. ISSN 0973-5763.

ČERNECKÝ, J., KONIAR, J., BRODNIANSKÁ, Z. 2012. *Možnosti optimalizácie tvaru teplovýmenných plôch výmenníkov tepla s využitím experimentálnych metód a fyzikálneho modelovania.* Vedecká monografia. Zvolen: Vydavateľstvo Technickej univerzity vo Zvolene, 2012. 172 s. ISBN 978-80-228-2325-8.

IGAZ, R., ČERNECKÝ, J. 2014. *Efektívnosť prestupu tepla pri prirodzenom prúdení* v *závislosti od povrchovej profilácie teplovýmennej plochy*. Zvolen: Technická univerzita vo Zvolene, 2014. 98 s. ISBN: 978-80-228-2670-9.

KOLEDA P., BARCÍK, Š., VANČO, M., NOCIAROVÁ A. 2017. Thermal treatment and its effect on energetic efficiency of thermal threated oak wood face milling. In *Acta Facultatis Technicae*, vol. 22, no. 2, pp. 63-74. ISSN 1336-4472.

KOLEDA, P., HRČKOVÁ, M. 2017. Color detection of thermal modified wood using Matlab. In *Acta Facultatis Technicae,* vol. 22, no. 2, pp. 9-16. ISSN 1336-4472.

LENHARD, R., JANDAČKA J., MALCHO, M. 2009. Influence of distance and height ribs on boundary layer in to the passive roof cooling convector. In *Acta Metallurgica Slovaca*, vol. 15, pp. 168 – 173. ISSN 1338-1156.

LEWANDOWSKI, W. M., RYMS, M., DENDA, H., KLUGMANN-RADZIEMSKA, E. 2014. Possibility of thermal imaging use in studies of natural convection heat transfer on the example of an isothermal vertical plate. In *International Journal of Heat and Mass Transfer*, vol. 78, pp. 1232-1242. DOI: 10.1016/j.ijheatmasstransfer.2014.07.024.

LU, Q., QIU, S., SU, G., TIAN, W., YE, Z. 2010. Experimental research on heat transfer of natural convection in vertical rectangular channels with large aspect ratio. In *Experimental Thermal and Fluid Science*, vol. 34, no. 1, pp. 73 – 80. DOI: 10.1016/j.expthermflusci.2009.09.004.

MARTYNENKO, O. G., KHRAMTSOV, P. P. 2005. *Free-convective heat transfer*. Berlin: Springer, 2005. 516 p. DOI: 10.1007/3-540-28498-2.

PAVELEK, M. 2001. *Interferometrický výzkum přestupu tepla* v *soustavě vertikálních desek*. Teze habilitační práce. Brno: VUTIUM v Brne, 2001. ISBN 80-214-1821-4.

ROELEVELD, D., NAYLOR, D. 2014. Flow visualization of natural convection in vertical channels with opposing buoyancy forces. In *Experimental Thermal and Fluid Science*, vol. 54, pp. 61-70. DOI: 10.1016/j.expthermflusci.2014.01.015.

The contribution was created within the project VEGA 1/0086/18 "The Research of Temperature Fields in the System of Shaped Heat Exchange Surfaces" funded by the Ministry of Education, Science, Research, and Sport of the Slovak Republic.

Corresponding author:
Ing. Zuzana Brodnianská, PhD., tel.: +421455206 678, e-mail: zuzana.brodnianska@tuzvo.sk

GRANULOMETRY OF SAWDUST FROM THE PROCESS OF LONGITUDINAL MILLING OF HEAT-TREATED WOOD

GRANULOMETRIA PILÍN Z PROCESU POZDĹŽNEHO FRÉZOVANIA TEPELNE UPRAVENÉHO DREVA

Martin Kučerka [a], Alena Očkajová

Department of Technology, Faculty of Natural Sciences, Matej Bel University, Tajovského 40, 97401 Banská Bystrica, Slovakia, email: [a] martin.kucerka@umb.sk

ABSTRACT: The submitted contribution deals with the granulometric composition of sawdust from the process of longitudinal milling of heat-treated spruce and oak wood depending on the treatment temperatures at 160 °C, 180 °C, 200 °C and 220 °C. Sieve analysis was used to determine the share of individual fractions, with growth in the finest fraction with increasing treatment temperature. With oak a notable change in the granulometric composition of the sawdust already appeared at a treatment temperature of 160 °C and with spruce at a treatment temperature of 200 °C. The assumptions of reduced solidity and sturdiness of the wood on behalf of increasing brittleness as well as the differing influence of treatment temperature on the degradation of individual components of the wood with broadleaved and coniferous tree species were confirmed. A share of the dust fraction of size ≤ 0.08 mm was recorded only at treatment temperatures of 200 and 220 °C for both oak and spruce in a percentage share from 1.77% to 4.96%.

Key words: milling, heat-treated wood, oak, spruce, granulometry

ABSTRAKT: Predložený príspevok pojednáva o granulometrickom zložení piliny z procesu pozdĺžneho frézovania tepelne upraveného dreva smreka a duba v závislosti na teplote úpravy 160 °C, 180 °C, 200 °C a 220 °C. Sitovou analýzou sa určil podiel jednotlivých frakcií, s nárastom jemnejšej frakcie so zvyšujúcou sa teplotou úpravy. Pri dube sa výrazná zmena v granulometrickom zložení piliny prejavila už pri teplote úpravy 160 °C a pri smreku až pri teplote 200 °C. Potvrdili sa predpoklady zníženej pevnosti dreva a húževnatosti dreva v prospech zvýšenia krehkosti dreva ako aj rozdielny vplyv teploty úpravy na degradáciu jednotlivých zložiek dreva pri listnatých a ihličnatých druhoch dreva. Podiel prachovej frakcie s rozmerom ≤ 0,08 mm bol zaznamenaný len pri teplotách úpravy 200 a 220 °C aj pri dube aj pri smreku v podiele od 1,77 % do 4,96 %

Kľúčové slová: frézovanie, tepelne upravené drevo, dub, smrek, granulometria

INTRODUCTION

On the basis of experiments previously carried out by the targeted treatment of wood (with high temperatures and so on), we acquire material with different physical-mechan-

ical properties – positive and negative. The change of these properties is associated in particular with a change in the chemical properties of the wood. At high temperatures, the original structural polymers of wood decompose, and new water-insoluble substances are formed along with substances with toxic or repugnant effects. Wood thus treated is more resistant to biological damage, and its hygroscopicity falls (Reinprecht & Vidholdová 2008), which is the advantage of this type of wood treatment. This is caused in particular by chemical changes in the hemicellulose, which is subject to various depolymerization and dehydration reactions, resulting in different monomers, which enter into condensation reactions leading to the origin of new hydrophobic substances, which is reflected in the decline of the hygroscopicity of the wood and increased dimensional stability. At higher temperatures (180 to 260 °C) chemical reactions of lignin occur for the origin of new structures with biocidal effects, the result of which is an increase in the durability of the wood, which is also a positive element of this type of wood treatment. On the other hand, however, with this depolymerisation of cellulose from a temperature of 150 °C nano-tears and micro-tears arise in the cell walls, in the individual layers, resulting in more brittle cell walls, which cause a lowering of the wood's solidity (especially its bending and tensile strength) and sturdiness, which limits the use of the wood thus treated, especially for construction purposes (Reinprecht & Vidholdová 2008; Kačíková & Kačík, 2011; ThermoWood Handbook, 2003; Čabalová et al., 2016; Budakci et al., 2013).

The bending strength fell by about 50% at treatment temperatures of 200 to 220 °C (Bengtsoon et al. 2002; Bekhta & Niemz 2003; Reinprecht & Vidholdová 2008; and ThermoWood Handbook 2003) presents the decline in bending strength from 5 to 30%, similarly also the Anonymous (2002), but only at a treatment temperature of 240 °C. The shear strength at 230 °C fell in a radial direction by about 25%, in the tangential direction by about 40%, and at 190 °C about 20% in both directions (ThermoWood Handbook 2003).

Thermowood is examined from various aspects, especially from the viewpoint of changes in the chemical, physical-mechanical, biological and optical properties (Gunduz et al. 2009; Reinprecht & Vidholdová 2008; Kačíková & Kačík 2011; ThermoWood Handbook 2003; Čabalová et al. 2016; Welzbacher et al. 2007; Bemgtsoon et al. 2002), but also from the aspect of workability, energy consumption in machining processes, and the resulting quality of the surface (Budacki et al., 2013; Kvietková et al. 2015; Kaplan et al. 2018; Sandak et al. 2017; Kubš et al. 2016; Koleda et al. 2018). Since in the process of machining another secondary semi-product arises – sawdust – which can in many cases be further processed, or waste (wood dust), which causes a health and safety risk at the workplace, thermowood was also examined from this angle of view (Dzurenda et al. 2010; Dzurenda & Orlowski 2011; Barcík & Gašparík 2014; Kučerka & Očkajová 2018; Mikušová et al. 2019; Kminiak & Dzurenda 2019).

Among the basic strength properties of wood which share in the creation of chips or sawdust are bending strength, longitudinal pulling and pressure on fibres, perpendicular pull on fibres in the case of longitudinal cutting, and in a certain way shear strength is also manifested (Siklienka et al., 2017). On the basis of the above-mentioned characteristics on the decline of mechanical properties (especially bending and tensile strength) and the characteristics of solidity during the chip-forming process, an increased share of finer fractions to dust in the processing of heat-treated wood is assumed (Král & Hrázský 2005; Reinprecht & Vidholdová 2008).

The aim of the submitted contribution is to determine the granulometric composition of sawdust obtained during the longitudinal milling of heat-treated wood, spruce and oak, on a lower spindle milling machine, depending on treatment temperature (temperatures of 160 °C, 180 °C, 200 °C and 220 °C), with confirmation or refutation of the influence of reducing the solidity of heat-treated wood on an increased share of the fine and dust fractions.

MATERIAL AND METHODS

Experimental samples – 2 species of wood, sessile oak (Quercus petraea) and Norway spruce (Picea abies (L.) H. Karst.). The sessile oak and Norway spruce were extracted at the location Vlčí jarok (Budča), 440 m. a. s. l. The oak and spruce trunks were sawed radially into boards, and these were processed into testing samples of size 20 x 100 mm with a length of approximately 700 mm. The samples were subsequently dried to a residual moisture of 8%. The entire process was carried out in the Research and Development Workshops at the Technical University in Zvolen.

Methods of heat treatment and the working the samples

The processed samples of size 20 x 100 x 700 mm were heat treated in the Arboretum FLD (ČZU Prague) in Kostelec nad Černými lesy. For heat treatment a S400/03 (LAC Ltd., Czech Republic), chamber was used, intended for heat treatment of wood with ThermoWood technology. For each treatment temperature variant, 5 sample units were prepared.

The process of heat treatment for individual temperatures and phases of heating, treatment and cooling for individual tree species and the time intervals of operation are in the contribution of Kučerka and Očkajová (2018).

Machinery

A lower spindle milling machine ZDS-2 (Liptov machine shop, Slovakia) was used. Feeding was carried out using the feeding device Frommia ZMD 252/137 (Maschinenfabrik Ferdinand Fromm, Fellbach, Germany).

Tool – milling head FH 45 Stanton SZT (Turany, Slovakia), with the parameters: diameter of milling head – 125 mm, diameter of milling head with protruding blade 130 mm, thickness of milling head 45 mm, number of blades 2, cutting material – steel MAXIMUM SPECIAL 55: 1985/5, front rake angle $\gamma = 25°$.

Cutting conditions – cutting speed $v_c = 40$ m.s^{-1}, feed rate $v_f = 10$ m.min^{-1}, depth of reduction = 1 mm.

Granulometric analysis

Samples for granulometric analysis of sawdust from the milling process were taken isokinetic from the suction pipe in line with STN 9096 (83 4610): “Manual determination

of mass concentration of particulate matter", during the cutting of individual heat-treated samples of wood.

The granulometric composition of the sawdust was determined by sieve analysis. For this purpose a special set of sieves on top of one another was used (2 mm; 1mm; 500 µm; 250 µm; 125 µm; 80 µm; 63 µm; 32 µm; and the bottom), placed on the vibration stand of a sieving machine (Retsch AS 200c), with a settable frequency for interrupting the sieving (20 seconds) and with an amplitude for deviating the sieves (2mm/g), in line with the STN 153105/ STN ISO 3310 – 1.

Granulometric composition was obtained by weighing the shares remaining on the sieves after sieving on an electronic laboratory Radwag WPS 510/C/2 scale (Radwag Balances and Scales, Radom Poland), with a capacity of 510 g and a precision of weighing of 0.001g. For each variant three sievings were done and the results are given as their average value.

RESULTS

The results of the experiment carried out are given in the form of figures 1 and 2.

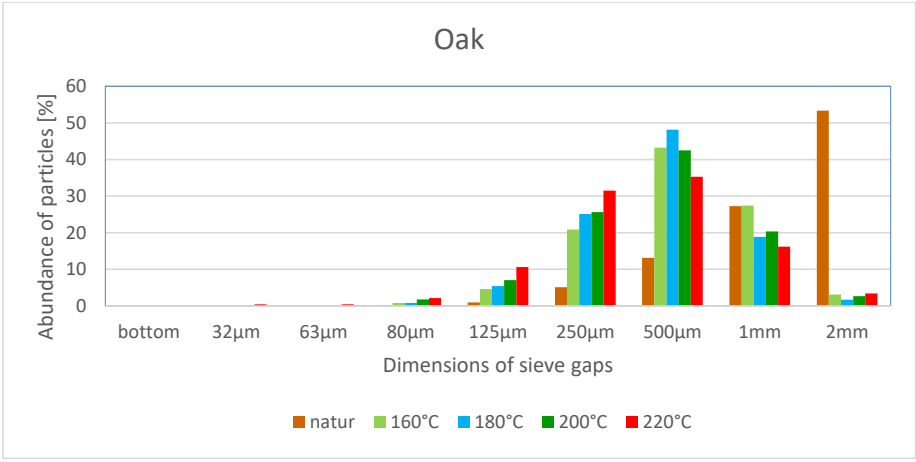

Fig. 1 Granulometric composition of oak sawdust depending on treatment temperature
Obr. 1 Granulometrické zloženie dubových pilín v závislosti na teplote termickej modifikácie

With natural oak the highest share of sawdust was recorded on the sieve (2 mm), up to 53.35% versus 1.67 – 3.40% with other treatment temperatures. With the evaluation of the coarse sawdust (sieves 2 mm and 1 mm) natural oak shows an 80% share, and the shares at treatment temperatures (160, 180, 200 a 220 °C) range from 19.57 – 30.50%. A significant change in the shares of sawdust can be seen on the 500 µm sieve, where the share of sawdust for natural oak is 13.16%; a similar percentage shares occur for treatment temperatures of 160, 180 and 200 °C, in the range from 42.48 – 48.12%, with the lowest share of

this fraction at the treatment temperature of 220 °C, namely 35.32%, but with the highest share of sawdust on the 250 µm sieve, namely up to 31.49% versus 5.08% for natural oak. For medium coarse sawdust (500 and 250 µm sieves) the percentage shares are the lowest for natural oak at 18.24 %, and the highest value is at the treatment temperature of 180 °C namely 73.22%; at heat treatment at 220 °C this value is 66.81%. On other sieves is sawdust which are characterised as fine. A significant difference can still be seen on the 125 µm sieve, where for natural oak the percentage share of sawdust on this sieve is 0.92%, and at a treatment temperature of 220 °C this share is the highest, namely at 10.64%. If we assess the share of dust fractions ≤ 80 µm, their value moves in the range from 0.23% for natural oak to 2.99% for the treatment temperature of 220 °C.

With oak it's possible on the basis of granulometric analysis to state that the stratification on the individual sieves is different depending on the treatment temperature, with a decline in the coarse fraction and growth in the medium coarse fraction as well as the fine fraction with growing treatment temperature of the wood.

With granulometric composition of spruce sawdust it's possible to see a slightly different stratification of sawdust than with oak, Figure 2.

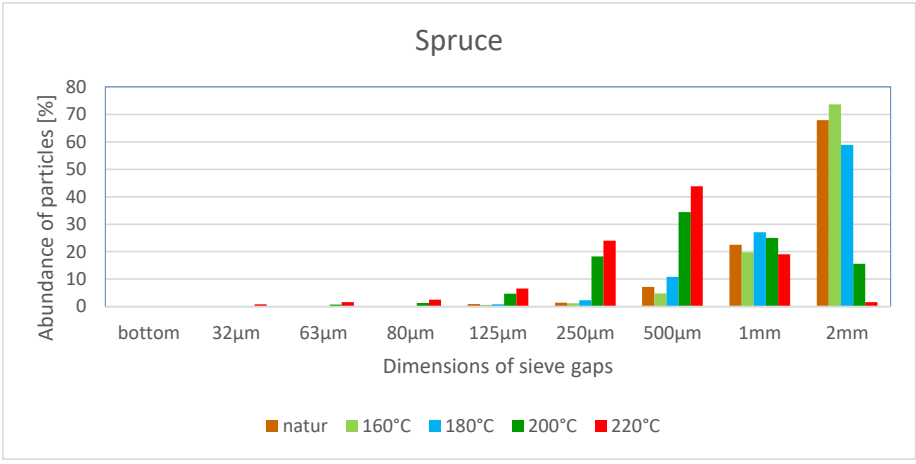

Fig. 2 Granulometric composition of spruce sawdust depending on treatment temperature
Obr. 2 Granulometrické zloženie smrekových pilín v závislosti na teplote termickej modifikácie

Similar results for the percentage shares of individual sawdusts (coarse and moderately coarse fractions) were obtained with natural spruce and treatment temperatures of 160 and 180 °C, where the share of coarse fraction (sieves 2 mm and 1 mm) represented from 86.04% (treatment temperature of 180 °C) to 90.43% (natural spruce), and the share of moderately coarse fraction (500 µm and 250 µm) was from 5.99% for a treatment temperature of 160 °C through 13.18% for a treatment temperature of 180 °C, as well as the fine fraction, where values under 1% were recorded. At a treatment temperature of 200 °C the share of coarse fraction falls to 40.54%, which is half compared to the natural wood, and at a treatment temperature of 220 °C this values achieves only 20.66%. The values of the moderately coarse fraction (sieves 500 µm and 250 µm) range from 52.70% a treat-

ment temperature of 200 °C to 67.77% for a treatment temperature of 220 °C, which is approximately 8-fold growth in comparison with natural wood. The share of fine fractions shows values from 6.76% for a treatment temperature of 200 °C to 11.57% for a treatment temperature of 220 °C. The share of dust fraction ≤ 80 μm was recorded only at the treatment temperatures of 200 and 220 °C, in the range from 2.03 – 4.96%.

DISCUSSION

The obtained results also correspond with the results of previous studies, where in processes of machining with an exactly defined geometry of the cutting chock, e.g. sawing (Dzurenda et al. 2010; Dzurenda & Orlowski 2011), or milling (Barcík & Gašparík 2014; Kminiak & Dzurenda 2019) with increasing treatment temperature increases the share of finer sawdust to dust, and therefore, it can be stated that with this method of machining the influence of a decline in the solidity and sturdiness of the wood (i. e. increasing the brittleness of the wood) is manifested in the granulometric composition of the sawdust, not changing the mass or density of the heat treated wood as with sanding (Kučerka & Očkajová 2018; Očkajová et al. 2018; Hlásková et al. 2018; Mikušová et al. 2019).

On the basis of the experiments conducted, it can be said that the assumptions of many researchers regarding changes to the physical-mechanical properties of heat-treated wood as a consequence of chemical changes of the individual components of the wood was confirmed, and that with the chip-forming process with longitudinal milling a lower sturdiness as well as lower tensile properties were manifested, and the wood behaved like more brittle material, with a higher share of moderately coarse and fine sawdust.

CONCLUSION

Since oak and spruce were milled, a certain difference was recorded even with those wood species, the heat treatment of which did not run the same, because, with the wood of deciduous species with a higher share of hemicellulose and a lower share of lignin, degradation occurs more than with evergreen trees with a higher share of lignin, which degrades at higher temperatures.

Therefore, we state that the changes in the granulometric composition in oak are expressed immediately at a temperature of 160 °C, and a similar course also occurred with higher temperatures, while with spruce the results are similar for natural wood and a treatment temperature of 160 and 180 °C, and a significant change in the granulometry manifested with a treatment temperature of 200 and 220 °C.

ACKNOWLEDGMENT

This article was created with the support of VEGA 1/0315/17 “Research of relevant properties of thermally modified wood at contact effects in the machining process with the prediction of obtaining an optimal surface.”

LITERATURE

ANONYMOUS. 2002. The Plato technology - a novel wood upgrading technology. Plato International BV, Arnhem, Netherlands, 14 s.

BARCÍK, Š., GAŠPARÍK, M. 2014. Effect of Tool and Milling Parameters on the Size Distribution of Splinters of Planed Native and Thermally Modified Beech Wood. In BioResources, 9(1): 1346−1360.

BEKHTA, P., NIEMZ, P. 2003. Effect of high temperature on the changes in colour, dimensional stability and mechanical properties of spruce wood. In Holzforsch, 539-546.

BEMGTSOON, C., JERMER, J., CLANG, A., EK-OLAUSSON, B. 2002. Investigation of some technical properties of heat-treated wood. ISBN 03-40266

BUDAKCI, M., ILCE, A. C., GURLEYEN, T., UTAR, M. 2013. Determination of the Surface Roughness of Heat-Treated Wood Materials Planed by the Cutters of a Horizontal Milling Machine. In BioResources, 8(3): 3189−3199.

ČABALOVÁ, I., KAČÍK, F., ZACHAR, M., DÚBRAVSKÝ, R. 2016. Chemical changes of hardwoods at thermal loading by radiant heating. In Acta Facultatis Xylologiae. Zvolen, 58(1): 43-50.

DZURENDA, L., ORLOWSKI, K., GRZESKIEWICZ, M. 2010. Effect of thermal modification of oak wood on sawdust granularity. In Drvna Industrija, 61(2): 89-94.

DZURENDA, L., ORLOWSKI, K. 2011. The effect of thermal modification of ash wood on granularity and homogeneity of sawdust in the sawing process on a sash gang saw PRW 15-M in view of its technological usefulness. In Drewno, Volume 54: 27−37.

GUNDUZ, G., KORKUT, S., AYDEMIR, D., BEKAR, I. 2009. The density, compression strength and surface hardness of heat-treated hornbeam (Carpinus betulus L.) wood. In Maderas. Ciencia y tecnología, 11(1): 61-70.

HLÁSKOVÁ, Ľ., KOPECKÝ, Z., RUOSEK, M., ROGOZINSKI, T., ŽELEZNÝ, A., HANINEC, P. 2018. Dust emissions during sanding of thermally modified beech wood. In Chip and chipless woodworking processes, 11 (1): 51-57, 2018. ISSN 1339-8350 (online)

KAČÍKOVÁ, D., KAČÍK, F. 2011. Chemical and mechanical changes during thermal treatment of wood. (Chemické a mechanické zmeny dreva pri termickej úprave). Zvolen: TU vo Zvolene. ISBN 978-80-228-2249-7

KAPLAN, L., KVIETKOVÁ, M., SEDLECKÝ, M. 2018. Effect of the Interaction between Thermal Modification Temperature and Cutting Parameters on the Quality of Oak Wood. In BioResources, 13(1): 1251−1264; DOI: 10.15376/biores.13.1.1251-1264.

KMINIAK, R., DZURENDA, L. 2019. Impact of sycamore maple thermal treatment on a granulometric composition of chips obtained due to processing on a CNC machining mentre Sustainability (Switzerland), Volume 11, Issue 3, 30 January 2019,

KOLEDA, P., BARCÍK, Š., NOCIAROVÁ, A. 2018. Effect of technological parameters of machining on energy efficiency in face milling of heat-treated oak wood. In BioResources, 13(3), 6133-6146.

KRÁL, P., HRÁZSKÝ, J. 2005. Využití nového materiálu ThermoWood. Materiály pro stavbu 1/2005.

KUBŠ, J., GAFF, M., BARCÍK, Š. 2016. Factors Affecting the Consumption of Energy during the Milling of Thermally Modified and Unmodified Beech Wood. In BioResources, 11(1): 736-747.

KUČERKA, M., OČKAJOVÁ, A. 2018. Thermowood and granularity of abrasive wood dust. Acta Facultatis Xylologiae Zvolen, 60 (2): 43-51, 2018. DOI: 10.17423/afx.2018.60.2.04

KVIETKOVÁ, M., GAFF, M., GAŠPARÍK, M., KAPLAN, L., BARCÍK, Š. 2015. Surface Quality of Milled Birch Wood after Thermal Treatment at Various Temperatures. In BioResources, 10(4): 6512-6521.

MIKUŠOVÁ, L., OČKAJOVÁ, A., DADO, M., KUČERA, M., DANIHELOVÁ, Z. 2019. Thermal Treatment´s Effect on Dust Emission During Sanding of Meranti Wood. In BioResources, 14(3), 5316-5326

OČKAJOVÁ, A., KUČERKA, M., BANSKI, A. 2018. The influence of heat treatment on granularity of sand wood dust. In Chip and chipless woodworking processes, 11 (1): 123-130, 2018. ISSN 1339-8350 (online)

REINPRECHT, L., VIDHOLDOVÁ, Z. 2008. ThermoWood – preparing, properties and applications. Thermodrevo – príprava, vlastnosti a aplikácie. Zvolen: TU Zvolen. ISBN 978-80-228-1920-6

SANDAK, J., GOLI, G., CETERA, P., SANDAK, A., CAVALLI, A., TODARO, L. 2017. Machinability of Minor Wooden Species before and after Modification with Thermo-Vacuum Technology. Materials 2017, 10, 121; DOI: 10.3390/ma10020121.

SIKLIENKA, M., KMINIAK, R., ŠUSTEK, J., JANKECH, A. 2017. Delenie a obrábanie dreva. Zvolen : Technická univerzita vo Zvolene, s. 357. ISBN 80-228-2845-1.

STN ISO 9096 (83 4610). 2004. Ochrana ovzdušia. Stacionárne zdroje znečisťovania. Manuálne stanovenie hmotnostnej koncentrácie tuhých znečisťujúcich látok.

STN 1531 05/ STN ISO 3310-1: 2000. Súbor sít na laboratórne účely.

ThermoWood Handbuch [online] [cit. 2010-04-10]. Dostupné z: https://asiakas.kotisivukone.com/files/en.thermowood.palvelee.fi/downloads/ThermoWood_Handbuch.pdf [accessed May 2019].

WELZBACHER, C.R., BRISCHHE, C., RAPP, A.O. 2007. Influence of tretment temperature and duration on selected biological, mechanical, physical and optical properties of thermally modified timber. In Wood Material Science and Enfineering. Vol. 2, Issue 2, 2007, pp. 66-76

Corresponding author:
Ing. Martin Kučerka, PhD., tel.: +421 48 446 7219, e-mail: martin.kucerka@umb.sk